8-2014

Studies on efficient spectrum sharing in coexisting wireless networks.

Guanying Ru
University of Louisville

STUDIES ON EFFICIENT SPECTRUM SHARING IN COEXISTING WIRELESS NETWORKS

By

Guanying Ru
B.S., Zhengzhou University, Zhengzhou, China, 2006, EE
M.S., Zhengzhou University, Zhengzhou, China, 2009, EE

A Dissertation
Submitted to the Faculty of the
University of Louisville
J.B. Speed School of Engieering
in Partial Fulfillment of the Requirements
for the Degree of

Doctor of Philosophy

Department of Electrical and Computer Engineering
University of Louisville
Louisville, Kentucky

August 2014

STUDIES ON EFFICIENT SPECTRUM SHARING IN COEXISTING WIRELESS NETWORKS

By

Guanying Ru

A Dissertation Approved on

June 13, 2014

by the Following Dissertation Committee:

_____

Dissertation Director
Hongxiang Li

_____

Jacek M. Zurada

_____

Michael L. McIntyre

_____

Lihui Bai

_____

Dongfeng Wu

ACKNOWLEDGMENTS

I would like to thank my Ph.D. advisor Dr. Hongxiang Li for his constant guidance, understanding and encouragement in both work and life. Dr. Li supported me in all ways an advisor can do for a student: he provided me insightful comments and guidance on topic selection; he gave me sufficient freedom to work on the problems that are interesting to me; he provided me great chances to collaborate with many people in both academia and industry; he demonstrated how to write papers and grant proposals, as well as how to give nice presentations; he also provided me generous support in choosing a career path, and etc. I cherish our student-teacher relationship developed during these years.

I am very grateful to Dr. Jacek Zurada, Dr. Michael McIntyre, Dr. Lihui Bai, Dr. Dongfeng Wu for being my committee members. Dr. Zurada's positive attitude towards working and life is very inspiring. Dr. McIntyre was always very supportive and nice to talk with. Dr. Bai allowed me to audit her optimization courses such that I can learn the optimizations systematically, also many thanks for her insightful comments and suggestions on my work in Chapter 2. Dr. Wu always gave me prompt support, and she encouraged me a lot both in study and life.

I would also like to express my great appreciation to Dr. Xin Liu in UC Davis for providing me a precious research experience at Davis and for sharing her knowledge in optimization and viewpoints in the trend of wireless communications. The insightful discussions with her opens my mind.

Lots of thanks to Dr. Rajendra Katti and Dr. Melnykov Volodymyr for serving as my Ph.D. committee members when I was at North Dakota State University (NDSU).

The in-depth discussions on interesting research problems in security and random process with them broadened my knowledge base. Many thanks to Dr. James H Graham for helping me smoothly transfer to UofL and adjust to my new working environment in UofL. Great thanks to my Master advisor Dr. Shouyi Yang for visiting my group from Zhengzhou University to UofL for potential collaborations, and also thanks a lot to my Master teacher Dr. Yanhui Lu for many insightful research discussions.

Thanks to Dr. Yong Cheng for discussions in Chapter 2, Dr. Huasen Wu for discussions in Chapter 3, Dr. Lingjia Liu, Dr. Zixia Hu for discussions in Chapter 4. Also I thank Ms. Lisa Bell for proofreading my dissertation and for being always very patience and helpful over these years.

Thanks to my friends and colleagues in University of Louisville: Dr. Tuan Tran, Dr. Yinan Cui, Marwa Ismail, Dr. Hui Wang, Dr. Bin Li, Dr. Qinwei Fan, Xiaohui Zhang, Wenqi Liu, Qingyun Li, Chen Cao, Nadieh Mohamadim, Guangyang Xu, Shanshan Li, Jin Shang, Dr. Minlun Li, Xiaomei Li, Dr. Chaolei Zhang, etc. I also want to express my appreciations to friends and colleagues when I was in North Dakota State University: Dr. Siqian Liu, Dr. Yang Du, Claudia Sampaio, Yingjie Yang, Varinder Singh, Reihaneh Lavafi, Kai Johnson, Dr. Zonghui Li, Xin Wang, Yang Liu, etc. Also, lots of thanks to my colleagues in UC Davis: Dr. Dan Xu, Dr. Eric Jung, Dr. Huasen Wu, Yichuan Wang, Wei Zhou, Keke Liu, Yu Liu, Dr. Qiuju Diao, etc. Thank you all very much for helpful discussions and all the great time you spent with me.

Finally, I would like to thank my parents and grandpa for their unconditional love and for raising me up. What's more, I am indescribably indebted to my mom for having taken very good care of my father and grandpa. Their love is of great spiritual power for me to accomplish my Ph.D. degree. I dedicate this dissertation to them.

ABSTRACT

STUDIES ON EFFICIENT SPECTRUM SHARING IN COEXISTING WIRELESS NETWORKS

Guanying Ru

June 13, 2014

Wireless communication is facing serious challenges worldwide: the severe spectrum shortage along with the explosive increase of the wireless communication demands. Moreover, different communication networks may coexist in the same geographical area. By allowing multiple communication networks cooperatively or opportunistically sharing the same frequency will potentially enhance the spectrum efficiency. This dissertation aims to investigate important spectrum sharing schemes for coexisting networks.

For coexisting networks operating in interweave cognitive radio mode, most existing works focus on the secondary network's spectrum sensing and accessing schemes. However, the primary network can be selfish and tends to use up all the frequency resource. In this dissertation, a novel optimization scheme is proposed to let primary network maximally release unnecessary frequency resource for secondary networks. The optimization problems are formulated for both uplink and downlink orthogonal frequency-division multiple access (OFDMA)-based primary networks, and near optimal algorithms are proposed as well.

For coexisting networks in the underlay cognitive radio mode, this work focuses on the resource allocation in distributed secondary networks as long as the primary network's rate constraint can be met. Global optimal multicarrier discrete distritbuted

(MCDD) algorithm and suboptimal Gibbs sampler based Lagrangian algorithm (GSLA) are proposed to solve the problem distributively.

Regarding to the dirty paper coding (DPC)-based system where multiple networks share the common transmitter, this dissertation focuses on its fundamental performance analysis from information theoretic point of view. Time division multiple access (TDMA) as an orthogonal frequency sharing scheme is also investigated for comparison purpose. Specifically, the delay sensitive quality of service (QoS) requirements are incorporated by considering effective capacity in fast fading and outage capacity in slow fading. The performance metrics in low signal to noise ratio (SNR) regime and high SNR regime are obtained in closed forms followed by the detailed performance analysis.

TABLE OF CONTENTS

LIST OF FIGURES

CHAPTER 1
INTRODUCTION

Technical innovations of mobile wireless communications are rapidly and profoundly changing people's daily lives. Fueled by the fourth generation (4G) wireless technologies and standards, the increasing smart devices as well as the social networking tools and video sharing resources forced the wireless communication experiencing a profound revolution from all aspects. According to [1, 2], the number of 3G/3.5G subscribers has increased to almost 1.2 billion in 2011 and will reach 4.27 billion by 2017; and according to Global System for Mobile Communications Alliance (GSMA) Intelligence [3] the number of 4G-LTE connections will increase to 2.5 billion till 2020. Global mobile data traffic will increase about 11-fold between 2013 and 2018, surpassing 15 exabytes per month in 2018 [4]. Therefore, for future mobile communications, high-speed high-quality data transmissions are required to support various multimedia services.

Considering all wireless communication demands, the fundamental theory of communications dates back to 1948, when Claude E. Shannon [5] first defined channel capacity, which is the upper limit of reliable communication rate with respect to its channel characteristics, specifically,

$$C = B \log_2 \left(1 + \frac{P|h|^2}{N_0 B}\right) \text{(bits/Hz)},$$

where B denotes the channel bandwidth (Hz), P is the transmission power (Watt), $|h|^2$ is the channel power gain between the transmitter and the receiver, and N_0 represents the noise power spectral density (W/Hz). Note that most wireless applications work in

the radio frequency between 30 MHz to 30 GHz. The reason is because such frequency range is not affected by the earth's curvature and can penetrate the ionosphere. Also, the required antenna size for good reception is to inversely proportional to the square of the signal frequency.

With limited usable frequency resource and the pervasive communication demands, the frequency scarcity has become a primary bottleneck for wireless communications. What is more, most of the usable radio frequency has been pre-regulated by Federal Communications Commission (FCC) for different applications long time ago. Nowadays, some spectrum bands become overcrowded while others are under-utilized. Hence, how to improve the spectrum efficiency to accommodate the ever-increasing communication demand becomes a main challenge for wireless communications. This dissertation will investigate the advanced frequency sharing schemes for coexisting networks.

The following sections will briefly introduce the wireless communications developing history from first generation to fourth generation, followed by the main techniques investigated in this dissertation. Finally, the motivation as well as the outline of this dissertation are provided.

1.1 Wireless Communications Evolution

1.1.1 Wireless Communication History

In past decades, mobile communication networks evolved from the first generation to the fourth generation. The first generation (1G) uses analog modulation with limited transmission rate; while the second generation (2G), which emerged in the early 1990s, is based on digital communication. The digitalization is realized by adding an Analog to Digital (A/D) converter before the radio frequency (RF) transmitter, and a

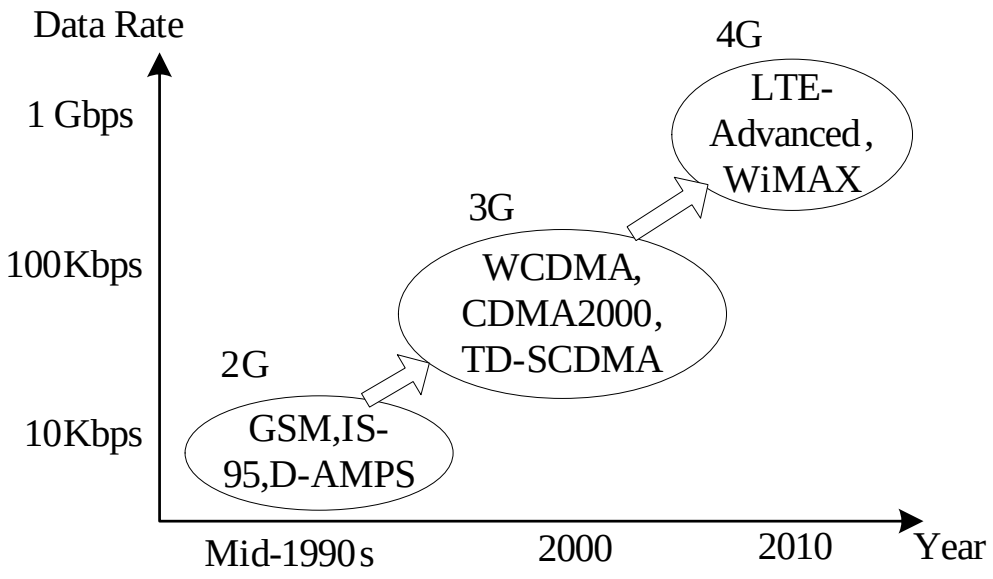

FIGURE 1.1 – The evolution of communication systems.

Digital to Analog (D/A) converter after the RF receiver. Compared to analog systems, digital systems have better security, higher communication quality, and higher frequency efficiency, etc. Ever since 2G communication, digital modulations play important roles to improve the communication speed. With the development of the 2G technique and the wide application of the cellular phone, the demands for data services were growing. While 2G systems were designed to carry speech and low bit rate data, third generation (3G) systems target higher data rate services. The use of packet-switching for data transmission distinguishes the 3G technology from the 2G technology. Current wireless communications are at the beginning of the fourth generation (4G). The evolution of digital communication systems is shown in Figure 1.1.

1.1.2 4G Wireless Communications

Existing mobile wireless communication systems can be generalized into the following categories from the application perspectives: cellular networks, broadcast networks, WI-Fi/WiMax networks, Ad hoc networks, sensor networks and green networks, heterogeneous network, and etc. In the 4G system, different wireless communication standards are expected to be integrated into one unique communication system. It will also enable a comprehensive and secure all-IP based solution, such as IP phone, ultra-broadband Internet access, High Definition Television (HDTV) broadcast, and stream multimedia. The 4G system will also provide full mobility and connectivity, which requires the free roaming from standard to standard or from service to service. In July 2003, International Telecommunication Union (ITU) made a requirement for the 4G system known as the IMT-Advanced standard: the transmission data rate should be above 1 Gbps at the stationary condition, and the transmission data rate should be above 100 Mbps at moving speed [6]. Both 3GPP long term evolution (LTE) and Worldwide Interoperability for Microwave Access (WiMAX) are candidates for 4G systems. So far, LTE has better market penetration than WiMax due to its compatibility with previous standards.

To meet the high-level performance requirement, the system structure evolution will greatly contribute to the communication performance. One of the main differences between the 3G network and the 4G network lies in the network structure [7]. Specifically, before 4G, Radio Network Controller (RNC) nodes controlled the radio resources and mobility over multiple base stations. In 4G networks, RNC is no longer needed, the evolved 4G base stations (eNB) manage the radio resource and mobility in the cell and sector to accommodate all users' communications, also an eNB can directly communicate with other eNBs. Such simplified network structure gives more capabilities and responsibilities to eNB, as a result, the response time is reduced to meet timely

communication demands.

In addition to the system structure evolution, the advanced 4G technologies include:

1. Efficient modulation techniques, such as the orthogonal frequency division multiplexing (OFDM) technology which can easily combat the multipath effect in broadband systems;

2. Intelligent systems, such as the cognitive radio that can adjust with the varying transmission conditions;

3. Wireless access technologies, such as orthogonal frequency-division multiple access (OFDMA) and multiple carrier code-division multiple access (MC-CDMA);

4. Multi-systems' cooperation and convergence, e.g. hybrid broadcast and unicast network;

5. Advanced antenna technologies, such as Multiple-Input Multiple-Output (MIMO) techniques that can combat the interference and greatly enhance the system capacity;

6. The advanced encoding and decoding techniques, such as turbo coding, low-density parity-check codes (LDPC), dirty paper coding (DPC).

1.2 Main Technologies

The main technologies covered in this dissertation are introduced, respectively, i.e., the OFDM and orthogonal frequency division multiple access (OFDMA) technology, cognitive radio, DPC scheme as well as its application in hybrid broadcast and unicast system.

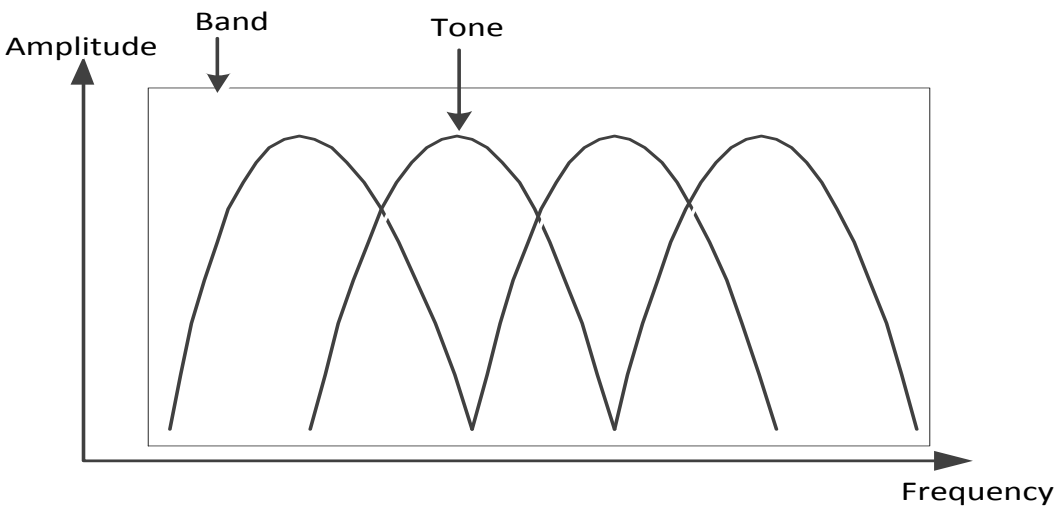

FIGURE 1.2 – Subcarrier overlap in OFDM system.

1.2.1 OFDM and OFDMA Technology

1.2.1.1 OFDM modulation OFDM is a multicarrier transmission technique used to achieve high data rate in a multipath-fading environment. With the decrease of the bandwidth in each subchannel, the symbol duration per subchannel increases. Hence, the overall wideband frequency-selective fading can be treated as flat fading on each subchannel. At the receiver side, only a trivial frequency domain single-tap equalizer is needed to overcome the overall frequency selective fading. Comparing with the traditional frequency division multiplexing (FDM) technique, OFDM has higher frequency efficiency by allowing the adjacent independent (orthogonal) subcarriers to overlap with each other without individual carrier guard band, as is shown in Figure 1.2. Due to its advantages, OFDM is widely used in many wireless communication systems (e.g., IEEE 802.16, IEEE 802.20, IEEE 802.22, 3GPP LTE/LTE-Advanced, and so on) [8].

1.2.1.2 OFDMA accessing technology OFDMA is a multiuser access version of OFDM. It is the combination of OFDM and the frequency division multiple ac-

cess (FDMA) concept. The two other versions are OFDM-TDMA and OFDM-CDMA; however, neither of these two can exploit the frequency diversity. Comparing with OFDM-TDMA and OFDM-CDMA, OFDMA allows multiple users to transmit at the same time on different subcarriers. Specifically, *the total bandwidth is divided into parallel subcarriers, and each subcarrier is assigned to at most one user in a given time slot.* One advantage of OFDMA is the elimination of intra-cell interference which means users do not interfere with each other. Another intrinsic advantage of OFDMA is capability of exploiting the multi-user diversity of diverse frequency-selective channels through intelligent resource allocation [9].

To enhance the system capacity, in OFDMA-based wireless communication systems, resources (power, bandwidth) have to be assigned to multiple users in such a way that the overall system capacity or power consumption is optimized. As a matter of fact, OFDMA resource allocation has become a hot topic in the past decade and has been studied widely in both academia [9–11] and industry.

In typical single cell mobile communication systems, a base station (BS) performs resource allocation according to the channel status information (CSI), and sends the so-called MAP information (i.e. resource allocation information) to its corresponding mobile stations (MSs); MSs send or receive data using the resources allocated by the BS. The information transmission link from BS to MS(s) is called downlink; while the link from MS(s) to BS is called uplink. The basic system structure for the OFDMA downlink system is shown in Figure 1.3.

1.2.2 Cognitive Radio

In recent years, the communication demands increased dramatically, which challenges the traditional fixed spectrum assignment policies such as by Federal Communications Commission (FCC). According to the present frequency usage, some licensed

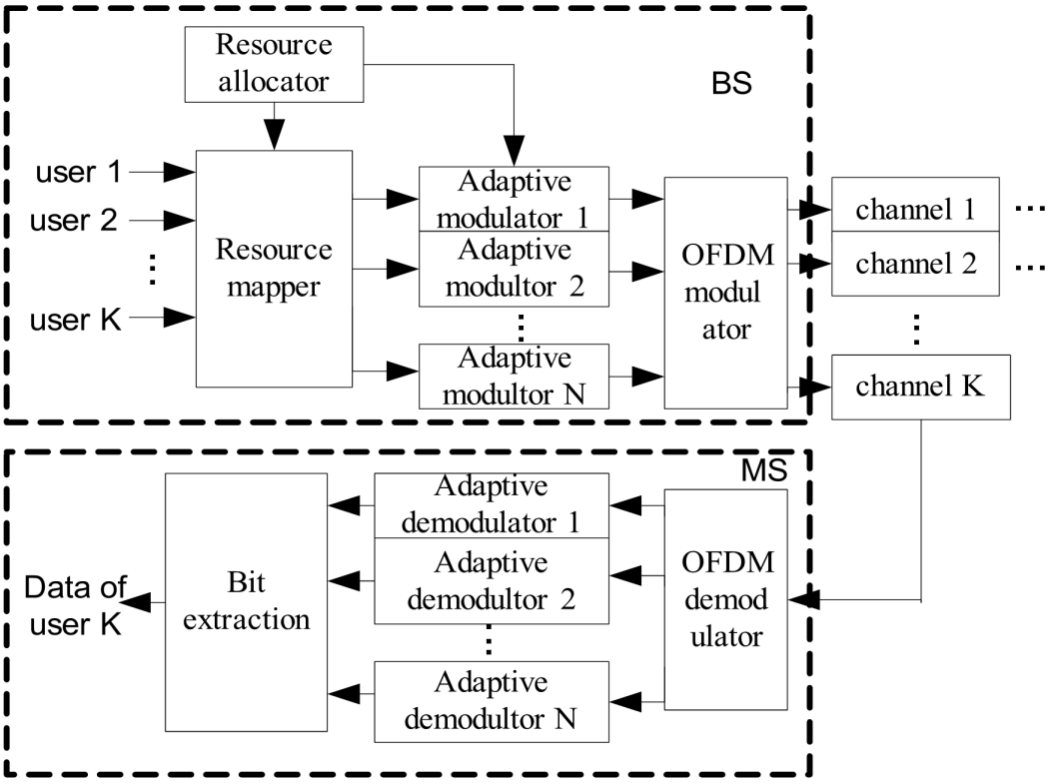

FIGURE 1.3 – OFDMA downlink structure.

frequency bands are seldom used, some bands are partially occupied, and only part of the frequency bands are heavily used [12]. This indicates the fixed spectrum assignment policy greatly affects the frequency efficiency. Hence, cognitive radio (CR) which can use a primary network's frequency band in an opportunistic way or a sharing way was proposed to improve the spectrum efficiency. The definition for CR given by Haykin [13] is: "an intelligent wireless communication system that is aware of its surrounding environment (i.e., outside world), and uses the methodology of understanding-by-building to learn from the environment and adapt its internal states to statistical variations in the incoming RF stimuli by making corresponding changes in certain operating parameters (e.g., transmit-power, carrier-frequency, and modulation strategy) in real-time, with two primary objectives in mind: 1) highly reliable communications whenever and wherever

needed; 2) efficient utilization of the radio spectrum."

Cognitive radio (CR) provides a promising solution to the problem of overcrowded and inefficient wireless spectrum usage [13–17]. The main principle of the CR is to allow the secondary users (SUs) to implement a variety of spectrum sharing techniques such as *underlay*, *overlay*, or *interweave* to transmit their signals without affecting the primary users' (PUs) communication [14]. Particularly, the "underlay" technique controls the SUs' transmission power over the operating bandwidth in a way that SU signals may interfere with the primary signal within a tolerable limit. The "overlay" technique allows SU transmitter to exploit the structure of the primary message and perform interference pre-cancellation (such as dirty paper pre-coding) for non-intrusive SU transmission. Note that the overlay transmitter is complicated and usually requires SU to know the PU signals in advance. Different from the first two techniques, "interweave" technique is *an opportunistic communication scheme by utilizing the spectrum holes in the primary transmission to carry out the SU transmission.*

1.2.3 Dirty Paper Coding

Dirty Paper Coding (DPC) was first introduced by M. Costa in 1983 [18]. Over the past years, DPC technique has allowed the wireless broadband industry to approach capacity-achieving rates [18–22].

The basic idea of DPC is illustrated in Figure 1.4. Assume v is the desired signal, s is the interference and n is the AWGN noise. If the interference s is non-causally known at the transmitter, the Costa's results shows that by adding a pre-coder at the transmitter, the receiver can demodulate source v as if the interference were not present. That is, the capacity of interference channel is the same as that of the AWGN channel without interference.

DPC also provides an intriguing alternative to receiver-end superposition coding.

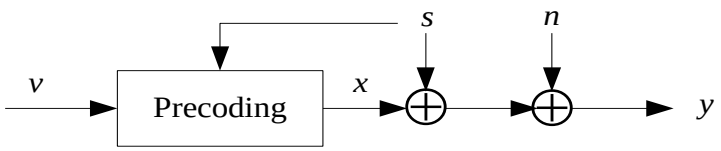

FIGURE 1.4 – Dirty paper pre-coding.

The significant advantage of DPC over superposition coding lies in that the interference is precanceled at the transmitter side. It happens that in wireless downlink transmission the interference can be considered as another modulated signal which is automatically known by the transmitter; therefore, the interference can be easily canceled in advance using DPC pre-coding.

The realization of DPC can be very complex in order to perfectly achieve the DPC performance. However, the near optimal DPC pre-coding designs can be very simple and efficient, for example, the structured DPC (SDPC) scheme proposed in [22] can approach the promised capacity limit by only involving simple add and modulo operations.

1.2.3.1 Hybrid Broadcast and Unicast Network One important application of DPC pre-coding is the hybrid broadcast and unicast system proposed in [23]. The *broadcast* network sends the same content over a reliable unidirectional channel to all users simultaneously, while the *unicast* network refers to point to point communication such as the cellular phone service. In the past, the broadcast and unicast evolved independently on different frequency bands through different infrastructures. Until recently, the pioneering work has been done to design a new hybrid broadcast and unicast network based on DPC [23].

As mentioned in the previous session, in a cognitive radio system, the primary users do not collaborate with the secondary users and they have higher priority than secondary users also. Although it provides more opportunities for spectrum usage, cog-

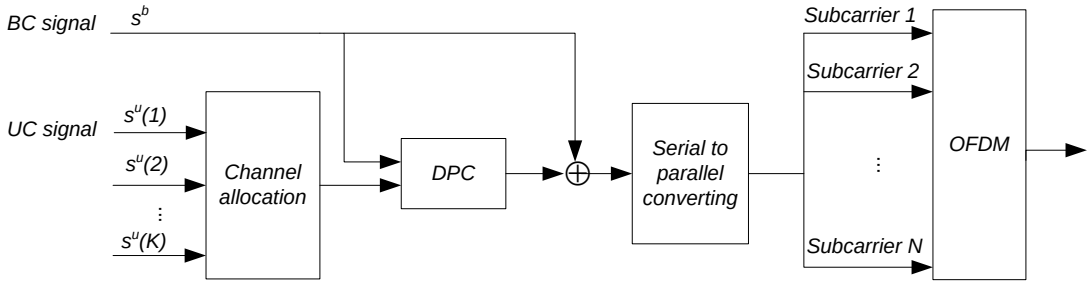

FIGURE 1.5 – Collaborative hybrid modem.

nitive radio is not the best option for broadcast and unicast networks. According to broadcast and unicast characteristics, they naturally complement each other. Moreover, with the new mobile TV (also called triple play service) as an emerging application [24], a more intensive collaboration can be done between broadcast and unicast networks to achieve further frequency efficiency.

The proposed hybrid broadcast and unicast (or say hybrid cellular) model by [23] is to allow broadcast and unicast transmitting simultaneously on the same frequency band using the dirty paper coding (DPC) technique. Specifically, the hybrid transmitter designed based on OFDM modulation and DPC precoding is shown in Figure 1.5. This hybrid cellular transmitter simultaneously sends the broadcast and unicast signals on the same channel. Since these signals are **known** "interference" to each other, the DPC is used to pre-cancel the broadcast interference for unicast users. In contrast to cognitive radio, this new form of collaboration can further enhance the spectrum efficiency.

1.3 Motivation

Considering the frequency sharing schemes between multiple coexisting networks, it can be generalized into three working modes:

1. Mode I: Multiple networks sharing the common frequency resource orthogonally.

2. Mode II: Multiple networks transmit on the same frequency simultaneously, and different networks interfere with each other.

3. Mode III: Multiple networks transmit on the same frequency simultaneously, however the interference is pre-canceled/post-canceled according to encoding/decoding techniques.

In cognitive radio, the three modes are named interweave mode (for mode I), underlay mode (for mode II), and overlay mode (for mode III). Due to the operational simplicity and effectiveness, the interweave mode and underlay mode are the most widely accepted working mode. However, the overlay mode may suffer from intolerable information exchange between the primary and secondary network.

The third mode requires encoding/decoding techniques to cancel the interference. DPC pre-coding has been proved for its capacity achieving performance [25]. The DPC-based scheme requires huge amount of information exchange when transmitters are at different locations, such as overlay cognitive radio systems, cooperative Ad hoc networks and distributed MIMO systems [26, 27]. However, when the DPC-based system has common transmitter sends signals to different systems, unbearable information exchange can be avoided, such as the hybrid cellular system introduced in Section 1.2.3.1.

This dissertation will investigate the interweave and underlay cognitive radio systems, as well as the DPC-base systems when multiple networks sharing the same transmitter for coexisting networks.

1.4 Outline

The rest of this dissertation is organized as follows:

Chapter 2 studies the resource allocation in interweave cognitive radio systems. The frequency saving problem is proposed for the primary network to save its required

frequency resource under QoS provisions. The optimization problems are formulated for both uplink and downlink OFDMA-based primary networks. Efficient algorithms are proposed to solve this problem near optimally. As a result, the secondary network may be able to sense the potential increase of available spectrum holes when the primary network is not heavily loaded.

Chapter 3 focuses on the underlay cognitive radio system, where we investigate the resource allocation in a distributed secondary network. The total utility of the secondary network under individual link's power constraint and primary user's rate constraint is maximized. Based on Gibbs sampling tools, the optimal algorithm and near optimal algorithm are provided to update the secondary users' power distributively.

Chapter 4 investigates the performance of the DPC-based hybrid downlink system in contrast to the TDMA-based downlink system. The delay sensitive QoS requirements are considered by using effective capacity in fast fading and outage capacity in slow fading. The low SNR metrics (minimum energy per bit and the wideband slope) and high SNR metrics (high SNR slope and power offset) are obtained in closed forms. The impact of the QoS requirements on the performance, the optimal cancellation order of the DPC scheme, and etc, are also provided. Further investigations and conclusions are drawn for Rayleigh fading channels. Sufficient simulation and numerical results are provided as well.

Finally, this dissertation is summarized in Chapter 5 with future research topics.

CHAPTER 2
FREQUENCY SAVING SCHEME FOR OFDMA-BASED INTERWEAVE COGNITIVE NETWORKS

In this chapter, the interweave mode cognitive radio is investigated. Most of the current research on interweave cognitive radio focuses on how can secondary networks effectively sense and access spectrum holes [14, 28, 29]. However, the primary network's involvement has been neglected. Hence, this chapter will introduce a new concept which can enhance the cognitive system's overall performance from the perspective of the primary network's resource allocation schemes. Specifically, a novel optimization objective has been proposed for the primary network: minimizing required frequency resource, on the premise that both the power constraints and users' quality of service (QoS) demands can be met. With the frequency saving objective, the primary system can release the unnecessary frequencies for secondary users. For OFDMA-based primary networks, the problem is formulated to minimize the required number of subcarriers for both uplink and downlink with certain power constraints and QoS rate requirements. This problem is a mixed-NP hard problem, and efficient near optimal solutions are proposed for both downlink and uplink transmission.

2.1 Background and Motivation

Due to the increasing communication demands, multiple wireless networks' (multi-radio) coexistence [13] has become an inevitable trend. Meanwhile, a hot research topic has always been how to improve the resource (frequency and power) utilization efficiency.

Under the context of multi-network co-existence, the existing resource allocation methods can be classified into three categories:

1. Single network dynamic resource allocation. It assumes each network independently allocates its resource without considering the other co-existing networks. The resource allocation within this category mainly consists of margin adaptive (MA) and rate adaptive (RA) approaches [30, 31]. The objective of MA is to minimize the total transmission power with the constraints of bandwidth and individual user's QoS requirements, and the objective of RA is to maximize the system throughput under the available power and bandwidth constraints.

2. Spectrum sharing in cognitive radio (CR) [13]. For the interweave mode, it allows the secondary users to share the spectrum in an opportunistic way when the primary users are silent. However, the primary system is unaware of the existence of the secondary users.

3. Joint resource allocation with inter-network cooperation. In this approach multiple networks jointly allocate the shared resources to achieve mutual benefits. For example, [23] proposed a collaborative hybrid network that supports both TV broadcasting and cellular data access on a single-frequency platform that can greatly enhance the aggregate capacity.

Intuitively, it is expected that the combination of the above three approaches can further improve the resource utilization efficiency. However, under the context of multi-network co-existence, most existing optimization objectives are either too selfish or unrealistic. Consider a primary and secondary network, and secondary users can only access the idle frequency of the primary network. With dynamic resource allocation, the primary cellular users tend to use all the frequency resource to maximize their performance according to the MA or RA optimization objective. As a result, the performance

of the secondary network can be jeopardized due to an insufficient amount of available frequencies. Meanwhile, these two coexisting networks cannot be cast into the collaborative hybrid structure in [23] because they do not share the same transmitter. In this case, if the primary network is aware of the existence of the secondary network and the latter is willing to somehow share the cost, at least some limited coordination can be performed between the two networks. As is well known, the scarcest resource in wireless communications is the radio spectrum. A fundamental question in multi-radio coexistence is: how to minimize the required frequency resource of a primary network without sacrificing its performance (i.e., guaranteed QoS to its users)?

To date, most existing research on OFDMA resource allocation focuses on either single cellular networks (see [23, 31–33] and references therein) or on secondary systems [13] [34, 35], without inter-network coordination. In this chapter, a new resource allocation objective is proposed to minimizes the required number of subcarriers in an OFDMA-based primary network, on the premise that both the power constraints and the users' QoS requirements can be met. The motivation of such a frequency saving objective can be found in many applications. In addition to the cognitive system where the subcarriers saved by the primary network can be used by the secondary users, the cellular system itself can also benefit from the frequency savings (For example, the saved frequencies can be used by other cellular applications such as mobile TV broadcasting).

The main contributions of this chapter are summarized as follows:

1. In contrast to the existing RA and MA optimization objectives, a new frequency saving optimization problem is established for both uplink and downlink primary networks;

2. In the downlink case, the "bisection search and feasibility test algorithm for multi-user frequency adaptive optimization" (BF-MUFA) is proposed, which has near optimal performance;

3. For the uplink, low complexity greedy methods to obtain very tight upper bound and lower bound for multi-user frequency adaptive optimization is derived. The proposed greedy methods can also be easily adapted to the downlink case to eliminate the bisection searching scope.

2.2 System Model and Problem Formulation

2.2.1 System Model

The proposed hybrid cognitive radio system is shown in Figure 2.1 which is consist of a primary network and a secondary network. The primary network is the traditional centralized network where primary base station (PBS) can manage the wireless resource allocation to meet primary users' requirements; and the co-existing secondary network can be either centralized or distributed. For example, the secondary network can be a cognitive Femtocell system with a small base station [36] or a distributed Ad hoc network [37]. Also assume there is a dedicated (wired or wireless) control channel to exchange the control information, as described in [36]. When the secondary network has a communication requirement, the 1-bit request information REQ (1 or 0) is sent through the control channel to the primary base station.

When the primary network is overloaded, i.e., not all PUs' QoS constraints can be met, the admission control should be carried out to maximize the primary network's effective user number. If all users' QoS constraints can be met, the primary network checks if there is any request from the secondary network. If $REQ = 0$, PBS carries out the traditional resource allocation algorithm to maximize its own performance, such as MA or RA. If $REQ = 1$, PBS will minimize the number of required subcarriers in the primary network. Accordingly, the ideal operational procedure for PBS is shown in Figure 2.2. This chapter mainly focuses on the case when $REQ = 1$, and the admission

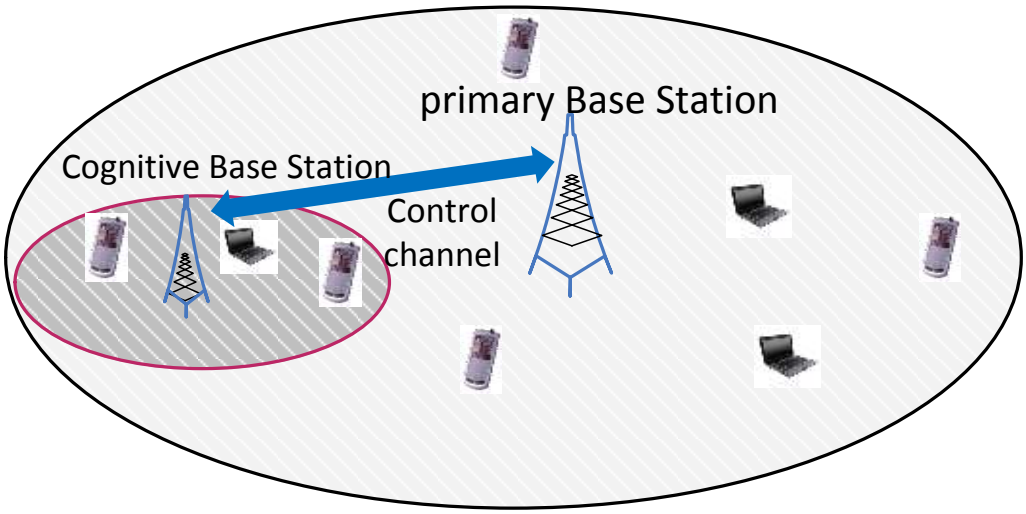

FIGURE 2.1 – Proposed cognitive system model.

control is beyond the research scope. For details on admission control, please refer to [38–41].

2.2.2 Problem Formulation

Specifically, consider the OFDMA-based primary network with K users and N subcarriers. The subcarrier bandwidth is B. Assume this priamry network receives a request from the secondary network, i.e. $REQ = 1$. Let $P_{k,n}$ denote the power allocated to the k-th user. Then the maximum achievable data rate of the k-th user on subcarrier n is:

$$C_{k,n} = B \log_2 \left(1 + P_{k,n} \cdot \frac{|H_{k,n}|^2}{\sigma_{k,n}^2}\right), \tag{2.1}$$

where $H_{k,n}$ is the instantaneous frequency response of user k on subcarrier n, and $H_{k,n}$ is assumed to be known at both the transmitter and receiver; $\sigma_{k,n}^2$ is the corresponding noise power which is assumed to be the same for all users on all subcarriers. Define channel signal to noise ratio (SNR) $\frac{|H_{k,n}|^2}{\sigma_{k,n}^2}$ as $e_{k,n}$. Denote matrix $\boldsymbol{X}$ as the subcarrier

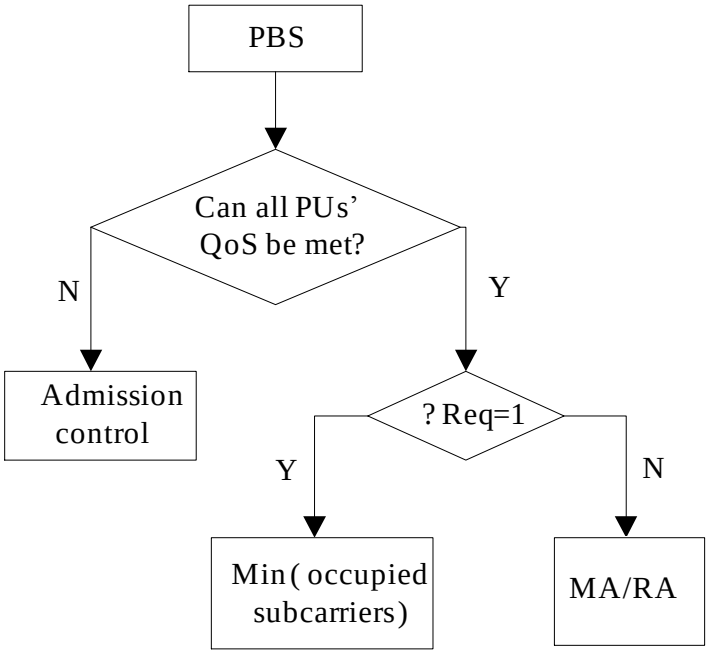

FIGURE 2.2 – Operational procedure of PBS.

allocation schedule, i.e. the (k, n)-th element of $\boldsymbol{X}$ is:

$$X_{k,n} = \begin{cases} 1 & \text{subcarrier } n \text{ is assigned to user } k \\ 0 & \text{otherwise} \end{cases} \tag{2.2}$$

Hence, the overall maximum rate for user k in this system is:

$$C_k = \sum_{n=1}^{N} X_{k,n} C_{k,n} \tag{2.3}$$

Assume user k's QoS requirement is specified by its transmission rate R_k. Thus, the frequency minimization problem can be formulated as follows:

$$\mathcal{P}_0 : \min \quad f = \sum_{k=1}^{K} \sum_{n=1}^{N} X_{k,n} \tag{2.4}$$

For downlink transmission where the signals are sent by the base station to all users, the objective (2.4) is subject to:

$$\text{Downlink:} \sum_{k=1}^{K} X_{k,n} \leq 1, \ \forall \, n; \tag{2.5a}$$

$$X_{k,n} \in \{0, 1\}, \ \forall \, n, k \tag{2.5b}$$

$$C_k \geq R_k, \forall \, k \tag{2.5c}$$

$$P_{k,n} \geq 0, \ \forall \, n, k \tag{2.5d}$$

$$\sum_{k=1}^{K} \sum_{n=1}^{N} X_{k,n} P_{k,n} \leq P_T \tag{2.5e}$$

where (2.4) is the objective function. The OFDMA constraints (2.5a) indicate that each subcarrier can be used by no more than one user at any time slot to avoid multi-user interference; conditions in (2.5b) restrict $X_{k,n}$ either equal to 1 or 0; inequalities (2.5c) make sure each user's QoS demand is met; inequalities (2.5d) restrict the power from being negative. For the downlink case, the transmission is subject to a total transmission power constraint (2.5e).

For the uplink transmission, the multiple users are transmitting different signals to the base station; hence, each user is subject to an individual constraint. Accordingly, the objective (2.4) is subject to:

$$\text{Uplink:} \sum_{k=1}^{K} X_{k,n} \leq 1, \ \forall \, n; \tag{2.6a}$$

$$X_{k,n} \in \{0, 1\}, \ \forall \, n, k \tag{2.6b}$$

$$C_k \geq R_k, \forall \, k \tag{2.6c}$$

$$P_{k,n} \geq 0, \ \forall \, n, k \tag{2.6d}$$

$$\sum_{n=1}^{N} X_{k,n} P_{k,n} \leq P_k, \ \forall \, k \tag{2.6e}$$

Note that the only difference between uplink constraints (2.6) and downlink constraints (2.5) lies its individual the power constraints for each user in (2.6e).

2.3 Frequency Saving Algorithms

In this section, near optimal algorithms for downlink and uplink OFDMA are investigated, respectively. In the downlink case, the bisection and feasibility test combined algorithm for multi-user frequency adapting optimization (BF-MUFA) is proposed, and the original problem is decomposed into two sub-problems. In the uplink, low complexity greedy algorithms are proposed to obtain both a tight lower bound and a tight upper bound.

First, this section begins with the single user optimization. Followed by the multi-user downlink optimization, and multi-user uplink optimization.

2.3.1 Optimal Solution for Single User System

If the system has only one user, i.e., point-to-point transmission (downlink and uplink optimization are reduced into the same question), then problem $\mathcal{P}_0$ is trivial. Obviously, with the given power, the user rate is a mono-increasing function of the number of subcarriers. Hence, the optimal solution can be easily obtained by the bisection method combined with the traditional single user waterfilling algorithm.

Recall that the traditional single user waterfilling algorithm is casted into a convex optimization problem as follows:

$$\begin{aligned} \max \quad & \sum_{n=1}^{N} B \log_2(1 + P_n \tfrac{|H_n|^2}{\sigma_n^2}) \\ \text{subject to:} \quad & \sum_{n=1}^{N} P_n \leq P_T \\ & P_n > 0 \, \forall \, n \end{aligned} \tag{2.7}$$

To find the optimal power allocation, form the Lagrangian as follows:

$$L(\mathbf{P}) = \sum_{n=1}^{N} B \log_2(1 + P_n \frac{|H_n|^2}{\sigma_n^2}) + \lambda(P_T - \sum_{n=1}^{N} P_n) \tag{2.8}$$

Next differentiate the Lagrangian and set the derivative equal to zero:

$$\frac{\partial L(\mathbf{P})}{\partial P_n} = \frac{B/\ln 2}{1 + P_n \frac{|H_n|^2}{\sigma_n^2}} \frac{|H_n|^2}{\sigma_n^2} - \lambda = 0 \tag{2.9}$$

Hence, solving the above equations with the constraint that $P_n \geq 0$, the power allocation on subcarrier n can be denoted as:

$$P_n = \begin{cases} \frac{B}{\lambda \ln 2} - \frac{1}{\frac{|H_n|^2}{\sigma_n^2}} & \text{if } \frac{B}{\lambda \ln 2} > \frac{1}{\frac{|H_n|^2}{\sigma_n^2}} \\ 0 & \text{otherwise} \end{cases} \tag{2.10}$$

Combining with the total power constraints, let $\sum_{n=1}^{N} P_n = P_T$, i.e.,

$$\sum_{n=1}^{N} \left(\frac{B}{\lambda \ln 2} - \frac{1}{\frac{|H_n|^2}{\sigma_n^2}}\right)^+ = P_T, \tag{2.11}$$

can yield that:

$$\lambda = \frac{NB}{\left(P_T + \sum_{n=1}^{N} \frac{1}{\frac{|H_n|^2}{\sigma_n^2}}\right) \ln 2} \tag{2.12}$$

Plug (2.12) into (2.10), the optimal power allocation scheme on each subcarrier can be obtained.

Note that the objective of the traditional water-filling algorithm is to maximize the user's throughput under the total power constraints. Regarding to the problem $\mathcal{P}_0$, in order to minimize the total occupied subcarriers under the user's rate constraint, the single user frequency adapting algorithm (SUFA) is introduced as follows (Algorithm 2.1). Let $\boldsymbol{e}$ be the channel SNR array with this user's SNR on n-th subcarrier as e_n, other parameters are as defined in problem formulation section. Note that in Step 3, the waterfilling algorithm is described as above in (2.7) – (2.12) which can easily obtain the global optima for single user resource allocation.

Algorithm 2.1 Single user frequency adapting algorithm (SUFA).

Input: P_T, R, $\boldsymbol{e}$;

Output: f, $\boldsymbol{X}$;

Step 1: Initialize $f_{\min} = 1$ and $f_{\max} = N$;

$E \leftarrow$ sort subcarriers according to SNR $\boldsymbol{e}$ in the descending order;

Step 2: $f = \text{int}\big((f_{\min} + f_{\max})/2\big)$;

Step 3: $[C, \boldsymbol{X}] \leftarrow \text{waterfilling}\big(P_T, E(1:f)\big)$;

Step 4: If $C \geq R$, then set $f_{\max} = f$; else set $f_{\min} = f$;

Step 5: If $f_{\min} = f_{\max}$, stop; otherwise $\downarrow$ Step 2;

2.3.2 Downlink OFDMA Frequency Optimization (Multi-User System)

From the former analysis, the bisection method can be used to derive the optimal solution for the single user OFDM system. However, in the multi-user case, the optimization problem $\mathcal{P}_0$ is nontrivial, and to solve this problem optimally needs a brutal forth search. Hence, a low complexity optimization algorithm for multi-user system is important for practical purpose. Inspired by the single user case, the question is brought up: "Can a similar method be used for the multi-user case?".

To answer this question, Lemma 2.1 provides a shed on the relationship between minimum required power and minimum required frequency.

Lemma 2.1. *In a given OFDMA system with K users and N possible subcarriers, the minimum total power required to satisfy all users' QoS requirements is the monodecreasing function of f, where f is the number of subcarriers that are allowed to use.*

Proof. In the single user case, this lemma was proved in the Appendix A of literature [42] mathematically. Also, by discovering the internal logic, this lemma can be proved as follows. Suppose the single-user system is using f number of subcarriers, the total power required to fulfill its rate requirement is P_{min}. Given one more subcarrier s', and assume this new subcarrier s' has better channel gain than any of the existing sub-

carrier s, then the water-filling solution from (2.10) implies that only strong channels will be used, hence this new subcarrier will be used. According to Shannon capacity expression, the power required by s' to achieve the previous capacity gained on s will be reduced. Therefore, when having this new subcarrier in the pool, the minimum total power required will be reduced or at least remain the same.

Similarly, in a multi-user system, it is safe to assume two cases with $f = f_1$ and $f = f_2$, while $f_2 = f_1 + 1$. Denote the total minimum power required when $f = f_1$ and $f = f_2$ as P_{T1} and P_{T2}, respectively. By the contradiction method, suppose Lemma 2.1 is not true, which means $P_{T2} > P_{T1}$. For $f = f_2$, assume all users maintain their subcarrier schedule as when $f = f_1$, except for user k who has one more subcarrier to use. Therefore, to meet all users' QoS, user k's power requirement decreases, while other users' remain the same; hence, $P_{T2} \leq P_{T1}$, which results in a contradiction of this assumption. Above all, Lemma 2.1 is proved. □

Note that **the number of subcarriers f is in one-dimensional space**, and **the total power constraint is also in one-dimensional space.** Supported by Lemma 2.1, the following bisection feasibility test combined method is proposed to solve the optimization problem $\mathcal{P}_0$ (Algorithm 2.2). The BF-MUFA contains mainly an outer loop and an inner loop. The outer loop adjusts the number of subcarriers by the bisection method, and it chooses the best subcarriers from the subcarrier pool (Step 2 and Step 3); the inner loop tests the feasibility of meeting users' QoS with the given power constraint for the chosen subcarrier group of the outer loop by comparing the minimum power required to meet QoS demands with the available total power (Step 4 and Step 5). Let $\boldsymbol{R}$ be the set that contains all users' rate requirements, and f_{opt} be the optimal number of subcarriers.

The aforementioned procedure contains two sub-problems (S1 and S2) which take up most of the computational complexity. Especially, the subproblem S2 is to minimize the total power required with individual user's rate constraint, which is proved

Algorithm 2.2 Bisection and feasibility test combined algorithm for multi-user frequency adapting optimization (BF-MUFA).

Input: P_T, $\boldsymbol{R}$, $\boldsymbol{e}$;

Output: f, $\boldsymbol{X}$;

Step 1: Initialize $f_{\min} = 0$ and $f_{\max} = N$;

Step 2: $f = \mathrm{int}\big((f_{\min} + f_{\max})/2\big)$;

Step 3: Find the best f number of subcarriers E_f, such that if $f \geq f_{\mathrm{opt}}$, $E_f \supseteq E_{\mathrm{opt}}$;

Step 4: $[P_{\min}, \boldsymbol{X}] \leftarrow \min \mathrm{power}(\boldsymbol{R}, E_f)$ according to **S2**;

Step 5: If $P_{\min} \leq P_t$, then set $f_{\max} = f$; else set $f_{\min} = f$;

Step 6: If $f_{\min} = f_{\max}$, stop; otherwise $\downarrow$ Step 2;

to be NP-complete in section 2 of [43]. Consequently, the problem $\mathcal{P}_0$ can be proved as NP-hard.

S1: Find the best f number of subcarriers-set E_f, such that if $f \geq f_{\mathrm{opt}}$, $E_f \supseteq E_{\mathrm{opt}}$, where E_{opt} represents the optimal set of subcarriers.

To meet S1's requirement, an exhaustive search is required. So a suboptimal method is derived. Among all possible N subcarriers, select f number of subcarriers with the highest weight. Weigh each subcarrier s by $\sum_{k=1}^{K} \alpha_{k,s} e_{k,s}$. The parameter $\alpha_{k,s}$ is determined by the possibility that it will be used by user k. In this work, it is assumed $\alpha_{k,s} = R_k/|\boldsymbol{R}|$, where $|\boldsymbol{R}|$ is the norm-1 of the vector $\boldsymbol{R}$.

S2: Total power minimization:

$$P_{min} = \min \sum_{k=1}^{K} \sum_{n=1}^{N} X_{k,n} P_{k,n} \tag{2.13}$$

$$\text{Subject to}: \sum_{k=1}^{K} X_{k,n} \leq 1, \ \forall n; \tag{2.14a}$$

$$X_{k,n} \in \{0,1\}, \ \forall \, n,k \tag{2.14b}$$

$$\sum_{n=1}^{N} X_{k,n} B \log_2(1 + P_{k,n} e_{k,n}) \geq R_k, \ \forall \, k \tag{2.14c}$$

$$P_{k,n} \geq 0, \forall \, n,k \tag{2.14d}$$

Sub-problem S2 is the traditional MA optimization, though it is proved to be NP-complete [43, 44]. Among all the existing algorithms for MA optimization, the dynamic programming based resource allocation (DPRA) [42] is a recent method with low complexity and good performance. Specifically, the DPRA method is shown as Algorithm 2.3:

Algorithm 2.3 The dynamic programming based resource allocation algorithm (DPRA).

Input: $\boldsymbol{R}$, $\boldsymbol{e}$;

Output: $P_{\min}$, $\boldsymbol{X}$;

Step 1: For each subcarrier n, find $e_n^* = \max\limits_{1 \leq k \leq K} e_{k,n}$,

rearrange the channel indexes, such that $e_1^* > e_2^* > ... > e_N^*$.

Step 2: Initialize iteration counter $i = 0$,

let the initial serving channel set of each user k as all subcarriers, i.e.,

$X_k^{(0)} = 1, 2, ..., N$.

Step 3: (N-level of deletion decisions) For $n = 1 : N$

Step 3.1: decide the best user k^* on sorted subcarrier n:

if the total power required to meet all users' rate requirements when n

is allocated to k^* instead of other users can be minimized;

Step 3.2: update the serving subcarriers for other users $k \neq k^*$, i.e.,

$X_k^{(n)} = X_k^{(n-1)}$rule out subcarrier n;

However, the DPRA method is a single loop method, and it cannot be refined simply by repeating it. Inspired by [42] and [45], a new algorithm based on the La-

grangian dual decomposition method is proposed in this chapter, which uses the DPRA's result as the initial solution and achieves better performance with low complexity.

The Lagrangian expression of the total power minimization problem **S2** is as follows:

$$L(\boldsymbol{P}, \boldsymbol{X}, \boldsymbol{\lambda}) =$$
$$\sum_{k=1}^{K}\sum_{n=1}^{N} X_{k,n}P_{k,n} + \sum_{k=1}^{K}\lambda_k\big(R_k - \sum_{n=1}^{N} X_{k,n}B\log_2(1+P_{k,n}e_{k,n})\big) \tag{2.15}$$

$$\text{Subject to}: \sum_{k=1}^{K} X_{k,n} \leq 1,\ \forall n; \tag{2.16a}$$

$$X_{k,n} \in \{0,1\},\ \forall\, n,k \tag{2.16b}$$

$$P_{k,n} \geq 0, \forall\, k,n \tag{2.16c}$$

$$\lambda_k \geq 0\ \forall\, k \tag{2.16d}$$

Then the Lagrangian dual objective function can be denoted as:

$$g(\boldsymbol{\lambda}) = \min_{\boldsymbol{P},\boldsymbol{X}} L(\boldsymbol{P}, \boldsymbol{X}, \boldsymbol{\lambda}) = \sum_{n=1}^{N} g_n(\boldsymbol{\lambda}) + \sum_{k=1}^{K}\lambda_k R_k \tag{2.17}$$

subject to the constraints in (2.16), wherein

$$g_n(\boldsymbol{\lambda}) = \min_{P_{k,n}} \sum_{k=1}^{K} X_{k,n}P_{k,n} - \sum_{k=1}^{K}\lambda_k X_{k,n}B\log_2(1+P_{k,n}e_{k,n}). \tag{2.18}$$

(2.17) is a relaxation of **S2** because:

1. By removing the constraint $\sum_{k=1}^{K} X_{k,n}B\log_2(1+P_{k,n}e_{k,n}) \geq R_k,\ \forall\, k$ relaxes the feasible space of **S2**.

2. $L(\boldsymbol{P}, \boldsymbol{X}, \boldsymbol{\lambda}) < P_{min}$ always holds because in the original space for all k, $\big(R_k - \sum_{k=1}^{K} X_{k,n}B\log_2(1+P_{k,n}e_{k,n}) \leq 0\big)$ and the Lagrange multiplier λ_k is non-negative.

In the OFDMA system, each subcarrier can be used by at most one user. Hence, (2.18) can be further denoted as:

$$g_n(\boldsymbol{\lambda}) = \min_{k,P_{k,n}} \big\{P_{k,n} - \lambda_k B\log_2(1+P_{k,n}e_{k,n})\big\}. \tag{2.19}$$

The subcarrier n is allocated only to user k^* such that:

$$k^* = \arg\min_k \left\{ P_{k,n} - \lambda_k B \log_2(1 + P_{k,n} e_{k,n}) \right\}. \tag{2.20}$$

With fixed λ_k, the problem (2.19) is a convex function of $P_{k,n}$. Thus, let the derivative of (2.19) over $P_{k,n}$ equal to 0, and the optimal power allocation to user k on subcarrier n can be expressed as:

$$P^*_{k,n} = \left(\lambda_k B \log_e 2 - \frac{1}{e_{k,n}}\right)^+. \tag{2.21}$$

Finally, the Lagrangian dual variable λ_k can be obtained from:

$$\sum_{n \in S_k} B \log_2 \left(1 + \left(\lambda_k B \log_e 2 - \frac{1}{e_{k,n}}\right)^+ e_{k,n}\right) = R_k, \tag{2.22}$$

in which S_k represents the set of subcarriers given to user k with $P_{k,n} > 0$. Hence:

$$\lambda_k = 2^{t/(B|S_k|)/(B \ln 2)}, \tag{2.23}$$

$$\text{where } t = R_k - \sum_{n \in S_k} B \log_2 e_{k,n}.$$

To optimally update this dual variable is nontrivial. Because of the discontinuity in the power allocation by (2.19), the existing methods, e.g. the ellipsoid method and subgradient based method, will result in slow convergence or even no convergence. Hence, by observing the above equations' structures, an efficient suboptimal algorithm is provided in Algorithm 2.4.

2.3.3 Uplink OFDMA Frequency Optimization (Multi-User System)

In the uplink OFDMA system, each user has an individual power constraint; hence, the former BF-MUFA with the total power constraint for the feasibility test is not applicable to the uplink case. However, low complexity greedy algorithms are obtained to find the upper bound and lower bound of the minimum number of required subcarriers for the uplink case. The general idea of the greedy algorithm is: rank users according to

Algorithm 2.4 Lagrangian dual decomposition based margin adaptive optimization (LDD-MA)

Input: $\boldsymbol{R}$, $\boldsymbol{e}$;

Output: $P_{\min}$, $\boldsymbol{X}$;

Step 1: Initialization.

Initialize the iteration counter $i = 0$, and preassign subcarriers according to the DPRA algorithm;

Step 2: For $n = 1$ to N, do the following computations

Step 2.1: Let $X_{k,n} = 1$, $\forall k$;

Step 2.2: derive λ_k from (2.23);

then obtain $P_{k,n}^*$ by plugging λ_k into (2.21) $\forall k$;

Step 2.3: Select the best user k^* for subcarrier n:

$$k^* \leftarrow \arg\min_k \left\{ P_{k,n} - \lambda_k B \log_2(1 + P_{k,n} e_{k,n}) \right\};$$

Step 2.4: for $k \neq k^*$, let $X_{k,n} = 0$, $P_{k,n} = 0$, and update λ_k by (2.23).

Step 3: $P_{\min}^{(i)} \leftarrow sum(P_{k_n})$;

Step 4: If $P_{\min}^{(i)} - P_{\min}^{(i-1)} \geq \xi$, then $i = i + 1$, and $\downarrow$ **Step 2**; otherwise, stop;

their QoS requirements [1], and then minimize the number occupied subcarriers for each subscriber using SUFA from the first user to the last one, until all users' QoS demands have been met. To obtain the upper bound, each subcarrier can be used by one user at most; to obtain the lower bound, each subcarrier is allowed to be shared among multiple users. The detail to attain the upper bound is presented in Algorithm 2.5.

Algorithm 2.5 Upper bound for multi-user frequency adapting optimization (UB-MUFA)

Input: $\boldsymbol{P}$, $\boldsymbol{R}$, $\boldsymbol{e}$;

Output: f_{UB}, $\boldsymbol{X}_{UB}$;

Step 1: $\{k^*\} \leftarrow sort(\text{QoS})$;

Step 2: For $k^* = 1$ to K

$X_{k^*} \leftarrow \text{SUFA}(P_{k^*}, R_{k^*}, e_{k^*})$, if $X_{k^*,n} = 1$, rule out subcarrier n; $\forall k \neq k^*$, $\forall n$;

Step 3: $f_{UB} \leftarrow count(X_{k,n} = 1)$;

Step 4: If all users' QoS requirements are satisfied, output f_{UB}, $\boldsymbol{X}_{UB}$;

Note that in this greedy algorithm, whenever multiple users compete for a same subcarrier, this subcarrier is assigned to the user with the lowest rate requirement. More importantly, the selected subcarriers consist a sufficient subcarriers-set E_f for the optimal solution, i.e. $E_f \supseteq E_{\text{opt}}$. The reason is that: if no subcarrier has been ruled out in Step 2, which means all users need distinct subcarriers to minimize the required frequency, then the greedy solution is the optimal solution; however, if some subcarriers are ruled out in Step 2, these subcarriers actually have already been given to the current user which means that they are already included as candidates for the optimal solution.

Similar to the UB-MUFA, a greedy algorithm is proposed as Algorithm 2.6 to obtain the lower bound. LB-MUFA differs from UB-MUFA in the following manner: give all frequency resource to each user, and no subcarrier is ruled out even if multiple

[1] The purpose is to serve the user with low QoS requirements first, in case any demanding user use too much system resource and jeopardies other users.

users occupy the same subcarrier; what is more, multi-user interference is not considered. Owing to the way that subcarriers are chosen for each user, the subcarriers selected from this approach are the necessary subcarriers to meet the users' requirements.

Algorithm 2.6 Lower bound for multi-user frequency adapting (LB-MUFA)

Input: $\boldsymbol{P}$, $\boldsymbol{R}$, $\boldsymbol{e}$;

Output: f_{LB}, $\boldsymbol{X}_{LB}$;

Step 1: For $k = 1$ to K, $\boldsymbol{X}_k \leftarrow \mathrm{SUFA}(P_{k^*}, R_{k^*}, e_{k^*})$;

Step 2: $f_{LB} \leftarrow count(X_{k,n} = 1)$;

Step 4: If all users' QoS requirements are satisfied, output f_{LB}, $\boldsymbol{X}_{LB}$;

Furthermore, for the downlink case, the UB-MUFA and LB-MUFA can also be used to eliminate the searching scope. For simplicity, assume each user has the equal power constraint as P_T/K in the UB-MUFA algorithm to obtain the upper bound; also, assume each user has P_T in the LB-MUFA as the power constraint to obtain a rough lower bound of minimum number of subcarriers. With the lower bound and upper bound being considered, the searching scope of BF-MUFA can be reduced greatly.

2.4 Experimental Results

This section provides simulation results to validate the algorithms proposed in Section III. For an OFDMA system with 20 users and 128 subcarriers, Figure 2.3 compares the novel LDD-MA algorithm and the DPRA algorithm proposed in [42]. After extensive simulations, the observation is whenever the system has more users, higher QoS requirements, or fewer subcarriers, the more improvement of LDD-MA from DPRA can be achieved.

Figures 2.4 and 2.5 are the typical numerical results of downlink OFDMA, which show the number of required subcarriers as a function of SNR and number of users K, respectively. In Figures 2.4 and 2.5, "Random" represents the results obtained by first

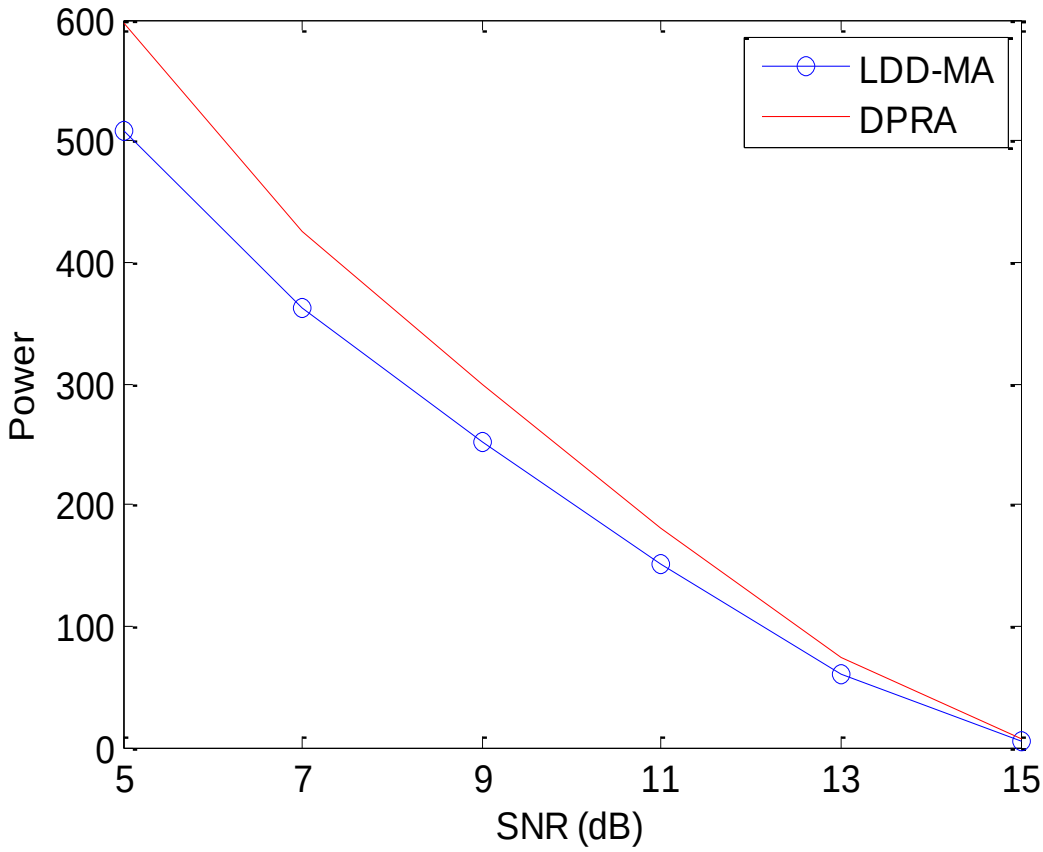

FIGURE 2.3 – Comparison between LDD-MA and DPRA.

predefining each user has equal total available power and then randomly assigning subcarriers to users until their QoS demands are met; "BF-MUFA" is the aforementioned algorithm using the bisection search and feasibility test. Simulation for Figure 2.4 assumes the 128 subcarriers are shared between 20 users, and each user has a random rate requirement. For Figure 2.5, it is assumed that each user has the same rate requirement, and SNR = 10 dB.

For the uplink, extensive simulations have shown that the upper bound and lower bound are extremely close so that the proposed UB-MUFA algorithm is almost always optimal, as is shown by Figures 2.6 and 2.7. Figure 2.6 and 2.7 show the relationship between SNR and the number of required subcarriers, as well as the number of users vs.

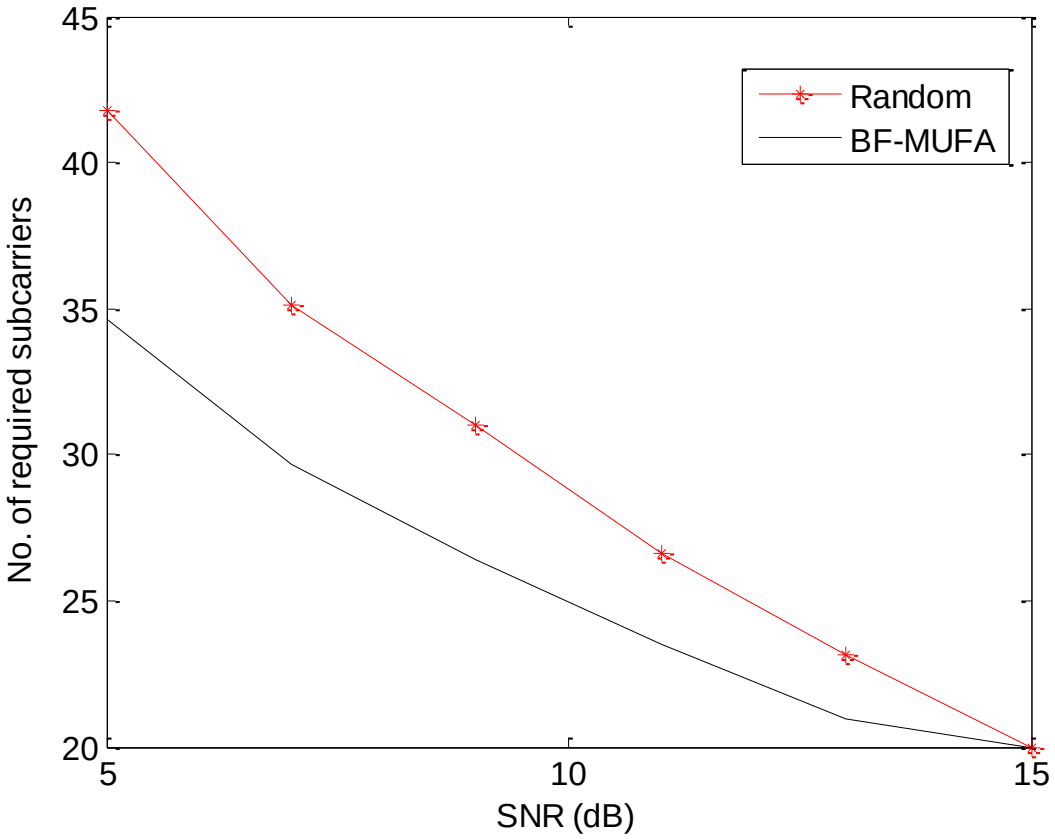

FIGURE 2.4 – SNR vs. No. of required subcarriers in downlink OFDMA.

the number of required subcarriers, respectively. In all cases, the proposed algorithms can significantly save the number of required subcarriers.

2.5 Conclusion

In this chapter, a novel spectrum optimization model is proposed, and the problem formulated for OFDMA-based primary systems to minimize the required number of subcarriers under the individual user's QoS constraint and the power constraint(s). The proposed model is effective to secondary networks when the primary network is not saturated. To solve this NP-hard mixed optimization problem efficiently, the BF-MUFA algorithm for downlink OFDMA and greedy algorithms for the uplink OFDMA system

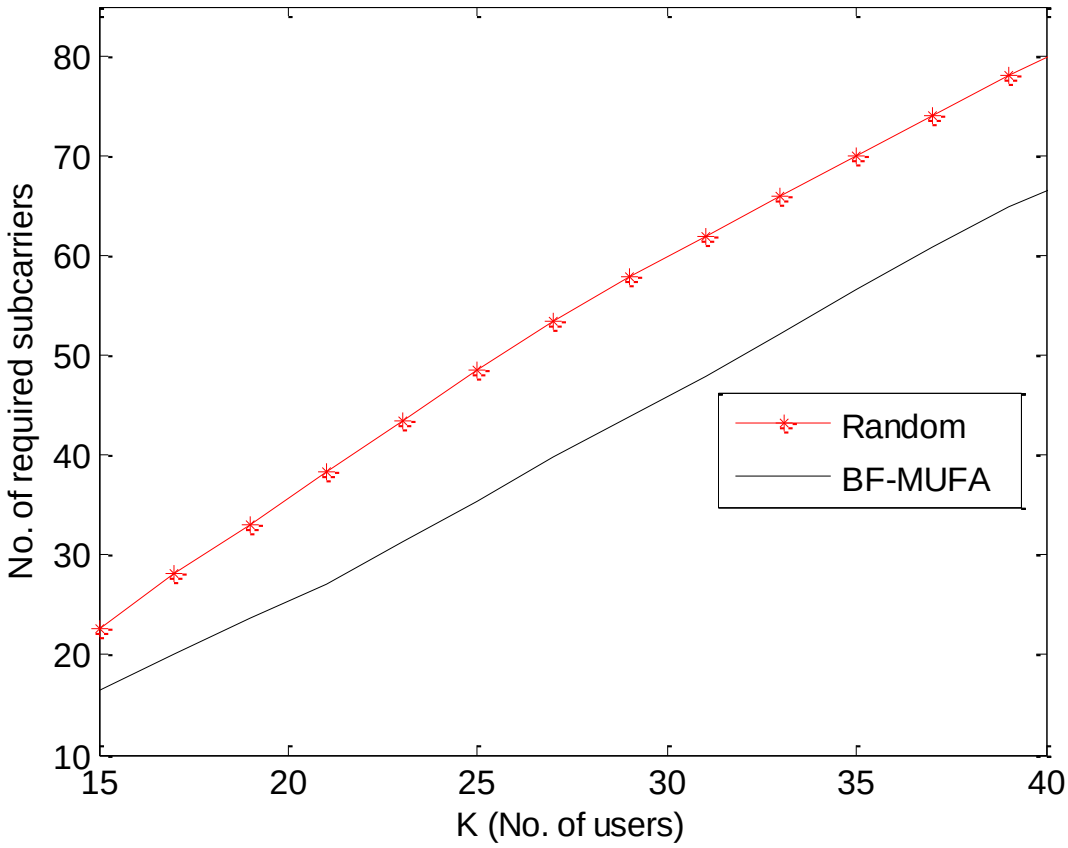

FIGURE 2.5 – K vs. No. of required subcarriers in downlink OFDMA.

are proposed and investigated. Simulation results show that the proposed algorithms can significantly save the number of required subcarriers. To solve the MA subproblem, the LDD-MA algorithm is proposed to greatly refine the existing DPRA algorithm; therefore, the performance of BF-MUFA algorithm for the downlink OFDMA system is guaranteed. The simulation results of UB-MUFA and LB-MUFA for the uplink OFDMA system show the tightness of both bounds. Hence, the UB-MUFA algorithm can be used to obtain near optimal results for the uplink OFDMA system.

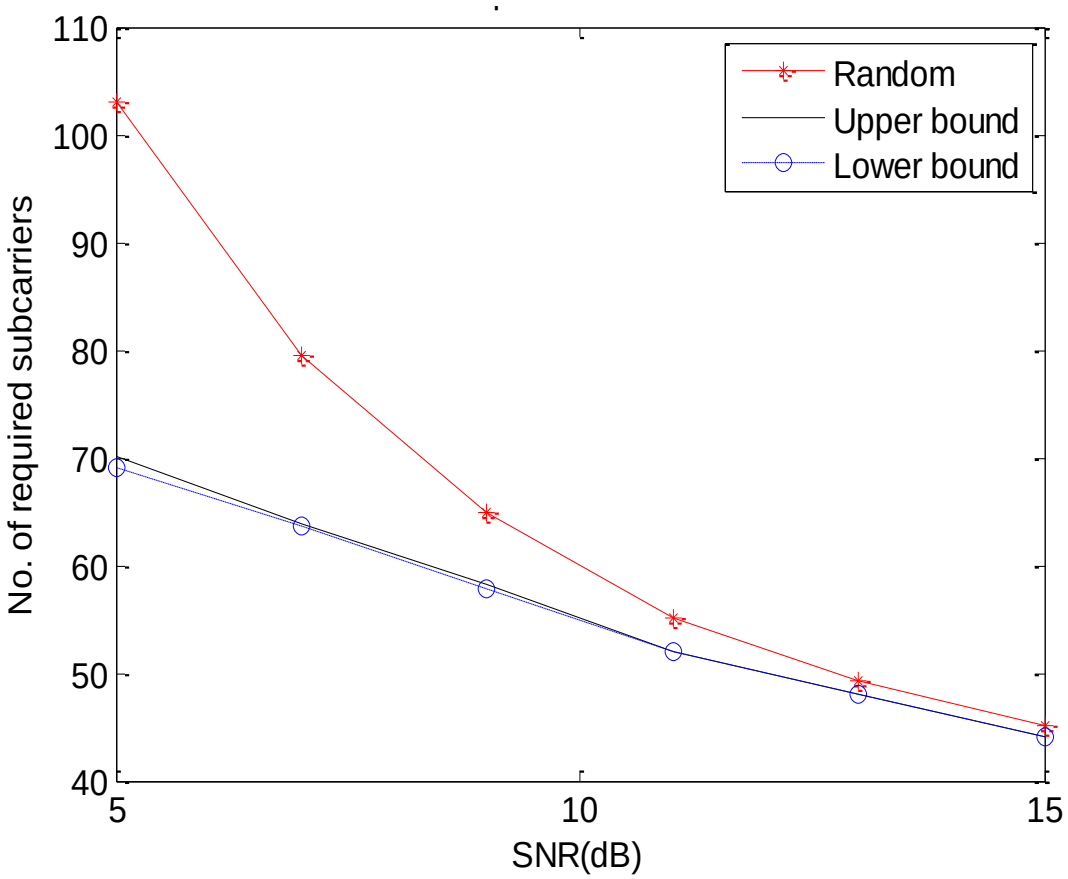

FIGURE 2.6 – SNR vs. No. of required subcarriers in uplink OFDMA.

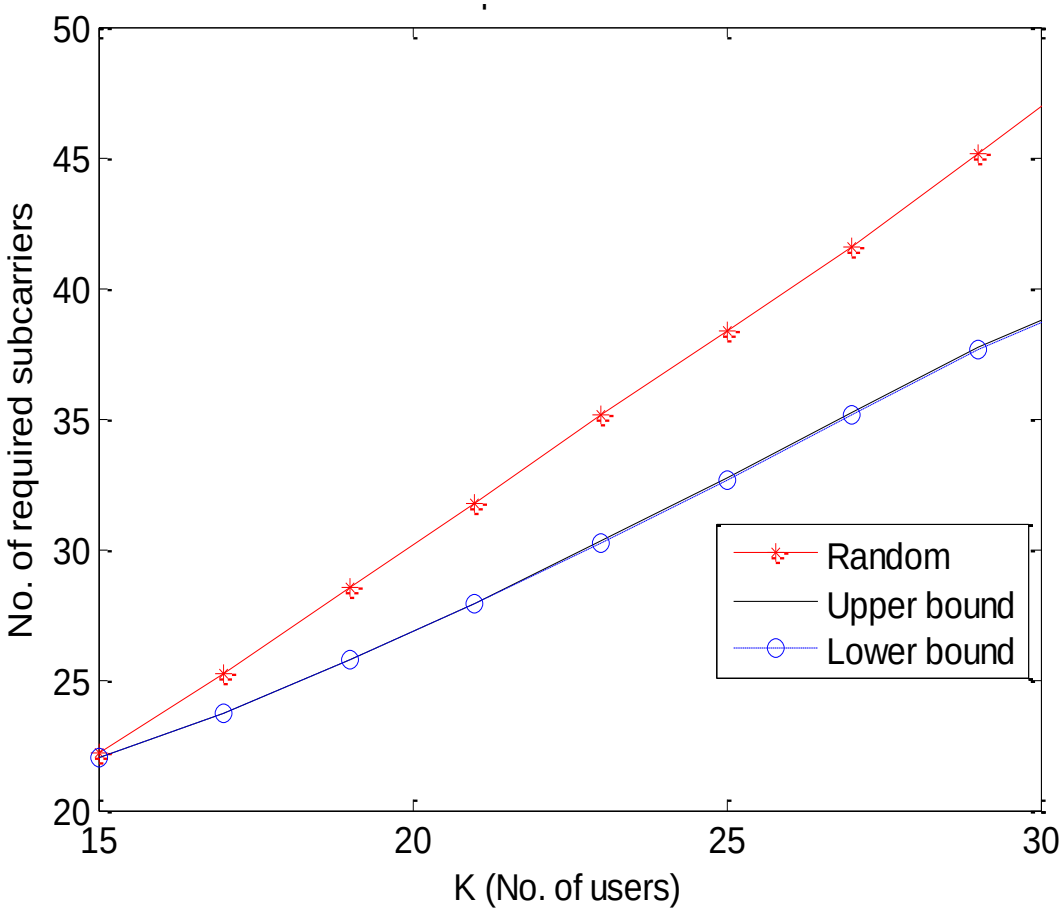

FIGURE 2.7 – K vs. No. of required subcarriers in downlink OFDMA.

CHAPTER 3
DISTRIBUTED OPTIMAL POWER CONTROL FOR UNDERLAY MULTICARRIER COGNITIVE SYSTEMS

In this chapter, the power optimization of the multicarrier secondary network underlying the primary network is investigated. Especially, when secondary network is distributed without a central infrastructure, the power optimization problem becomes more complicate. This chapter studies the interference coupled secondary network under individual secondary user's power constraint and primary user's rate constraint. A multicarrier discrete distributed (MCDD) algorithm based on Gibbs sampler is proposed. Although the problem is nonconcave, MCDD is proved to converge to the global optimal solution. To reduce the computational complexity and convergence time, the near-optimal Gibbs sampler based Lagrangian algorithm (GSLA) is proposed. Simulation results are provided to show the effectiveness of the proposed algorithms.

3.1 Background and Motivation

As is introduced in Chapter 1, cognitive radios can work in three different modes: underlay, overlay, and interweave. The former frequency saving algorithms in Chapter 2 are effective for the interweave mode since the cognitive users only access the spectrum holes in the primary transmission. However, the "underlay" technique allows secondary users' (SUs) to transmit simultaneously with the primary user in a way that SU signals may affect the primary signal within a tolerable limit. Among all these techniques, the underlay technique has great potential to improve the spectrum efficiency with reasonable cost, and it has recently attracted a lot of research attention [15, 32]. However,

one of the main challenges of the underlay approach has not been fully investigated. That is, how to allocate SU power across different cognitive links to maximize the SU transmission rate while guaranteeing the interference to PU signals is under the tolerable threshold? Such problem becomes more complicated when the secondary network operates in a distributed manners. Note that when multiple users with the OFDM modulation access the same subcarrier, it belongs to the multicarrier technique in general. In this chapter, multicarrier and OFDM are used interchangeably.

When multiple users simultaneously transmit on the same frequency, the optimization problem is typically nonconcave and more complicated because of the coupled interference across multiple transmitters. In the case of infrastructure-based networks, where the control processing is performed at a central node such as base station, the optimal power allocation has been studied in [46]. The key idea is to reformulate the weighted throughput maximization problem and then construct a sequence of shrinking polyblocks that gradually approximate the global optimal solution. On the other hand, the problem of power allocation in Ad hoc networks is more challenging due to the distributed and unsynchronized operation among users. In fact, cooperation may exist in Ad hoc based networks to allow information exchange among devices [16]. Furthermore, in multicarrier systems, the optimization becomes even more complex because it creates another degree of freedom over frequencies.

In multicarrier systems, the optimization problem is in general NP-hard. Up to date, many distributed power control strategies have been proposed for interference coupled multicarrier systems. The well-known Iterative Water Filling (IWF) algorithm originally proposed by [47] maximizes the sum rate with individual power constraints, and the Nash equilibrium can be achieved under certain conditions [48]. However, in IWF each user only maximizes its own rate without considering the overall system profit. Later on, [49] proposes distributed algorithms that can achieve global optima when the number of subcarriers goes to infinity; nevertheless, its high computational complexity

is unbearable for practical usage. In [50], global optimal is obtained by the centralized MARL algorithm in interference coupled multicarrier system. Unfortunately, those algorithms cannot be extended to Ad hoc based cognitive networks. For cognitive radio, a price based IWF with sum rate consideration is proposed by [51], which can reach Pareto optimal Nash equilibrium. Recently, [52] also proposes a game theory based algorithm in which each SU updates its power allocation based on the history of its counterpart. However, none of these algorithms can reach global optima distributively.

This chapter will investigate the interference coupled multicarrier cognitive network, where SUs underlay the primary system with limited information exchange. The concept of Gibbs sampler is used to optimize the power allocation in secondary networks. Gibbs sampler is a well studied optimization tool that originates in image processing [53] and gains popularity in statistics. Inspired by [54] which first used the Gibbs sampling method to optimize the single carrier interference coupled system, in this work Gibbs sampler is applied to the multicarrier CR network. To facilitate cooperative optimization, similar to [54], secondary users are allowed to broadcast their channel and power information instantly to the network. The proposed algorithms can distributively and asynchronously update power, based on the system status and estimated power probability distribution. In particular, the main contributions include:

1. The multicarrier discrete distributed algorithm (MCDD) is proposed with the proof of its global optimality;

2. Due to the high complexity of calculating the probability distribution and the long convergence time of MCDD, the suboptimal Gibbs sampler based Lagrangian algorithm (GSLA) is proposed to get a near optimal solution.

3.2 System Model and Problem Formulation

In this work, consider an Ad hoc secondary network consisting of M cognitive links that underlay the primary network. The primary network uses multicarrier transmission technology, such as OFDMA; and at any time during the operation, each subcarrier is assigned to at most one primary user. Hence, the system has no interference among PUs. Therefore, for simplicity, consider one primary user transmits on K subcarriers, and many SUs transmit simultaneously on these subcarriers with PU's minimum transmission rate being guaranteed.

Each cognitive link i consists of the transmitter T_i and the receiver R_i. Define $G_{ij}(k)$ as the channel power gain of the communication link between transmitter T_i and receiver R_j on subcarrier k; n_{ik} is the noise power of link i on subcarrier k which also include the interference from the primary user to link i on subcarrier k. Note that when the receiver R_i decodes its information on link i, all received signals from other links are considered as noise. In addition, denote $I_i(k)$ as the normalized channel power gain, which is defined as the ratio of the channel power gain between T_i and the PU over the channel power gain of the PU on subcarrier k. The system model is denoted as in Figure 3.1.

In this work, assume that all the nodes in the network form a complete graph in which each transmission is reliably received by other nodes. In particular, the secondary receivers exchange their channel information and overhear the primary user's channel gain during the network operation. The channel gain is assumed to be constant compared to the convergence time of the resource allocation algorithms.

Define the power profile of link i as $\boldsymbol{p}_i \triangleq [p_{i1}, \ldots, p_{iK}]^{\mathrm{T}}$, where p_{ik} denotes the transmission power of the transmitter T_i on subcarrier k. Further, define $\boldsymbol{p}_{-i} \triangleq [\boldsymbol{p}_1, \ldots, \boldsymbol{p}_{i-1}, \boldsymbol{p}_{i+1}, \ldots, \boldsymbol{p}_M]$ as the power profile of all other links except link i; and define $\boldsymbol{p} = [\boldsymbol{p}_{-i}, \boldsymbol{p}_i]$ as the power profile of the secondary network. Each transmitter T_i has the maximum transmission power constraint. For the primary user, define the power

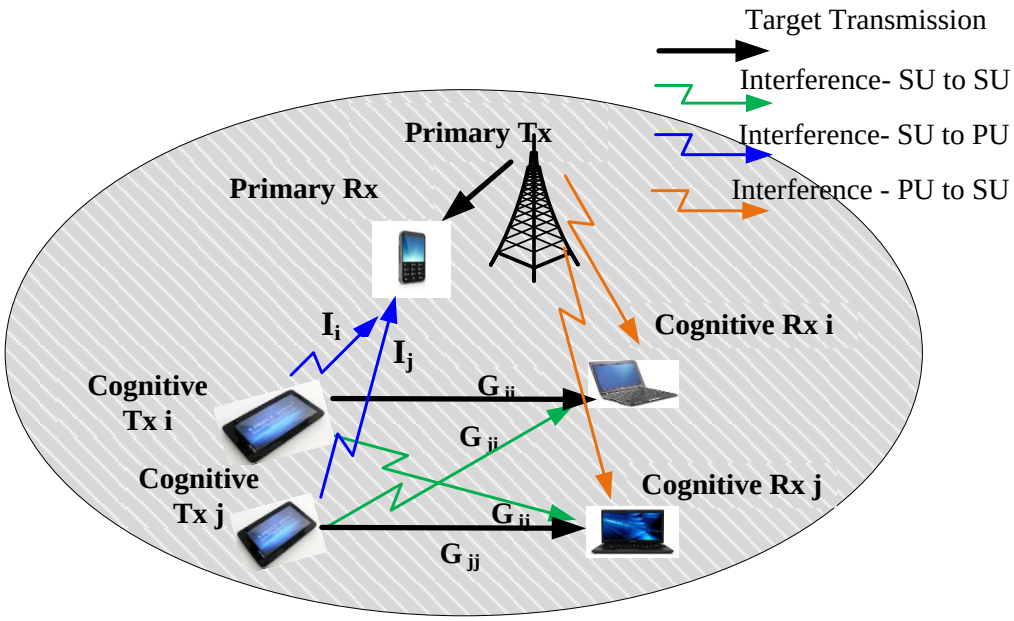

FIGURE 3.1 – Cognitive radio system model.

profile as $\mathbf{s}_i \triangleq [s_1, \ldots, s_K]^{\mathrm{T}}$, assume $\mathbf{s}$ is fixed regardless of the SUs' transmission strategy; and denote n_k as the noise power on subcarrier k. With that said, the signal to interference plus noise ratio (SINR) of link i on subcarrier k is

$$SINR_i(k) = \frac{G_{ii}(k)p_{ik}}{n_{ik} + \sum_{j \neq i} G_{ji}(i)p_{jk}}, \tag{3.1}$$

According to Shannon capacity, the maximum achievable rate on link i over all K subcarriers is given by

$$R_i(\boldsymbol{p}) = \sum_{k=1}^{K} \log\big(1 + SINR_i(k)\big). \tag{3.2}$$

As described in (3.2), the maximum achievable rate of each cognitive link depends on its power allocation, interference from all other links, and interference to the PU. Finding an optimal power allocation is challenging, due to the network dynamics and interference coupling between transmission links. Therefore, the main focus of this

work is to find a power allocation scheme $\boldsymbol{p}^*$ to maximize the sum Shannon capacity over all the cognitive links. Mathematically, the optimization problem is denoted as follows:

$$\mathcal{P}_0: \max_{\boldsymbol{p}} \; R = \sum_{i=1}^{M} R_i(\boldsymbol{p}) \tag{3.3}$$

$$\text{Subject to}: \sum_{k=1}^{K} p_{ik} \leq P_i^{\max}, \forall i \in \{1, 2, \ldots, M\} \tag{3.4a}$$

$$\sum_{k=1}^{K} \log\left(1 + \frac{s_k}{n_k + \sum\limits_{i=1}^{M} I_i(k) p_{ik}}\right) \geq R_{th} \tag{3.4b}$$

Where (3.4a) accounts for the constraint on the maximum transmission power of each cognitive transmitter, and (3.4b) accounts for the constraint on the guarantee of the minimum rate of the primary user. Due to the nonconcave objective function and SINR coupling structure, finding an optimal solution to this optimization problem is challenging even for the simple scenario of single carrier. Notice that in the case of centralized control, Qian et al. [46] proposes an algorithm that maximizes the network weighted throughput. However, for the multicarrier distributed cognitive systems, the global solution is still unsolved.

3.3 Distributed Power Allocation Algorithm

This section will investigate the distributed power allocation schemes to solve the problem ($\mathcal{P}_0$). Particularly, two distributed scheduling algorithms are proposed to allocate the transmission power for each cognitive link. The first scheme is based on the Gibbs sampler to stochastically select the transmission powers for the cognitive links following some distribution. Then the convergence of this proposed method is proved to converge to the optimal solution. Furthermore, to reduce the time complexity and convergence time of the first scheme, the Gibbs sampler based Lagrangian method is proposed in which the searching space is decreased which can still achieve the near optimal performance.

3.3.1 Multicarrier Discrete Distributed Algorithm

Assume a link i on subcarrier k can only take discrete power values p_{ik} from the set $\mathcal{P}_{ik} = \{0, \Delta P_{ik}, 2\Delta P_{ik}, \ldots, P_{ik}^{\max}\}$, where $P_{ik}^{\max}$ varies according to the power allocation in the previous state and the optimization constraints. Let each link i independently update its transmission power; therefore, with probability 1, no two links update at the same time [54].

To update power allocation on link i, the power allocation can be updated either on one random-selected subcarrier at a time or on all subcarriers at the same time. More specifically, the Gibbs sampler method is applied to update the power on different cognitive links asynchronously. The main principle of this method is to select the optimal parameter set by a sequence of transitions that leads to a desired distribution of the variable. In this chapter, the distribution function is adopted from the one proposed in [53, 54].

3.3.1.1 Case 1– Update on One Random Selected Subcarrier Each Time For the case of random-selected subcarrier update method, the power of user i on subcarrier k is updated at random time epochs $\{e_{ik1}, e_{ik2}, \ldots\}$. Particularly, user i iteratively and asynchronously updates each p_{ik} according to a probability distribution where the larger total utility R has a higher probability of being selected. Specifically, at the time epoch e_{ikn}, transmission power is updated to $p_{ik}(e_{ikn})$ according to the following probability distribution

$$\Pr(p_{ik}|p_{-ik}, \boldsymbol{p}_{-i}) = \frac{\exp\big(-\frac{\beta}{R(p_{ik}, p_{-ik}, \boldsymbol{p}_{-i})}\big)}{\sum\limits_{p'_{ik} \in \mathcal{P}_{ik}} \exp\big(-\frac{\beta}{R(p_{ik}, p_{-ik}, \boldsymbol{p}_{-i})}\big)}, \tag{3.5}$$

where β is related to the temperature of the simulated annealing algorithm [53], p_{-ik} is the transmission power of user i on other subcarriers, and $\boldsymbol{p}_{-i}$ represents the transmission power allocation of other links right before time e_{ikn}. Recall that in the set $\mathcal{P}_{ik}$, $P_{ik}^{\max}$ varies according to the optimization constraints, as well as p_{-ik} and $\boldsymbol{p}_{-i}$. In the MCDD algorithm, instead of calculating $P_{ik}^{\max}$ which does not have a closed form, let

$\mathcal{P}'_{ik} = \{0, \Delta P_{ik}, \ldots, P_i^{\max} - \sum_{l \neq k} p_{il}\}$, then use the feasibility test to obtain the feasible set $\mathcal{P}_{ik} \subseteq \mathcal{P}'_{ik}$.

Then the proposed MCDD algorithm is denoted in Algorithm 3.1.

Algorithm 3.1 MCDD Algorithm-Case 1.

For any link i, at time epoch e_{ikn}

Step 1: Keep sensing information broadcast by other links;

Step 2: For all $p_{ik} \in \mathcal{P}'_{ik}$, test if the constraints (3.4a) and (3.4b) can be met:

–if not, $p_{ik} \notin \mathcal{P}_{ik}$;

–if yes, calculate $\Pr(p_{ik}|p_{-ik}, \boldsymbol{p}_{-i})$ according to (3.5)

Step 3: Update power $p_{ik}(e_{ikn})$ according to its distribution function;

Step 4: Broadcast updated power in the cognitive system.

3.3.1.2 Case 2 – Update on All Subcarriers Each Time For the case of updating all subcarriers at the same time, the power profile of user i on all subcarriers is assumed to be updated at time epochs $\{e_{i1}, e_{i2}, \ldots\}$. Let $\boldsymbol{\mathcal{P}}_i$ represent the set of overall power allocation schemes of user i. The power profile of link i is updated to $\boldsymbol{p}_i(e_{in})$ according to the following distribution,

$$\Pr(\boldsymbol{p}_i|\boldsymbol{p}_{-i}) = \frac{\exp\left(-\frac{\beta}{R(\boldsymbol{p}_i,\boldsymbol{p}_{-i})}\right)}{\sum_{\boldsymbol{p}'_i \in \boldsymbol{\mathcal{P}}_i} \exp\left(-\frac{\beta}{R(\boldsymbol{p}'_i,\boldsymbol{p}_{-i})}\right)}, \tag{3.6}$$

Similar to the first case, the closed form for $\boldsymbol{\mathcal{P}}_i$ cannot be obtained. Let user i exhaustively search all the possible power allocation schemes $\boldsymbol{\mathcal{P}}'_i$, then test the feasibility to obtain $\boldsymbol{\mathcal{P}}_i$. The proposed MCDD algorithm is summarized in Algorithm 3.2.

3.3.1.3 Optimality of MCDD In this subsection, the convergence and optimal performance of the MCDD algorithm is proved.

Theorem 3.1. *Starting from any initial power allocation, the MCDD algorithm con-*

Algorithm 3.2 MCDD Algorithm-Case 2.

For any link i, at time epoch e_{in}

Step 1: Keep sensing information broadcast by other links;

Step 2: For all $\boldsymbol{p}_i \in \boldsymbol{\mathcal{P}}'_{ik}$, test if the constraints (3.4a) and (3.4b) can be met:

–if not, $\boldsymbol{p}_i \notin \boldsymbol{\mathcal{P}}_{ik}$;

–if yes, calculate $\Pr(\boldsymbol{p}_i|\boldsymbol{p}_{-i})$ according to (3.6) ;

Step 3: Update power $\boldsymbol{p}_i(e_{in})$ according to its distribution function;

Step 4: Broadcast updated power in the cognitive system.

verges to a stationary distribution

$$\boldsymbol{\Pi} = \frac{\exp\left(-\frac{\beta}{R(\boldsymbol{p})}\right)}{\sum\limits_{\boldsymbol{p}' \in \boldsymbol{\mathcal{P}}} \exp\left(-\frac{\beta}{R(\boldsymbol{p}')}\right)}, \tag{3.7}$$

where $\boldsymbol{\mathcal{P}} = \{\boldsymbol{p}|\boldsymbol{p}_i \in \mathcal{P}_i, \forall i\}$.

Let $\boldsymbol{\mathcal{P}}^*$ *denote the set of optimal solutions to the problem* $(\mathcal{P}_0)$*, when* $\beta \to \infty$

$$\lim_{\beta \to \infty} \boldsymbol{\Pi} = \begin{cases} \frac{1}{|\mathcal{P}^*|}, & \boldsymbol{p} \in \boldsymbol{\mathcal{P}}^* \\ 0, & \textit{otherwise} \end{cases} \tag{3.8}$$

where $|\mathcal{P}^*|$ *denotes the cardinality of* $\mathcal{P}^*$.

Proof. According to the MCDD algorithm, at time t, the power allocation scheme $\boldsymbol{p}(t)$ only depends on the previous power allocation scheme $\boldsymbol{p}(t-1)$. Hence, the power updating of the cognitive system can be modeled as a Markov chain. Note that for any state $\boldsymbol{p}(t)$, all links have equal probability $1/M$ to update to this state since each link can update at any time independently. Also, no two links update at the same time with probability 1.

This theorem is proved in two cases:

Case 1: If link i updates power of one arbitrary subcarrier at a time, then power adjustment on any subcarrier has equal probability $1/K$ to update to $\boldsymbol{p}(t)$. There-

fore, the MCDD can be modeled as a Markov Chain with the transition matrix $\mathbf{\Omega} = [\Omega(\boldsymbol{p}(t), \boldsymbol{p}(t-1)), \forall \boldsymbol{p}(t), \boldsymbol{p}(t-1) \in \mathcal{P}]$, and

$$\mathbf{\Omega} = \frac{1}{M \times K} \sum_{i=1}^{M} \sum_{k=1}^{K} \mathbf{\Omega}_{ik}, \tag{3.9}$$

where $\mathbf{\Omega}_{ik} = [\Omega_{ik}(\boldsymbol{p}(t)|\boldsymbol{p}(t-1), \forall \boldsymbol{p}(t), \boldsymbol{p}(t-1) \in \mathcal{P}]$ with

$$\Omega_{ik}(\boldsymbol{p}(t)|\boldsymbol{p}(t-1)) = \tag{3.10}$$

$$\begin{cases} \Pr\big(p_{ik}(t)|p_{-ik}(t-1), \boldsymbol{p}_{-i}(t-1)\big), & \text{if } p_{-ik}(t-1) = p_{-ik}(t) \\ & \text{and } \boldsymbol{p}_{-i}(t-1) = \boldsymbol{p}_{-i}(t) \\ 0, & \text{otherwise} \end{cases} \tag{3.11}$$

Case 2: If link i updates power on all subcarriers at the same time, then the transition matrix can be modeled as:

$$\mathbf{\Omega} = \frac{1}{M} \sum_{i=1}^{M} \mathbf{\Omega}_{i}, \tag{3.12}$$

where

$$\Omega_{i}(\boldsymbol{p}(t)|\boldsymbol{p}(t-1)) = \begin{cases} \Pr\big(\boldsymbol{p}_{i}(t)|\boldsymbol{p}_{-i}(t-1)\big), & \text{if } \boldsymbol{p}_{-i}(t-1) = \boldsymbol{p}_{-i}(t) \\ 0, & \text{otherwise} \end{cases} \tag{3.13}$$

To prove the convergence behavior of this MCDD algorithm, the Markov Chain denoted in (3.9) and (3.12) should have stationary distributions. Note that updating for certain amount of times, all links will have updated their transmission powers at least once on all subcarriers. Thus, all the elements of the transition matrices (3.9) and (3.12) will be nonzero till certain time epochs. That is the Markov chains are irreducible, positive recursive, and aperiodic. Thus, the Markov chains converge to the stationary distributions. In particular, the stationary distribution is given as:

$$\mathbf{\Pi} = \frac{\exp\big(-\frac{\beta}{R(\boldsymbol{p})}\big)}{\sum\limits_{\boldsymbol{p}' \in \boldsymbol{\mathcal{P}}} \exp\big(-\frac{\beta}{R(\boldsymbol{p}')}\big)}. \tag{3.14}$$

Furthermore,

$$\begin{aligned}
\mathbf{\Pi} &= \frac{\exp\left(-\frac{\beta}{R(\boldsymbol{p})}\right)}{\sum\limits_{\boldsymbol{p}'\in\boldsymbol{\mathcal{P}}^*}\exp\left(-\frac{\beta}{R(\boldsymbol{p}')}\right)+\sum\limits_{\boldsymbol{p}'\in\boldsymbol{P}-\boldsymbol{\mathcal{P}}^*}\exp\left(-\frac{\beta}{R(\boldsymbol{p}')}\right)} \\
&= \frac{\exp\left(-\frac{\beta}{R(\boldsymbol{p})-R(\boldsymbol{p}*)}\right)}{\sum\limits_{\boldsymbol{p}'\in\boldsymbol{\mathcal{P}}^*}1+\sum\limits_{\boldsymbol{p}'\in\boldsymbol{P}-\boldsymbol{\mathcal{P}}^*}\exp\left(-\frac{\beta}{R(\boldsymbol{p}')-R(\boldsymbol{p}*)}\right)} \\
&\overset{\beta\to\infty}{\to} \begin{cases} \frac{1}{|\boldsymbol{P}^*|}, \text{ if } \boldsymbol{p}\in\boldsymbol{\mathcal{P}}^* \\ 0, \text{ otherwise} \end{cases}
\end{aligned} \tag{3.15}$$

Theorem 3.1 is proved. □

Remark 3.1. *The first approach that each link updates power on one subcarrier each time will result in very slow convergence. Intuitively, each link only updates one subcarrier at a time which requires a long time to converge.*

Remark 3.2. *The second approach that each link updates power on all subcarriers at a time converges much faster than the first method. However, to obtain the distribution function needs exhaustive search of the whole space that increases exponentially with the quantization level and the number of subcarriers.*

The performance differences between Algorithm 3.1 and Algorithm 3.2 are:

Performance	MCDD–Case 1	MCDD –Case 2
Convergence Speed	Slow	Fast
Searching Space	Small	Large

In the following sections, a near optimal algorithm is proposed by reducing the searching space of the Algorithm 3.2.

3.3.2 Gibbs Sampler Based Lagrangian Algorithm

In this subsection, in order to reduce the complexity and the convergence time of the MCDD algorithm, a Gibbs sampler based Lagrangian algorithm is proposed which approximates the optimal solution.

In the well-known single user waterfilling algorithm [47], without the constraint (3.4b), each user only maximizes its own utility with the same "waterlevel" for all subcarriers. In the cognitive scenario, if each time only one link i adjusts its power to maximize its individual rate while treating other users' interference as noise; then the Lagrangian function of user i can be written as:

$$\begin{aligned} L_i &= \sum_{k=1}^{K} \log\big(1+\frac{G_{ii}(k)p_{ik}}{\Delta_{ik}^{(1)}}\big) \\ &\quad +\lambda_i\big(P_i^{\max}-\sum_{k=1}^{K}p_{ik}\big)+\eta_i\bigg(\sum_{k=1}^{K}\log\big(1+\frac{s_k}{I_i(k)p_{ik}+\Delta_{ik}^{(2)}}\big)-R_{th}\bigg) \end{aligned} \quad (3.16)$$

where $\Delta_{ik}^{(1)} \triangleq n_{ik}+\sum_{j\neq i} G_{ji}(k)p_{jk}$, $\Delta_{ik}^{(2} \triangleq n_k+\sum_{j\neq i} I_j(k)p_{jk}$, λ_i and η_i are the nonnegative Lagrangian multipliers.

Take the derivative of L_i with respect to p_{ik}, and set it equal to zero, (3.17) is obtained:

$$\frac{G_{ii}(k)\Delta_{ik}^{(1)}}{\Delta_{ik}^{(1)}+G_{ii}(k)p_{ik}}-\lambda_i+\eta_i\big(\frac{-I_i(k)s_k}{(\Delta_{ik}^{(2)}+I_i(k)p_{ik}+s_k)(\Delta_{ik}^{(2)}+I_i(k)p_{ik})}\big)=0. \quad (3.17)$$

Unfortunately, the closed form of p_{ik} is not obtainable from (3.17). Further, the two-dimensional exhaustive search of Lagrangian parameters λ_i and η_i are required to obtain the whole value space of p_{ik}. Note that when condition (3.4a) is active and (3.4b) is inactive, the searching space can be obtained by setting $\eta_i = 0$, so only a one-dimensional search of λ_i is required. Similarly, when condition (3.4b) is active and (3.4a) is inactive, only a one-dimensional search of η_i is required. Hence, let link i use the combination of two one-dimensional searches to obtain its current power space. Specifically, link i first sets $\eta_i = 0$; then applies a one-dimensional exhaustive search on

λ_i and obtains all corresponding values of p_{ik} for each subcarrier as follows:

$$p_{ik} = \max\Big\{\frac{\Delta_{ik}^{(1)}}{\lambda_i} - \frac{\Delta_{ik}^{(1)}}{G_{ii}(k)}, 0\Big\}. \tag{3.18}$$

Then link i sets $\lambda_i = 0$, and obtains all possible values of p_{ik} from (3.23) through the exhaustive search of η_i. Specifically,(3.17) now becomes:

$$\frac{G_{ii}(k)\Delta_{ik}^{(1)}}{\Delta_{ik}^{(1)}+G_{ii}(k)p_{ik}} = \frac{\eta_i I_i(k) s_k}{(\Delta_{ik}^{(2)}+I_i(k)p_{ik}+s_k)(\Delta_{ik}^{(2)}+I_i(k)p_{ik})} \tag{3.19}$$

$$i.e., \tag{3.20}$$

$$\frac{1}{\frac{1}{G_{ii}(k)}+\frac{p_{ik}}{\Delta_{ik}^{(1)}}} = \frac{\eta_i I_i(k) s_k}{{p_{ik}}^2 I_i(k)^2 + p_{ik}\Big(s_k I_i(k) + 2\Delta_{ik}^{(2)} I_i(k)\Big) + {\Delta_{ik}^{(2)}}^2 + s_k \Delta_{ik}^{(2)}} \tag{3.21}$$

Furthermore, it can be denoted as:

$$\begin{aligned} {p_{ik}}^2 I_i(k)^2 + p_{ik}\left(s_k I_i(k) + 2\Delta_{ik}^{(2)} I_i(k) - \frac{\eta_i I_i(k) s_k}{\Delta_{ik}^{(1)}}\right) + \\ {\Delta_{ik}^{(2)}}^2 + s_k \Delta_{ik}^{(2)} - \frac{\eta_i I_i(k) s_k}{G_{ii}(k)} = 0 \end{aligned} \tag{3.22}$$

Let $\Delta_A = I_i(k)^2$, $\Delta_B = \left(s_k I_i(k) + 2\Delta_{ik}^{(2)} I_i(k) - \frac{\eta_i I_i(k) s_k}{\Delta_{ik}^{(1)}}\right)$, and $\Delta_C = {\Delta_{ik}^{(2)}}^2 + s_k \Delta_{ik}^{(2)} - \frac{\eta_i I_i(k) s_k}{G_{ii}(k)}$,

$$p_{ik} = \left(\frac{-\Delta_B \pm \sqrt{{\Delta_B}^2 - 4\Delta_A \Delta_C}}{2\Delta_A}\right)^+. \tag{3.23}$$

Intuitively, from (3.18) the channel with the lower interference has higher power; according to (3.23) the channel with stronger interference to the primary system has lower power.

Different from the MCDD algorithm which searches the whole space of the power allocation scheme, the size of the searching space is greatly reduced by allowing one user to adjust its power on all subcarriers at the same time using two one-dimensional searches according to (3.18) and (3.23). Without loss of generality, let $v_i = 1/\lambda_i$, and assume v_i and η_i of user i take discrete values from $\mathcal{V}_i = \{v_i^{\min}, v_i^{\min} + \Delta v_i, \ldots, v_i^{\max}\}$ and $\mathcal{H}_i = \{\eta_i^{\min}, \eta_i^{\min} + \Delta\eta_i, \ldots, \eta_i^{\max}\}$ respectively; wherein set $v_i^{\max} = \max_k\left(\frac{\Delta_{ik}^{(1)}}{G_{ii}(k)}\right) + P_i^{\max}$, $v_i^{\min} = \min_k\left(\frac{\Delta_{ik}^{(1)}}{G_{ii}(k)}\right)$, $\eta_i^{\max} = \max_k\left(1 + \frac{2P_i^{\max} I_i(k) + 2\Delta_{ik}^{(2)}}{s_k}\right)$, and $\eta_i^{\min} = 0$. Then,

the entire space of $\boldsymbol{p}$ derived from (3.18) and (3.23) belongs to $\hat{\boldsymbol{\mathcal{P}}}_i$ if and only if constraints (3.4a) and (3.4b) can both be met. Note that $\hat{\boldsymbol{\mathcal{P}}}_i$ is the subset of $\boldsymbol{\mathcal{P}}_i$ for the MCDD algorithm. Each user i updates its power $\boldsymbol{p}_i$ iteratively and asynchronously according to the following probability distribution

$$\Pr(\boldsymbol{p}_i|\boldsymbol{p}_{-i}) = \frac{\exp\big(-\frac{\beta}{R(\boldsymbol{p}_i,\boldsymbol{p}_{-i})}\big)}{\sum\limits_{\boldsymbol{p}_i'\in\hat{\boldsymbol{\mathcal{P}}}_i}\exp\big(-\frac{\beta}{R(\boldsymbol{p}_i',\boldsymbol{p}_{-i})}\big)}, \tag{3.24}$$

Pseudo code of the proposed GSLA is summarized as follows.

Algorithm 3.3 GSLA Algorithm.

For any link i, at time epoch e_{in}

Step 1: Keep sensing information broadcast by other links;

Step 2: For all $v_i \in \mathcal{V}_i$, $\eta_i \in \mathcal{H}_i$,

Obtain the corresponding $\boldsymbol{p}_i$ from (3.18) and (3.23);

Test if both (3.4a) and (3.4b) are met:

–if not, $\boldsymbol{p}_i \notin \hat{\boldsymbol{\mathcal{P}}}_{ik}$);

–if yes, calculate $\Pr(\boldsymbol{p}_i|\boldsymbol{p}_{-i})$ according to (3.24);

Step 3: Update power $\boldsymbol{p}_i(e_{in})$ according to its distribution function;

Step 4: Broadcast $\boldsymbol{p}_i(e_{in})$ in the cognitive system.

Theorem 3.2. *The GSLA algorithm converges to a stationary distribution.*

Proof. This can be proved similarly as the proof of Theorem 3.1. □

Note that, the convergence performance of GSLA algorithm can be proved, however it is still a suboptimal algorithm because the reduced searching space may miss the optimal solution.

Remark 3.3. *The GSLA algorithm is preferred when dealing with a large number of subcarriers. This is because its convergence speed is much faster compared to the first*

case of the MCDD algorithm; also the searching space of the second case of MCDD is greatly reduced.

3.4 Simulations

This section will evaluate the proposed algorithms via simulations. In particular, consider a secondary system consisting of five cognitive communication links, i.e., $M = 5$. The PU and SUs are randomly located in a 10 m$\times$10 m area. The channel power gains in the secondary network independently belong to exponential distributions with mean values as $1/d_{i,j}^2$, where $d_{i,j}$ denotes the distance between the SU transmitter i and receiver j; and the channel power gains between SUs and PU are drawn similarly. In addition, set the transmission power for all subcarriers of the primary user as the same and $s_k = 1$ mW. The power noises n_{ik} and n_k are set equal to 1 μW for all users and subcarriers. Although from Theorem 3.1 large β is preferred, this simulation set β as 2000 because very large β could result in numerical problems in calculating the probability distribution.

The first experiment simulates a scenario where five cognitive communication links share two subcarriers with the primary user. Set the primary user's rate threshold as 5 bps and the secondary users' maximum power equal to 1 mW. The throughput of the secondary network using different technique is indicated in Figure 3.2. Note that the MCDD algorithm shown in Figure 3.2 is obtained by allowing a link updating the power over all subcarriers at a time. As expected, all the techniques converge to their stable value after a small number of iterations. In particular, IWF results in the worst performance as the transmitter of each cognitive link selfishly maximizes its own transmission rate. Consequently, it increases the interference to the other links; thus, overall it decreases the sum throughput of the network. On the contrary, the MCDD technique achieves the best performance by adjusting the transmission power based on

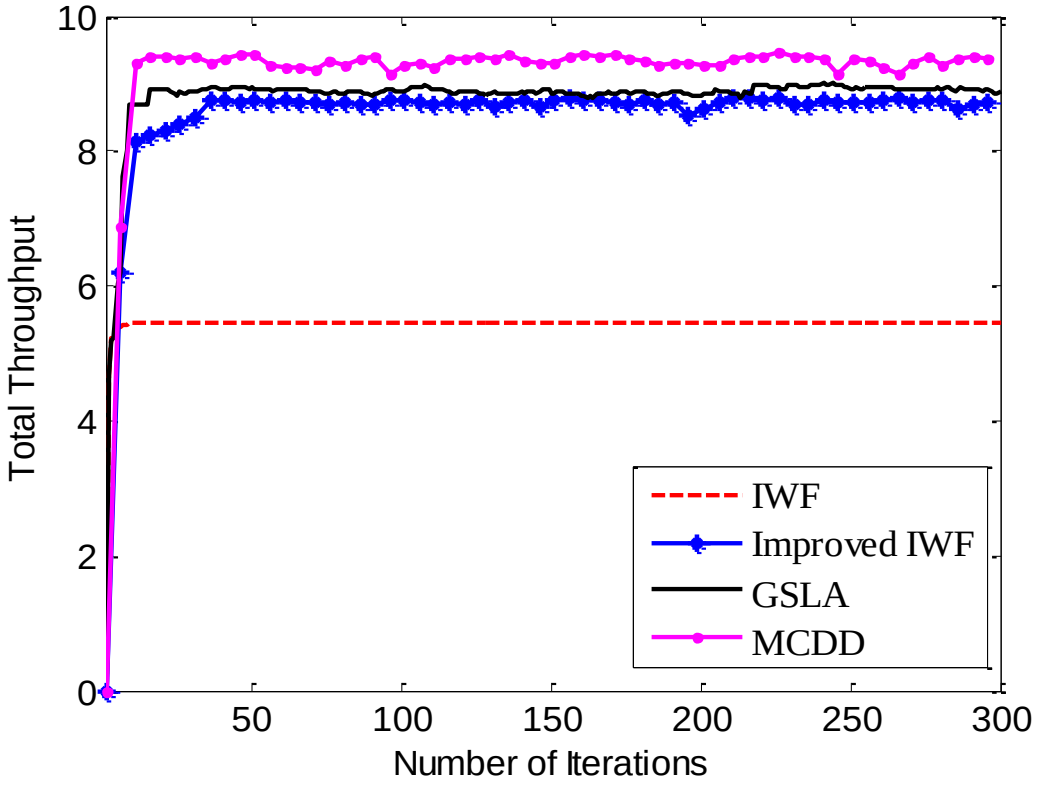

FIGURE 3.2 – Throughput of a 5-link cognitive network with 2 subcariers.

the overall system utility.

The second experiment considers a scenario consisting of five cognitive communication links that share twenty subcarriers with the primary user. The primary user's rate threshold is set to 50 bps . Further, assume each secondary user has a maximum power as 5 mW. Since the MCDD algorithm performs on a very large searching space, which increases exponentially with the number of subcarriers, this simulation focuses only on comparing the performance gain of the GSLA algorithm with that of IWF and the Improved IWF algorithms. Figure 3.3 depicts the sum throughput of the cognitive network using different techniques. As seen, the IWF results in the worst performance. On the other hand, GSLA achieves the best performance. The intuition is that GSLA

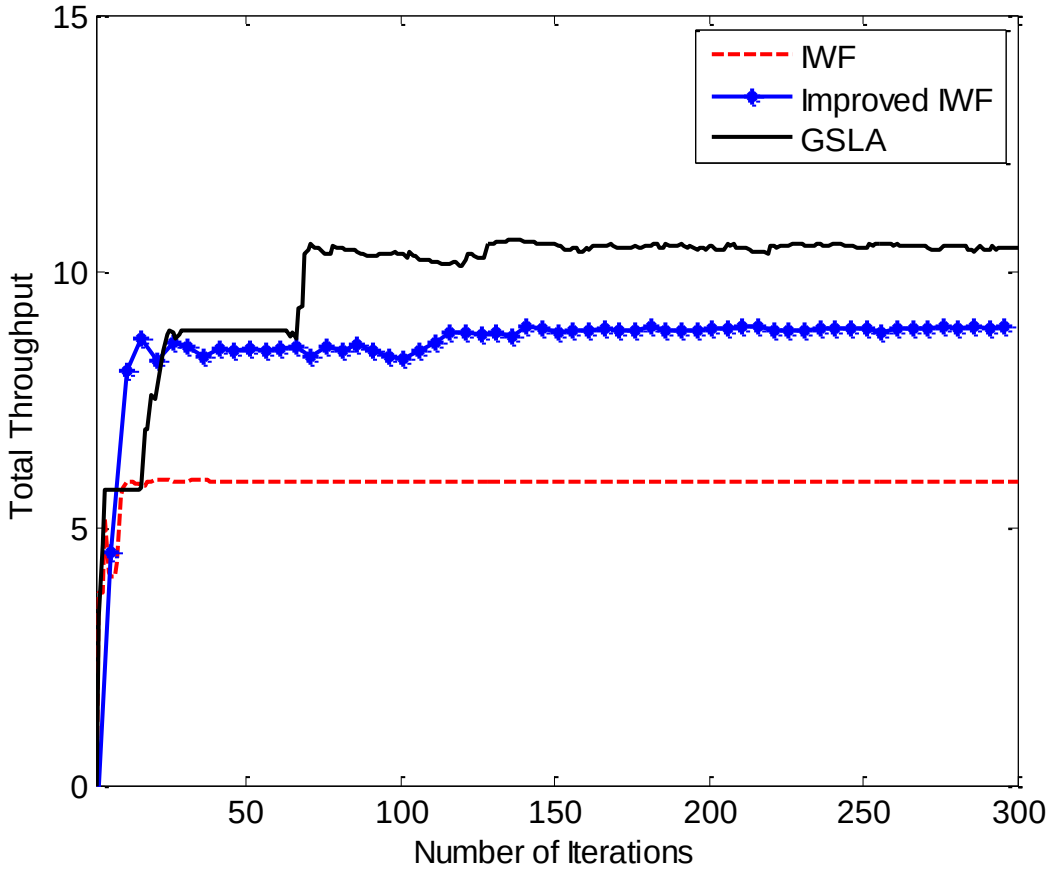

FIGURE 3.3 – Throughput of a 5-link cognitive network with 20 subcariers.

operates on a larger searching space, i.e., combination of two one-dimensional spaces, while the Improved IWF performs only a simple one-dimensional search.

3.5 Conclusion

This chapter investigated the problem of optimal power allocation in an interference coupled multicarrier cognitive network, which subjects to the primary user's rate constraint. In particular, several distributed algorithms were proposed with limited information exchange between the cognitive nodes in order to approximate the optimal solution of the nonconcave objective problem. The proposed MCDD algorithm has

been proven to converge to the global optimal solution. In addition, in order to increase the convergence rate and decrease the complexity of the MCDD algorithm, the GSLA algorithm was proposed by reducing the searching space while still obtaining a high performance. Simulation results were provided to show the performance gains of the proposed schemes.

CHAPTER 4

DPC VERSUS TDMA IN DELAY SENSITIVE COMMUNICATION OVER BROADCAST FADING CHANNELS

In the previous chapters, the underlay mode and the interweave mode of the cognitive radio systems were investigated, where the primary network and the secondary network are using different transmitters. However, as is mentioned in Chapter 1, when multiple coexisting networks are transmitting on the same frequency simultaneously, advanced dirty paper coding (DPC) scheme can be used to precancel the interference for better performance. As mentioned in Chapter 1, the DPC-based systems with multiple distributed antennas will suffer from unbearable amount of information exchange; however, when multiple networks are converged into a hybrid network using the common transmitter, e.g, the hybrid broadcast and unicast system proposed by [23], the side information can be avoided.

Therefore, this chapter will investigate a DPC-based hybrid system that has common transmitter serving different networks. For comparison purpose, the time division multiple access (TDMA) scheme is also investigated. Furthermore, the QoS requirements are considered by using *effective capacity* for a user in fast fading scenario and *outage capacity* for a user in slow fading scenario. Note that the abstract mathematical model will apply for users that working in different networks and in the same network as well. Specifically, the performance of DPC and TDMA schemes are studied over the two-user broadcast channel in low SNR regime and high SNR regime, respectively; in low SNR regime, the *minimum energy per bit* and the *wideband slope region* are the main performance metrics; in high SNR regime, the *high SNR slope* and the *power offset*

are considered as the main metrics.

4.1 Background and Motivation

This chapter focuses on the transmission schemes for multiuser broadcasting (downlink) systems, i.e., the common transmitter sends signals to several different users that belong to the same network or different networks. What is more, it is assumed that the instantaneous channel state information is not available at the transmitter side.

In mutiluser wireless communications, time division multiple access (TDMA) and dirty paper coding (DPC) are two primary multiple access techniques. Specifically, TDMA is an orthogonal spectrum sharing scheme where multiple users transmit on different time slots to avoid multi-user interference. Due to its simplicity in system implementation, TDMA has been widely used in practical wireless systems. DPC is a non-orthogonal spectrum sharing scheme where multiple signals are pre-coded and transmitted on the same frequency at the same time. Despite its added complexity, DPC is becoming an emerging wireless multiple access scheme due to its well known capacity achieving performance in downlink channels [25]. From information theoretic point of view, a number of existing studies on TDMA and DPC can be found in the literature [55–59], where Shannon capacity was used as the performance metric to unveil the fundamental limits of these two multiple access schemes.

It is well known that the classic Shannon capacity is a physical layer metric that cannot capture the upper layer quality of service (QoS) requirements. Particularly, with the increasing communication demand, many wireless services are delay sensitive [60–62]. Along a different line, the delay limited capacity (a.k.a zero-outage capacity) enforces zero delay bound violation probability, which restricts the system to operate pessimistically in fading channels (e.g. the delay limited capacity becomes zero in Rayleigh fading channels). To balance the requirements on delay and transmission rate, effective

capacity was proposed as the maximum constant arrival rate that can be supported by a stochastic service process with a probabilistic delay constraint [63]. While the effective capacity can well capture the delay requirement in fast fading channel, it becomes very small in slow fading channel due to relatively large channel coherent time. For slow fading channel without CSIT, outage capacity defines the maximum data transmission rate that the received data are decoded with certain outage probability. By allowing the system to lose some data in the event of deep slow fading, the received data can be decoded instantly to meet the delay requirement. Therefore, effective capacity and outage capacity are used in this work as the performance metric for fast fading channel and slow fading channel, respectively. For tractability, the delay sensitive multiuser capacity region in both low and high SNR regimes as well as the impact of delay requirements on system performance will be investigated.

For a point-to-point channel, it is well known that the minimum received energy per bit is -1.59 dB, which is achieved as the spectral efficiency (bits/s/Hz) approaches zero. However, in [64] Verdú pointed out the spectral efficiency must be nonzero in practical systems, and he proposed the wideband slope concept to characterize the second order approximation of the spectral efficiency. Thereafter, minimum energy per bit and wideband slope together are often used to characterize the low SNR performance [55, 65–70]. In high SNR regime, Lozano et al. pointed out that high SNR slope only captures the scaling effect but cannot assess the power required for a certain capacity, so they proposed the concept of power offset as a complementary metric [71]. Since then, most studies on high SNR capacity analysis, e.g. [66, 72], adopt both high SNR slope and power offset as the performance metrics.

Existing works on effective capacity in low or high SNR are available in [65–68]. For point-to-point transmission, [65] investigated the performance of SISO system using effective capacity in low SNR regime; [66] investigated the performance of MIMO system using effective capacity in both low SNR regime and high SNR regime. For

multiuser communication system in low SNR regime, [67] and [68] studied the energy efficiency for multiple access channel and interference channel respectively, where each user has an individual power constraint. To the best of our knowledge, effective capacity has not been studied in downlink channels. With regard to outage capacity of multiuser systems, existing works are available for both low SNR case [69] and high SNR case [72]. For users with different performance metrics, recent work [70] investigated a hybrid cellular system in low SNR regime, where effective capacity and outage capacity are used for unicast users and broadcast users, respectively. This chapter will investigate the effective capacity of multiuser downlink systems in both low SNR and high SNR regimes. Moreover, the heterogeneous QoS constraints will also be investigated by extending previous work [70] to general cases in low and high SNR regime.

The original contributions of this work are:

1. In low SNR regime, the closed form minimum energy per bit and the wideband slope for DPC and TDMA are obtained regarding to effective capacity region as well as hybrid capacity region.

2. In low SNR regime, the impact of the QoS requirements on the performance, turning points on wideband slope, performance comparison between DPC and TDMA, optimal cancellation order of the DPC scheme, as well as the near-optimal resource allocation are provided, respectively.

3. In high SNR regime, the high SNR slope and power offset for DPC and TDMA are obtained regarding to sum effective capacity as well as sum hybrid capacity.

4. In high SNR regime, the impact of the QoS requirements, the optimal DPC cancellation order, the impact of the resource sharing factor on sum effective/hybrid capacity are investigated.

5. For Rayleigh fading channel model, further investigations are provided for both

high SNR and low SNR regimes.

The rest of this chapter is organized as follows. Section 4.2 provides system model and capacity region for different transmission scenarios. Then, Section 4.3 focuses on performance analysis of DPC and TDMA in low SNR regime, where the minimum energy per bit and the wideband slope in both fast fading and hybrid fading (fast fading + slow fading) are thoroughly studied. For high SNR regime, rigorous performance analysis of DPC and TDMA is presented in Section 4.4, where the high SNR slope and power offset are used as the performance metric. Finally, a conclusion is drawn in Section 4.5.

4.2 System Model and Problem Formulation

4.2.1 System Model

This work focuses on a two-user broadcast fading channel, given the mathematical model as follows:

$$Y_1 = h_1 X + n_1 \tag{4.1a}$$

$$Y_2 = h_2 X + n_2 \tag{4.1b}$$

where Y_i is the received signal of user i; X represents the transmitted signal; n_i denotes the Gaussian noise of user i; h_i is the channel gain of user i.

In this downlink transmission, the transmitter is subject to a total power constraint P which is shared between two users. Denote the channel noise power spectral density as N_0 and the channel bandwidth as B; as a result, the signal-to-noise ratio can be expressed as SNR $= \frac{P}{N_0 B}$. Assume the transmitter only knows the statistical channel state information and receivers have perfect channel state information. For the TDMA scheme, the information for user 1 and user 2 will be transmitted separately in

different time periods without mutual interference. In contrast, for the DPC scheme, the transmitter sends two users' encoded signal simultaneously in time and frequency.

4.2.2 Effective Capacity and Outage Capacity

This subsection introduces the effective capacity as the performance metric for error free transmission in fast fading channel and outage capacity as the performance metric that bears error in slow fading channel, respectively. The main difference between effective capacity and outage capacity is: effective capacity describes an error free capacity and has a QoS exponent which directly reflects the statistical delay requirement; while the outage capacity bears error, which is preferred for deep slow fading channel.

4.2.2.1 Effective Capacity Effective capacity is a probabilistic delay constrained capacity defined for small scale fading channel by Wu and Negi[63]. According to [63], effective capacity $C(\theta)$ describes as the maximum constant arrival rate that a given service process can support in order to guarantee a statistical delay requirement (i.e. delay violation probability).

Let $D(t)$ represents the delay that a source packet is experiencing at time t, assume the probability of steady state delay $D(\infty)$ exceeding a delay bound D_{max} is required to be no greater than ϵ:

$$Pr_{delay} = Pr\{D(\infty) \geq D_{max}\} \leq \epsilon. \tag{4.2}$$

As is shown in [73] that the delay violation probability is related to the buffer overflow probability as follows:

$$Pr\{D(\infty) \geq D_{max}\} \leq c\sqrt{Pr\{Q(\infty) \geq Q_{max}\}}, \tag{4.3}$$

where c is some positive constant, $Q(\infty)$ is the steady state queue length of the buffer, and $Q_{max} = C(\theta)D_{max}$. Therefore, the statistical delay requirement in (4.2) can be

upper-bounded by a buffer overflow probability requirement:

$$Pr\{Q(\infty) \geq Q_{max}\} \leq \frac{\epsilon^2}{c^2}. \tag{4.4}$$

According to [74], for a queuing system with stationary ergodic arrival and service processes, and under certain conditions, the queue length process $Q(t)$ converges to a random variable $Q(\infty)$ in a distribution that satisfies

$$\begin{aligned} -\lim_{Q_{max}\to\infty} \frac{\log_e\big(\Pr\{Q(\infty) > Q_{max}\}\big)}{Q_{max}} &= \theta, \\ i.e. \lim_{Q_{max}\to\infty} \Pr\{Q(\infty) > Q_{max}\} &= \lim_{Q_{max}\to\infty} e^{-\theta Q_{max}}, \end{aligned} \tag{4.5}$$

where $Q(\infty)$ is the stationary queue length, and θ is the asymptotic decay rate of buffer occupancy. Smaller θ represents looser delay requirement, and larger θ corresponds to a more strict delay requirement. The statistical delay constraint of the traffic will be met if the measured decay rate of the buffer occupancy $\hat{\theta}$ is greater than the required θ.

Let $r(\tau)$ represents the instantaneous service rate of a wireless system at time τ, then $Q(t) = C(\theta)t - \int_0^t r(\tau)\, d\tau$. According to the large deviation principle (LDP):

$$\begin{aligned} \Pr\{Q(\infty) \geq Q_{max}\} &= \lim_{t\to\infty} \Pr\left\{ C(\theta)t - \int_0^\infty r(\tau)\, d\tau \geq Q_{max} \right\} \\ &= \lim_{t\to\infty} \Pr\left\{ \int_0^\infty r(\tau)\, d\tau \geq -C(\theta)t + Q_{max} \right\} \\ &\overset{\text{LDP}}{=\!=} \lim_{t\to\infty} \frac{\mathbb{E}\{e^{-\theta\int_0^\infty r(\tau)d\tau}\}}{e^{-\theta C(\theta)t + \theta Q_{max}}} \\ &= \lim_{t\to\infty} \frac{\mathbb{E}\{e^{-\theta\int_0^\infty r(\tau)d\tau}\}}{e^{-\theta C(\theta)t}} e^{-\theta Q_{max}} \end{aligned} \tag{4.6}$$

Based on (4.5) and (4.6), the effective capacity $C(\theta)$ can be denoted as:

$$C(\theta) = -\lim_{t\to\infty} \frac{1}{\theta t} \log_e \mathbb{E}[e^{-\theta\int_0^t r(\tau)d\tau}]\ \forall\theta \geq 0 \text{ bits/s}, \tag{4.7}$$

wherein $\mathbb{E}\{\cdot\}$ denotes the expectation. Note that, when $\theta = 0$, the effective capacity approaches ergodic capacity $\mathbb{E}\{r\}$ [75].

Furthermore, assume that the users are experiencing block fading with block length T and having different requirements on the asymptotic decay rate of buffer occupancy as θ_1 and θ_2. As a result, the effective capacity normalized with bandwidth B

(also called the spectrum efficiency with regard to effective capacity) for user i can be written as [75]:

$$C_i(\theta_i) = -\frac{1}{\theta_i TB} \log_e \mathbb{E}[e^{-\theta_i T r_i}] \text{ bits/s/Hz.} \tag{4.8}$$

According to (4.8), in slow fading scenario, i.e., when T is large, effective capacity can be very small due to the stringent delay requirement [76]. Therefore, effective capacity if often used for fast fading channels.

4.2.2.2 Outage Capacity As mentioned above, using effective capacity is too conservative for slow fading channel. Hence, in slow fading where the instantaneous SNR is assumed to be constant for a large number of symbols, the widely adopted outage capacity is considered as the figure of merit. The outage capacity defines the maximum data transmission rate that can be decoded with certain outage probability. Specifically, the outage capacity R^{oc} is expressed as:

$$R^{oc} : \Pr\{R(t) \leq R^{oc}\} = q^o, \tag{4.9}$$

where q^o denotes the outage probability. Corresponding to this outage probability, for given SNR at the transmitter side, there is a channel power gain threshold z_{th} as [77]:

$$z_{th} : \Pr\{z \leq z_{th}\} = q^o. \tag{4.10}$$

4.2.3 Effective Capacity Region and Hybrid Capacity Region

The following sections will investigate the *fast fading scenario* where both users are experiencing the fasting fading and using effective capacity, as well as the *hybrid fading scenario* where one user is in fast fading using effective capacity and the other user is in slow fading using outage capacity. Note that the case when both users are using outage capacity has been studied in [69].

In broadcasting channel, total wireless resource (power and time) needs to be shared between two users. Using the DPC scheme, signals for different users are sent

simultaneously, and the total power is shared between two users; while in the TDMA scheme, signals for different users are transmitted with full power on different fraction of time slot. Let α be the percentage of resource scheduled for user 1, and $0 \leq \alpha \leq 1$ (α denotes the power sharing factor for DPC and the time sharing factor for TDMA, respectively). Let z_i denote the instantaneous channel power gain for user i, i.e., $z_i = |h_i|^2$.

4.2.3.1 Effective Capacity Region When both users are experiencing the fast fading channels, for the DPC scheme, consider the interference from user 2 to user 1 is pre-canceled (also called as: user 2 is precanceled from user 1 for simplicity). Accordingly, the normalized effective capacity region for DPC is denoted as (4.11).

$$\bigcup_{\alpha\in[0,1]} \left\{ C_1^{DPC}(\theta_1) \leq -\frac{1}{\theta_1 TB}\log_e \mathbb{E}\left[e^{-\theta_1 TB\log_2(1+\alpha z_1 \mathrm{SNR})}\right], \right.$$
$$\left. C_2^{DPC}(\theta_2) \leq -\frac{1}{\theta_2 TB}\log_e \mathbb{E}\left[e^{-\theta_2 TB\log_2\left(1+\frac{(1-\alpha)z_2\mathrm{SNR}}{1+\alpha z_2 \mathrm{SNR}}\right)}\right] \right\}. \tag{4.11}$$

On the other hand, the normalized effective capacity region for TDMA can be represented as (4.12).

$$\bigcup_{\alpha\in[0,1]} \left\{ C_1^{TDMA}(\theta_1) \leq -\frac{1}{\theta_1 TB}\log_e \mathbb{E}\left[e^{-\theta_1 TB\alpha\log_2(1+z_1 \mathrm{SNR})}\right], \right.$$
$$\left. C_2^{TDMA}(\theta_2) \leq -\frac{1}{\theta_2 TB}\log_e \mathbb{E}\left[e^{-\theta_2 TB(1-\alpha)\log_2(1+z_2 \mathrm{SNR})}\right] \right\}. \tag{4.12}$$

4.2.3.2 Hybrid Capacity Region When user 1 is experiencing fast fading and user 2 is in slow fading, use effective capacity for user 1 and outage capacity for user 2. For user 2, assume the maximum allowable outage probability is q^o, recall from (4.10), its power gain threshold z_{th} is denoted as:

$$z_{th} : \Pr\{z_2 \leq z_{th}\} = q^o. \tag{4.13}$$

For simplicity, use R_2 to denote user 2's outage capacity.

For the DPC scheme, still consider the interference from user 2 to user 1 is pre-

canceled, and the normalized hybrid capacity region can be denoted as:

$$\bigcup_{\alpha\in[0,1]} \Bigg\{ C_1^{DPC}(\theta_1) \leq -\tfrac{1}{\theta_1 TB}\log_e \mathbb{E}\left[e^{-\theta_1 TB\log_2(1+\alpha z_1 \text{SNR})}\right], \\ R_2^{DPC} \leq \log_2\left(1+\tfrac{(1-\alpha)z_{th}\text{SNR}}{1+\alpha z_{th}\text{SNR}}\right) \Bigg\}. \tag{4.14}$$

The normalized TDMA hybrid capacity region can be expressed as:

$$\bigcup_{\alpha\in[0,1]} \Bigg\{ C_1^{TDMA}(\theta_1) \leq -\tfrac{1}{\theta_1 TB}\log_e \mathbb{E}\left[e^{-\theta_1 TB\alpha\log_2(1+z_1 \text{SNR})}\right], \\ R_2^{TDMA} \leq (1-\alpha)\log_2(1+z_{th}\text{SNR}) \Bigg\}. \tag{4.15}$$

4.3 DPC and TDMA Performance Analysis in Low SNR Regime

Either bandwidth $B \to \infty$ or total power $P \to 0$ can result in low SNR; however, different approaches will have different impacts on the performance [78]. The essential difference is that they impact the behavior of propagation delays differently. The case that $P \to 0$ has the much smaller propagation delay than the symbol duration, in contrast $B \to \infty$ results in large propagation delay compared with symbol duration. In this work, the low SNR analysis will focus on the case that $P \to 0$ while the bandwidth is fixed and finite.

This section will first introduce the two performance metrics in low SNR regime, i.e., minimum energy per bit and wideband slope. Next, the performance when both users are using effective capacity will be investigated. Specifically, the closed form minimum energy per bit and wideband slope region are obtained, followed by the performance comparison of TDMA and DPC, turning point on the slope region, optimal cancellation order of the DPC scheme, the low SNR resource allocation scheme, also the results are further investigated in Rayleigh fading channels. Next, similar performance investigations are carried out for hybrid capacity region in low power regime.

4.3.1 Minimum Energy Per Bit and Wideband Slope

Denote C as the general normalized capacity (bits per second per hertz), which can refer to either effective capacity or outage capacity. In the low SNR regime, the capacity C increases linearly with SNR and can be further expanded as:

$$C\left(\mathrm{SNR}\right) = \dot{C}(0)\mathrm{SNR} + \frac{1}{2}\ddot{C}(0)\mathrm{SNR}^2 + o\left(\mathrm{SNR}^2\right), \tag{4.16}$$

where $\dot{C}(0)$ and $\ddot{C}(0)$ respectively represent the first and second order derivative of C regarding to SNR at $\mathrm{SNR} = 0$.

The performance in low power regime is characterized in terms of minimum energy per bit and wideband slope. Specifically, according to [64], the *minimum transmission energy per bit* is defined as follows:

$$\frac{E}{N_0}_{\min} = \lim_{\mathrm{SNR}\to 0} \frac{\mathrm{SNR}}{C\left(\mathrm{SNR}\right)} = \frac{1}{\dot{C}(0)}, \tag{4.17}$$

where $\dot{C}(0)$ represents the first order derivative of $C(\mathrm{SNR})$ regarding to SNR at $\mathrm{SNR} = 0$.

The *wideband slope* S, defined by Verdú in [64], measures the increase of spectrum efficiency per 3dB of signal energy achieved at $\frac{E_i}{N_0}_{\min}$, specifically:

$$\begin{aligned} S &= \lim_{\frac{E_b}{N_0}\downarrow \frac{E_b}{N_0}_{\min}} \frac{C\left(\frac{E_b}{N_0}\right)}{10\log_{10}\frac{E_b}{N_0} - 10\log_{10}\frac{E_b}{N_0}_{\min}} 10\log_{10}2 \\ &= -\frac{2\left(\dot{C}(0)\right)^2}{\ddot{C}(0)}\log_e 2 \text{ (bits/s/Hz/3dB)}, \end{aligned} \tag{4.18}$$

where $\ddot{C}(0)$ represents the second order derivative of $C(\mathrm{SNR})$ at $\mathrm{SNR} = 0$.

As mentioned previously, the minimum energy per bit and wideband slope are defined at low SNR and approximated by derivatives at $\mathrm{SNR} = 0$. Note that, small minimum energy per bit and large wideband slope are always desired in the system design in terms of energy efficiency.

4.3.2 Analysis of Effective Capacity Region in Low Power Regime

This subsection will investigate the performance of DPC and TDMA scheme in low power regime when both users are using effective capacity as performance metrics.

First calculate the minimum transmission energy per bit defined as (4.17) for both schemes, according to their achievable DPC effective capacity region in (4.11) and TDMA effective capacity region in (4.12), respectively.

Theorem 4.1. *For all $k = C_1(\theta_1)/C_2(\theta_2)$, the minimum transmission energy per information bit for the broadcasting channel achieved by both DPC and TDMA are:*

$$\frac{E_1}{N_0}^{DPC}_{\min} = \frac{E_1}{N_0}^{TDMA}_{\min} = \left(\frac{1}{\mathbb{E}\{z_1\}} + \frac{1}{k\mathbb{E}\{z_2\}}\right)\log_e 2, \tag{4.19}$$

$$\frac{E_2}{N_0}^{DPC}_{\min} = \frac{E_2}{N_0}^{TDMA}_{\min} = \left(\frac{k}{\mathbb{E}\{z_1\}} + \frac{1}{\mathbb{E}\{z_2\}}\right)\log_e 2. \tag{4.20}$$

Proof. Enforcing the constraint that $C_1(\theta_1)/C_2(\theta_2) = k$ on the achievable rate region (4.11) or (4.12), the resource sharing parameter α becomes a function of SNR, denoted as $\alpha(\text{SNR})$. The explicit solution for $\alpha(\text{SNR})$ is difficult to obtain. Fortunately, $\alpha(\text{SNR})$ at SNR $= 0$ can be obtained by taking the first order derivative of $C_1(\theta_1)$ and $C_2(\theta_2)$ at SNR $= 0$,

$$\dot{C}_1^{DPC}(\theta_1)|_{\text{SNR}=0} = \dot{C}_1^{TDMA}(\theta_1)|_{\text{SNR}=0} = \frac{\alpha(0)}{\log_e 2}\mathbb{E}\{z_1\}, \tag{4.21}$$

$$\dot{C}_2^{DPC}(\theta_2)|_{\text{SNR}=0} = \dot{C}_2^{TDMA}(\theta_2)|_{\text{SNR}=0} = \frac{1-\alpha(0)}{\log_e 2}\mathbb{E}\{z_2\}. \tag{4.22}$$

Since $\frac{C_1(\theta_1)}{C_2(\theta_2)} = k$ for all SNR, $\frac{\dot{C}_1(\theta_1)}{\dot{C}_2(\theta_2)}|_{\text{SNR}=0} = k$ holds for both DPC and TDMA schemes. Therefore, $\alpha(0)$ can be obtained as:

$$\alpha(0) = \frac{k\mathbb{E}\{z_2\}}{\mathbb{E}\{z_1\} + k\mathbb{E}\{z_2\}}. \tag{4.23}$$

Finally, by substituting (4.21), (4.22) and (4.23) into (4.17), Theorem 4.1 is proved. □

Remark 4.1. *According to Theorem 4.1, both DPC scheme and TDMA scheme have the same minimum energy per bit* $\frac{E_b}{N_0}_{min}$*, which is not affected by users' delay requirements. Furthermore, for user 1, the minimum transmission energy per bit decreases with rate ratio* k $(k = C_1(\theta_1)/C_2(\theta_2)$*; while for user 2, it increases with* k*.*

The minimum transmission energy per bit alone cannot tell which transmission scheme is more advantageous in terms of energy efficiency. Therefore, the slope regions of DPC and TDMA schemes are investigated. According to the wideband slope expression in (4.18) and the achievable effective capacity regions in (4.11)-(4.12), the following theorems are obtained.

Theorem 4.2. *In the DPC mode, for any* $k = C_1^{DPC}(\theta_1)/C_2^{DPC}(\theta_2)$*, the slope region for broadcast transmission in the low-power regime is:*

$$\left\{\left(S_1^{DPC}, S_2^{DPC}\right) : 0 \le S_1^{DPC} \le \frac{2k\left(A+k\right)}{k^2A_1 + kA_2 + A_3}, \right. \\ \left. 0 \le S_2^{DPC} \le \frac{S_1^{DPC}}{k}\right\}, \tag{4.24}$$

where $A = \frac{\mathbb{E}\{z_1\}}{\mathbb{E}\{z_2\}}$; $A_1 = \theta_1 TB\left(\frac{\mathbb{E}\left\{{z_1}^2\right\}}{\mathbb{E}\{z_1\}^2} - 1\right) + \frac{\mathbb{E}\left\{{z_1}^2\right\}}{\mathbb{E}\{z_1\}^2}\log_e 2$; $A_2 = 2\frac{\mathbb{E}\left\{{z_2}^2\right\}}{\mathbb{E}\{z_2\}^2}\log_e 2$; $A_3 = \theta_2 TB\frac{\mathbb{E}\{z_1\}}{\mathbb{E}\{z_2\}}\left(\frac{\mathbb{E}\left\{z_2^2\right\}}{\mathbb{E}\{z_2\}^2} - 1\right) + \frac{\mathbb{E}\{z_1\}}{\mathbb{E}\{z_2\}}\frac{\mathbb{E}\left\{z_2^2\right\}}{\mathbb{E}\{z_2\}^2}\log_e 2$.

Proof. Taking the second order derivative of $C_1^{DPC}(\theta_1)$ and $C_2^{DPC}(\theta_2)$ over SNR at SNR $= 0$, the following results are obtained:

$$\ddot{C}_1^{DPC}(\theta_1)\,|_{\text{SNR}=0} = \frac{2\dot{\alpha}(0)}{\log_e 2}\mathbb{E}\{z_1\} - \frac{\alpha(0)^2}{\log_e 2}\mathbb{E}\left\{{z_1}^2\right\} - \frac{\theta_1 TB\alpha(0)^2}{\left(\log_e 2\right)^2}\text{Var}\{z_1\}, \tag{4.25}$$

$$\ddot{C}_2^{DPC}(\theta_2)\,|_{\text{SNR}=0} = -\frac{2\dot{\alpha}(0)}{\log_e 2}\mathbb{E}\{z_2\} - \frac{1-\alpha(0)^2}{\log_e 2}\mathbb{E}\left\{{z_2}^2\right\} \\ -\frac{\theta_2 TB(1-\alpha(0))^2}{\left(\log_e 2\right)^2}\text{Var}\{z_2\}. \tag{4.26}$$

Similar to the proof of Theorem 4.1, by enforcing the constraint $C_1^{DPC}(\theta_1)/C_2^{DPC}(\theta_2) =$

k, the derivative of $\alpha(\text{SNR})$ at SNR $= 0$ i.e., $\dot{\alpha}^{DPC}(0)$ is denoted in (4.27).

$$\dot{\alpha}^{DPC}(0) = \frac{\alpha(0)^2\mathbb{E}\left\{{z_1}^2\right\}+\frac{\theta_1 TB\alpha(0)^2}{\log_e 2}\text{Var}\{z_1\}-\frac{k\theta_2 TB(1-\alpha(0))^2}{\log_e 2}\text{Var}\{z_2\}-k\left(1-\alpha(0)^2\right)\mathbb{E}\left\{z_2^2\right\}}{2\mathbb{E}\{z_1\}+2k\mathbb{E}\{z_2\}}. \quad (4.27)$$

Theorem 4.2 follows by plugging (4.21)-(4.23), (4.25)-(4.27) into (4.18). □

Theorem 4.3. *In the TDMA mode, for any $k = C_1^{TDMA}(\theta_1)/C_2^{TDMA}(\theta_2)$, the broadcast slope region in the low-power regime is:*

$$\left\{\left(S_1^{TDMA}, S_2^{TDMA}\right): \ 0 \le S_1^{TDMA} \le \frac{2k(A+k)}{k^2A_1+kA_4+A_3}, \ 0 \le S_2^{TDMA} \le \frac{S_1^{TDMA}}{k}\right\}, \quad (4.28)$$

where $A_4 = \left(\frac{\mathbb{E}\left\{z_2^2\right\}}{\mathbb{E}\{z_2\}^2} + \frac{\mathbb{E}\left\{{z_1}^2\right\}}{\mathbb{E}\{z_1\}\mathbb{E}\{z_2\}}\right)\log_e 2$, and other coefficients are the same as in Theorem 4.2.

Proof. Following the same approach as the proof of Theorem 4.2, first take the second order derivative of $C_1^{TDMA}(\theta_1)$ and $C_2^{TDMA}(\theta_2)$ over SNR at SNR $= 0$,

$$\ddot{C}_1^{TDMA}(\theta_1)\,|_{\text{SNR}=0} = \frac{2\dot{\alpha}(0)}{\log_e 2}\mathbb{E}\{z_1\} - \frac{\alpha(0)}{\log_e 2}\mathbb{E}\left\{{z_1}^2\right\} - \frac{\theta_1 TB\alpha(0)^2}{(\log_e 2)^2}\text{Var}\{z_1\}, \quad (4.29)$$

$$\ddot{C}_2^{TDMA}(\theta_2)\,|_{\text{SNR}=0} = -\frac{2\dot{\alpha}(0)}{\log_e 2}\mathbb{E}\{z_2\} - \frac{1-\alpha(0)}{\log_e 2}\mathbb{E}\{{z_2}^2\} - \frac{\theta_2 TB(1-\alpha(0))^2}{(\log_e 2)^2}\text{Var}\{z_2\}. \quad (4.30)$$

Then the derivative of the time sharing parameter $\alpha(\text{SNR})$ at SNR $= 0$ for TDMA scheme can be obtained as (4.31).

$$\dot{\alpha}^{TDMA}(0) = \frac{\alpha(0)\mathbb{E}\left\{{z_1}^2\right\}+\frac{\theta_1 TB\alpha(0)^2}{\log_e 2}\text{Var}\{z_1\}-\frac{k\theta_2 TB(1-\alpha(0))^2}{\log_e 2}\text{Var}\{z_2\}-k(1-\alpha(0))\mathbb{E}\left\{z_2^2\right\}}{2\mathbb{E}\{z_1\}+2k\mathbb{E}\{z_2\}}. \quad (4.31)$$

Plug (4.21)-(4.23) and (4.29)-(4.31) to (4.18), Theorem 4.3 is proved. □

Remark 4.2. *From Theorem 4.2 and 4.3, the slope region for both DPC scheme and TDMA scheme are decreasing when any user's delay requirement becomes more stringent.*

Based on the above theorems, the more detailed performance analysis of DPC and TDMA are provided next.

4.3.2.1 Turning Point on Wideband Slope From Theorem 4.2 and 4.3, each point on the slope region corresponds to a rate ratio k between user 1 and user 2. By investigating the relationship between wideband slope and rate ratio k, the observations are as follows. For DPC scheme:

- *User 1's wideband slope*: when $A_2 \geq AA_1$, user 1's wideband slope is a mono-increasing function of k; otherwise, user 1's wideband slope first increases with k till k_1, and then decreases with k, where $k_1 = \frac{A_3+\sqrt{{A_3}^2-AA_3(A_2-AA_1)}}{(AA_1-A_2)}$.
- *User 2's wideband slope*: when $A_3 \leq AA_2$, user 2's wideband slope is a mono-decreasing function of k; otherwise, user 2's wideband slope first increases with k till k_2, and then decreases with k, where $k_2 = \frac{-AA_1+\sqrt{(AA_1)^2+A_1(A_3-AA_2)}}{A_1}$

Similarly, for TDMA scheme, the above results hold by replacing coefficient A_2 with A_4, which is defined in Theorem 4.3.

4.3.2.2 Bandwidth Expansion Factor In order to compare the performance between DPC and TDMA in low power regime, use the *bandwidth expansion factor* σ, as in [55], which is defined as the ratio of the DPC wideband slope over the TDMA wideband slope. Specifically, for fast fading scenario, according to Theorem 4.2 and 4.3,

$$\begin{aligned}\sigma &= S_1^{DPC}/S_1^{TDMA} = S_2^{DPC}/S_2^{TDMA} \\ &= 1 + \tfrac{k(A_4-A_2)}{k^2A_1+kA_2+A_3}. \end{aligned} \tag{4.32}$$

where σ is the function of rate ratio k.

Consequently, when $\mathbb{E}\{z_1^2\} > \mathbb{E}\{z_1\}\mathbb{E}\{z_2\}$, $\sigma > 1$ holds, i.e., DPC outperforms TMDA.

4.3.2.3 Energy Efficiency in Rayleigh Fading Channel For Rayleigh fading channels, the channel power gain z_i belongs to exponential distribution for user i. Assume that the probability density function of z_i is $f(z_i) = \lambda_i e^{-\lambda_i z_i}$. Let $x = \lambda_2/\lambda_1$, then the DPC slope region and TDMA slope region in fast fading scenario can be further expressed as (4.33) and (4.34), respectively.

$$\left\{ \left(S_1^{DPC}, S_2^{DPC}\right) : \right.$$
$$0 \le S_1^{DPC} \le \frac{2k(x+k)}{k^2(\theta_1 TB + 2\log_e 2) + k4\log_e 2 + x(\theta_2 TB + 2\log_e 2)},$$
$$\left. 0 \le S_2^{DPC} \le \frac{S_1^{DPC}}{k} \right\}. \tag{4.33}$$

$$\left\{ \left(S_1^{TDMA}, S_2^{TDMA}\right) : \right.$$
$$0 \le S_1^{TDMA} \le \frac{2k(x+k)}{k^2(\theta_1 TB + 2\log_e 2) + k(2+2x)\log_e 2 + x(\theta_2 TB + 2\log_e 2)},$$
$$\left. 0 \le S_2^{TDMA} \le \frac{S_1^{TDMA}}{k} \right\}. \tag{4.34}$$

Figure 4.1 compares the envelope of the DPC slope region versus TDMA slope region under Rayleigh fading, where $x = 2$. The cases when both users do not have delay requirement i.e. $\theta_i TB = 0$, and ($\theta_1 TB = 2$, $\theta_2 TB = 1$), as well as ($\theta_1 TB = 4$, $\theta_2 TB = 10$) are investigated and compared. Note that when both users do not have QoS requirements, the obtained slope region is consistent with the results in [55]. The direction of the arrows indicates the increasing direction of the rate ratio k. Moreover, the turning points for user 1 and user 2, if exist, are marked in the figure. From Figure 4.1, the slope region shrinks when user(s) delay requirements becomes more stringent.

The bandwidth expansion factor σ for Rayleigh fading becomes:

$$\sigma = 1 + \frac{2(x-1)\log_e 2}{k^2(\theta_1 TB + 2\log_e 2) + k4\log_e 2 + x(\theta_2 TB + 2\log_e 2)}. \tag{4.35}$$

The performance gap between TDMA and DPC denoted as σ increases when x increas-

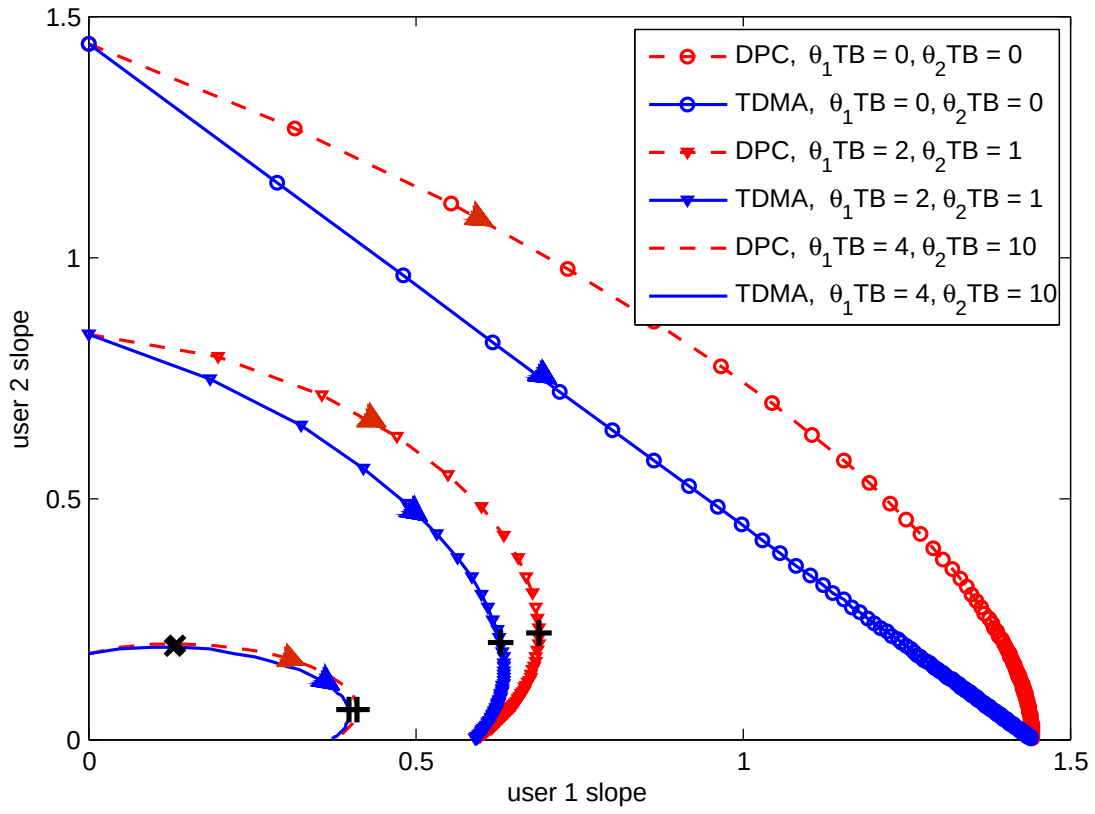

FIGURE 4.1 – Slope region under different delay requirement.

es, and σ decreases when θ_i increases. Figure 4.2 compares the slope region when $x = 2$ and $x = 10$ for ($\theta_1 TB = 2, \theta_2 TB = 1$). Figure 4.3 shows the bandwidth expansion factor for different scenario. From these three figures, when the delay constraints become more stringent and/or x becomes smaller, the bandwidth expansion factor decreases (i.e., the performance gap between DPC and TDMA scheme shrinks).

4.3.2.4 Cancellation Order of The DPC Scheme The above results are obtained based on the fixing DPC cancellation order as pre-canceling user 2 from user 1. However, this may not be optimal. For example, in Rayleigh fading channel, when $x = \lambda_2/\lambda_1 = 0.5$, Figure 4.4 shows the DPC slope region is smaller than TDMA slope region by canceling user 2 from user 1. Hence, it is important to investigate the optimal cancellation order for the DPC scheme.

In this section, the energy efficiencies are compared under different cancellation

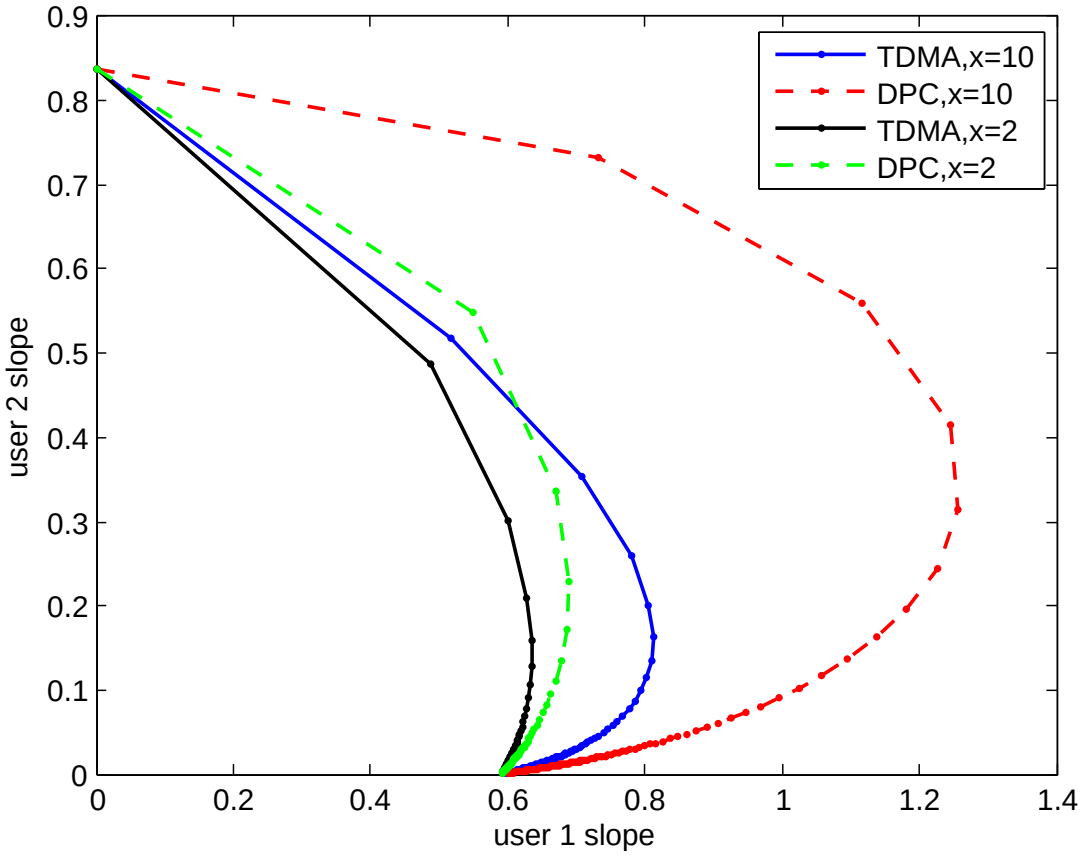

FIGURE 4.2 – Slope region under different channel gain

orders and decide the optimal cancellation order between two users. Note that, when canceling user 1 from user 2, the DPC capacity region for fast fading scenario becomes:

$$\bigcup_{\alpha\in[0,1]} \left\{ C_1^{DPC}(\theta_1) \leq -\frac{1}{\theta_1 TB}\log_e \mathbb{E}\left[e^{-\theta_1 TB\log_2\left(1+\frac{(1-\alpha)z_1\mathrm{SNR}}{1+\alpha z_1\mathrm{SNR}}\right)}\right], \right.$$
$$\left. C_2^{DPC}(\theta_2) \leq -\frac{1}{\theta_2 TB}\log_e \mathbb{E}\left[e^{-\theta_2 TB\log_2(1+\alpha z_2\mathrm{SNR})}\right] \right\}. \tag{4.36}$$

Similarly, the DPC energy efficiency when canceling user 1 from user 2 can be obtained as follows.

Corollary 4.1. For the DPC scheme, for all $k = C_1^{DPC}(\theta_1)/C_2^{DPC}(\theta_2)$, the minimum transmission energy per information bit when canceling user 1 from user 2 is the same as when canceling user 2 from user 1.

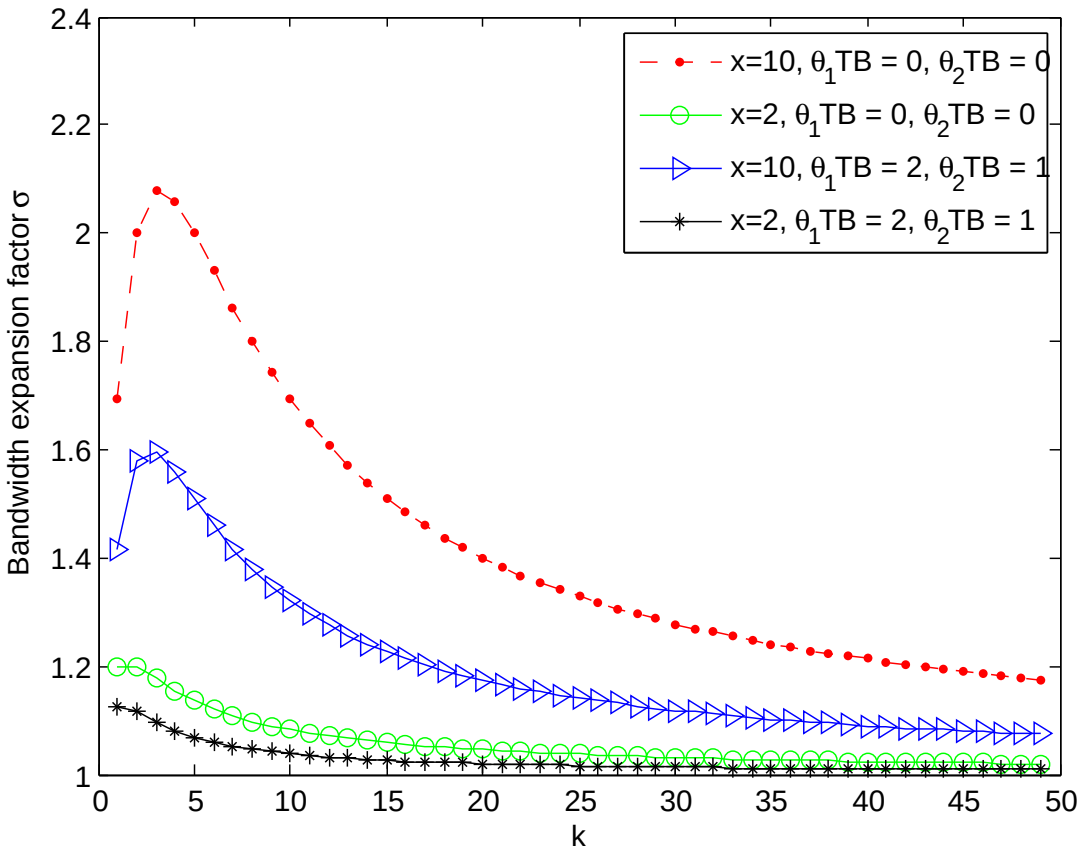

FIGURE 4.3 – DPC slope vs TDMA slope.

Corollary 4.2. For the DPC scheme, when canceling user 1 from user 2, for all $k = C_1^{DPC}(\theta_1)/C_2^{DPC}(\theta_2)$ the slope region becomes:

$$\left\{ \left(S_1^{DPC}, S_2^{DPC}\right) : 0 \leq S_1^{DPC} \leq \frac{2k\,(A+k)}{k^2 A_1 + kA_5 + A_3},\ 0 \leq S_2^{DPC} \leq \frac{S_1^{DPC}}{k} \right\}, \quad (4.37)$$

where $A_5 = 2\frac{\mathbb{E}\{z_1^2\}}{\mathbb{E}\{z_1\}\mathbb{E}\{z_2\}} \log_e 2$ and other coefficients are the same as in Theorem 4.2.

Consequently, the *bandwidth expansion factor* now becomes $\hat{\sigma} = 1 + \frac{k(A_4 - A_5)}{k^2 A_1 + kA_2 + A_3}$.

According to Corollary 4.1 and 4.2, Lemma 4.1 is obtained.

Lemma 4.1. *When broadcasting channel information is only known at the receiver side, for effective capacity region in the low power regime, the optimal DPC cancellation order is to precancel the interference from user 2 to user 1 when* $\frac{\mathbb{E}\{z_1^2\}}{\mathbb{E}\{z_1\}} \geq \frac{\mathbb{E}\{z_2^2\}}{\mathbb{E}\{z_2\}}$*, otherwise*

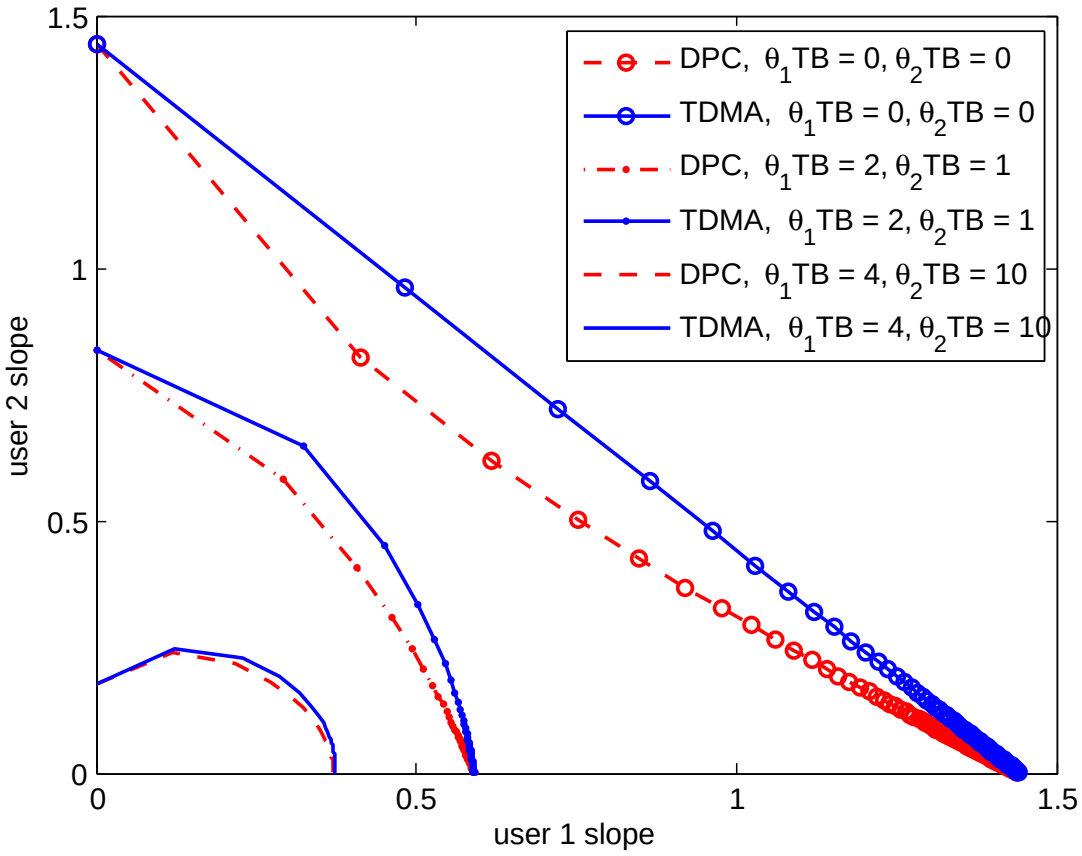

FIGURE 4.4 – Slope region with non-optimal DPC cancellation order

precancel user 1 from user 2. Moreover, using this optimal cancellation order, the DPC scheme always outperforms the TDMA scheme.

4.3.2.5 Near Optimal Resource Allocation in Low Power Regime This section will investigate the resource sharing principle in order to achieve the rate region for the DPC scheme and the TDMA scheme. Specifically, this section aims to obtain the resource sharing factor α such that $\frac{C_1(\theta_1)}{C_2(\theta_2)}|_\alpha = k$, where k is the expected rate ratio which can be any positive value, and $C_i(\theta_i)$ denotes the effective capacity of user i with QoS exponent θ_i. The closed form of resource sharing factor α can not be obtained in an analytical form. Hence, in the low power regime, use its first order approximation as follows:

$$\alpha(\mathrm{SNR}) \approx \alpha(0) + \dot{\alpha}(0)\mathrm{SNR}. \tag{4.38}$$

Recall that, $\alpha(0)$ and $\dot{\alpha}(0)$ are derived for DPC and TDMA as the intermediate results in (4.23), (4.27) and (4.31), respectively. Specifically, given the channel statistics and the QoS exponents, the approximated $\alpha(\mathrm{SNR})$ can be obtained. Note that, here the DPC scheme cancels user 2 from user 1.

In order to show the accuracy of the approximation of α, substitute the approximated α into the achievable effective capacity region in (4.11) and (4.12) for DPC and TDMA, respectively. Accordingly, the rate ratio $\hat{k} = C_1(\theta_1)/C_2(\theta_2)$ is obtained. For example, in the Rayleigh fading scenario, where $\mathbb{E}\{z_1\} = 1$, $\mathbb{E}\{z_1\} = 0.5$, and $\mathrm{SNR} = -10$dB, the rate ratio $\hat{k}$ obtained by using the approximated resource sharing factors is shown in Figure 4.5. From Figure 4.5, the resource sharing factor is approximated by (4.38) with high precision, especially when the delay constraints are loose.

4.3.3 Analysis of Hybrid Capacity Region in Low Power Regime

This subsection will investigate the performance of DPC and TDMA when one user is using effective capacity and the other user is using outage capacity as the performance metrics. Similar as the previous subsection, the minimum transmission energy per bit and slope region are obtained for both DPC and TDMA according to their achievable hybrid rate region in (4.14) and (4.15).

Looking into the DPC effective capacity region in (4.11) (or (4.12) for TDMA) in fast fading scenario, when user 2's channel power gain z_2 (random variable) is replaced with a constant threshold z_{th} for slow fading outage capacity, the effective capacity region becomes (4.14) (or (4.15) for TDMA) as the hybrid capacity region. Similarly, the results obtained for slow fading channels can be transformed to the hybrid fading scenario.

The minimum energy per bit for both schemes in hybrid fading scenario are

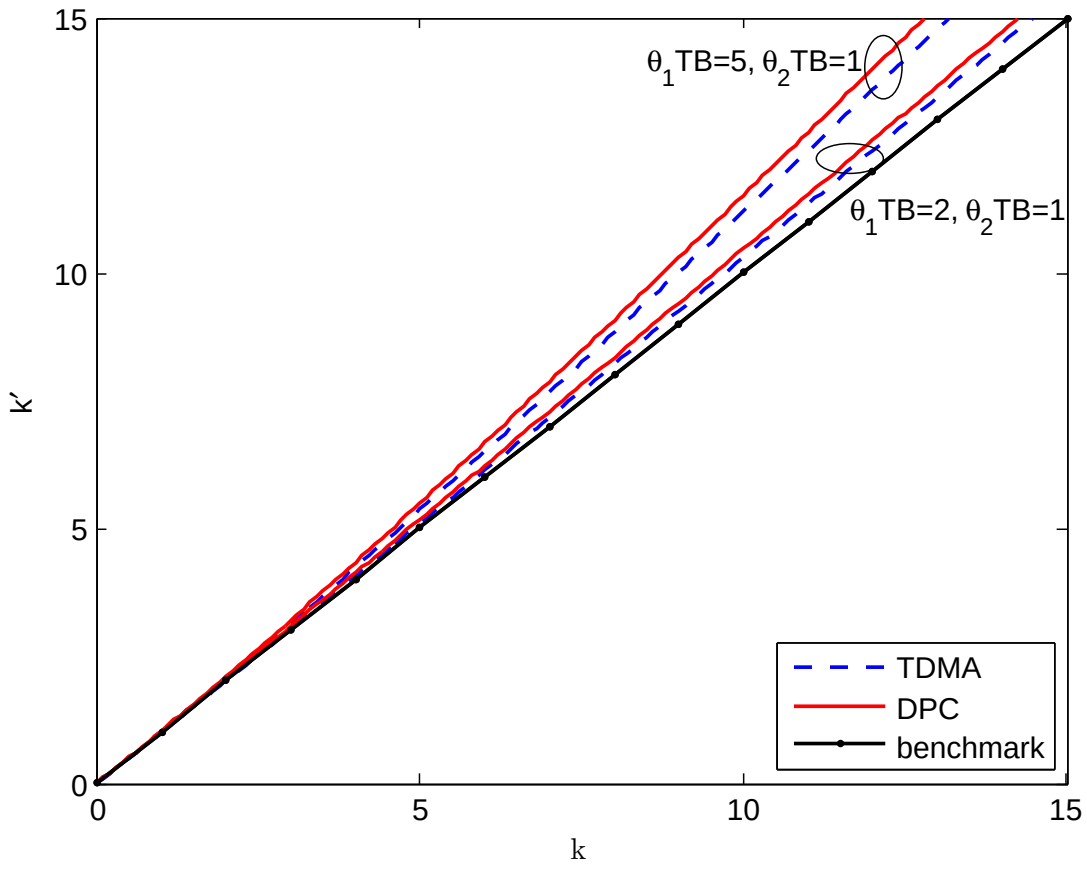

FIGURE 4.5 – Achieved rate ratio k' vs expected rate ratio k

shown in Corollary 4.3.

Corollary 4.3. Suppose the rate pair $(C_1(\theta_1), R_2)$ on the boundary of the achievable hybrid rate region (4.14) (4.15) satisfies $C_1(\theta_1)/R_2 = k$. Then, the minimum transmission energy per bit achieved by both TDMA and DPC are:

$$\frac{E_1}{N_0}^{TDMA}_{\min} = \frac{E_1}{N_0}^{DPC}_{\min} = \left(\frac{1}{kz_{th}} + \frac{1}{\mathbb{E}\{z_1\}}\right)\log_e 2, \tag{4.39}$$

$$\frac{E_2}{N_0}^{TDMA}_{\min} = \frac{E_2}{N_0}^{DPC}_{\min} = \left(\frac{1}{z_{th}} + \frac{k}{\mathbb{E}\{z_1\}}\right)\log_e 2. \tag{4.40}$$

Note that, though the results for hybrid fading can be derived from the fast fading scenario, the main difference is that for user 2, instead of considering the effective capacity with QoS exponent θ_2, outage capacity is used with outage probability as the QoS metric.

Remark 4.3. *According to Corollary 4.3, both TDMA scheme and DPC scheme have the same minimum energy per bit* $\frac{E_b}{N_0}_{min}$*. The minimum energy per bit is not affected by the user 1's delay requirement* θ_1*; however, it decreases with the user 2's outage probability* q^o*. Furthermore, for user 1, the minimum transmission energy per bit decreases with* k*, i.e. the rate ratio* $C_1(\theta_1)/R_2$*; while for user 2, it increases with* k*.*

The slope region of DPC and TDMA are shown in Corollary 4.4 and Corollary 4.5, respectively.

Corollary 4.4. In DPC mode, for any $C_1^{DPC}(\theta_1)/R_2^{DPC} = k$, the slope region in low-power regime for hybrid fading scenario becomes:

$$\left\{ \left(S_1^{DPC}, S_2^{DPC}\right) : 0 \le S_1^{DPC} \le \frac{2k\left(A'+k\right)}{k^2 A_1' + kA_2' + A_3'},\ 0 \le S_2^{DPC} \le \frac{S_1^{DPC}}{k} \right\}, \quad (4.41)$$

where $A' = \frac{\mathbb{E}\{z_1\}}{z_{th}}$, $A_1{}' = \theta_1 TB\left(\frac{\mathbb{E}\{{z_1}^2\}}{\mathbb{E}\{z_1\}^2} - 1\right) + \frac{\mathbb{E}\{{z_1}^2\}}{\mathbb{E}\{z_1\}^2}\log_e 2$, $A_2{}' = 2\log_e 2$, $A_3{}' = \frac{\mathbb{E}\{z_1\}}{z_{th}}\log_e 2$.

Corollary 4.5. In TDMA, for any $C_1^{TDMA}(\theta_1)/R_2^{TDMA} = k$, slope region in the low-power regime for hybrid fading scenario is:

$$\left\{ \left(S_1^{TDMA}, S_2^{TDMA}\right) : 0 \le S_1^{TDMA} \le \frac{2k\left(A'+k\right)}{k^2 A_1' + kA_4' + A_3'},\ 0 \le S_2^{TDMA} \le \frac{S_1^{TDMA}}{k} \right\} \quad (4.42)$$

where $A_4' = \left(1 + \frac{\mathbb{E}\{{z_1}^2\}}{z_{th}\mathbb{E}\{z_1\}}\right)\log_e 2$, and other coefficients are the same as in Corollary 4.4.

These results are consistent with the previous work in [70]. Furthermore, for hybrid fading scenario the observations are as follows.

4.3.3.1 Bandwidth Expansion Factor For hybrid fading scenario, according to Corollary 4.4 and Corollary 4.5, the *bandwidth expansion factor* becomes σ',

$$\sigma' = 1 + \frac{k\left(\frac{\mathbb{E}\{{z_1}^2\}}{z_{th}\mathbb{E}\{z_1\}} - 1\right)\log_e 2}{k^2 A_1' + kA_2' + A_3'}. \quad (4.43)$$

Hence, if $\mathbb{E}\{z_1^2\} > \mathbb{E}\{z_1\} z_{th}$, DPC always outperforms TDMA.

4.3.3.2 Cancellation Order of DPC Scheme The above results for DPC is obtained by fixing the cancellation order as canceling user 2 from user 1. However, when the cancellation order becomes canceling user 1 from user 2, the DPC capacity region for hybrid fading scenario becomes:

$$\bigcup_{\alpha\in[0,1]}\left\{C_1^{DPC}(\theta_1)\le -\tfrac{1}{\theta_1 TB}\log_e\mathbb{E}\left[e^{-\theta_1 TB\log_2\left(1+\frac{(1-\alpha)z_1\mathrm{SNR}}{1+\alpha z_1\mathrm{SNR}}\right)}\right],\right.$$
$$\left. R_2^{DPC}\le\log_2(1+\alpha z_{th}\mathrm{SNR})\right\}. \tag{4.44}$$

For all $k=C_1^{DPC}(\theta_1)/R_2^{DPC}$, the minimum energy per bit when canceling user 1 from user 2 is the same canceling user 2 from user 1, while the DPC slope region becomes:

$$\left\{\left(S_1^{DPC},S_2^{DPC}\right):0\le S_1^{DPC}\le\frac{2k\left(A'+k\right)}{k^2A_1'+kA_5'+A_3'},\ 0\le S_2^{DPC}\le\frac{S_1^{DPC}}{k}\right\}, \tag{4.45}$$

where $A_5'=2\frac{\mathbb{E}\left\{z_1^2\right\}}{\mathbb{E}\{z_1\}z_{th}}\log_e 2$, and other coefficients are the same as in Corollary 4.4. Consequently, the *bandwidth expansion factor* now becomes $\hat{\sigma}'=1+\frac{k(A_4'-A_5')}{k^2A_1'+kA_2'+A_3'}$.

Accordingly, Lemma 4.2 is obtained regarding to the optimal DPC cancellation order.

Lemma 4.2. *When broadcasting channel information is only known at the receiver side, for hybrid capacity region in the low power regime, the optimal DPC cancellation order is to precancel the interference from user 2 to user 1 when* $\mathbb{E}\{z_1^2\}\ge\mathbb{E}\{z_1\}z_{th}$*, and vice versa. Moreover, using this optimal cancellation order, the DPC scheme always outperforms the TDMA scheme.*

4.3.3.3 Turning Point on Wideband Slope For hybrid fading, in DPC mode, assume the optimal cancellation order is canceling user 2 from user 1, i.e., $\mathbb{E}\{z_1^2\}\ge\mathbb{E}\{z_1\}z_{th}$. When $A_2'>A'A_1'$, the user 1's wideband slope is a mono-increasing function of k; otherwise, it first increases with rate ratio k till a certain threshold k_0 and then decreases with k. Specifically, $k_0=\frac{A_3'+\sqrt{{A_3'}^2-A'A_3'\left(A_2'-A'A_1'\right)}}{\left(A'A_1'-A_2'\right)}$, where all the coefficients are defined in Corollary 4.4; while in TDMA mode, coefficient A_2' is replaced by A_4',

defined in Corollary 4.5. The user 2's wideband slope is always a mono-decreasing function of k.

4.3.3.4 Energy Efficiency in Hybrid Rayleigh Fading This subsection will investigate the scenario when user 1 is in fast Rayleigh fading and user 2 is in slow Rayleigh fading. Assume the probability density function of channel power gain z_i is $f(z_i) = \lambda_i e^{-\lambda_i z_i}$. Furthermore, the channel threshold for user 2 defined in (4.13) becomes $z_{th} = -\frac{\log_e(1-q^o)}{\lambda_2}$. Let $x = \lambda_2/\lambda_1$, consequently, the slope region for DPC and TDMA can be denoted as (4.46) and (4.47), respectively.

$$\left\{ \left(S_1^{DPC}, S_2^{DPC}\right) : 0 \le S_1^{DPC} \le \frac{2k(-\frac{1}{\log_e(1-q^o)}x+k)}{k^2(\theta_1 TB+2\log_e 2)+k2\log_e 2-x\frac{1}{\log_e(1-q^o)}\log_e 2}, \right.$$
$$\left. 0 \le S_2^{DPC} \le \frac{S_1^{DPC}}{k} \right\}, \tag{4.46}$$

$$\left\{ \left(S_1^{TDMA}, S_2^{TDMA}\right) : 0 \le S_1^{DPC} \le \frac{2k(-\frac{1}{\log_e(1-q^o)}x+k)}{k^2(\theta_1 TB+2\log_e 2)-k\frac{x}{\log_2(1-q^o)}2\log_e 2-x\frac{1}{\log_e(1-q^o)}\log_e 2}, \right.$$
$$\left. 0 \le S_2^{TDMA} \le \frac{S_1^{TDMA}}{k} \right\}. \tag{4.47}$$

When $x = 1$, the slope region is shown in Figure 4.6 for user 1 and user 2 with different QoS requirements. For DPC scheme, wideband slope region becomes smaller when user 1's delay requirement becomes tight or when user 2's outage probability requirement q^o becomes loose; when using TDMA scheme, it is only proved that wideband slope region become smaller as user 1's delay requirement becomes tight. Note that here the trend of the wideband slope for user 2 may seems not reasonable; however, the energy efficiency is determined by not only slope region but also minimum energy per bit which decreases with user 2's outage probability q^o.

4.4 DPC and TDMA Performance Analysis in High SNR Regime

This section will investigate the performance of DPC scheme and TDMA scheme in high SNR regime. Different from the previous sections where the capacity region is investigated, the sum capacity is considered as many other existing works [57, 58]. First

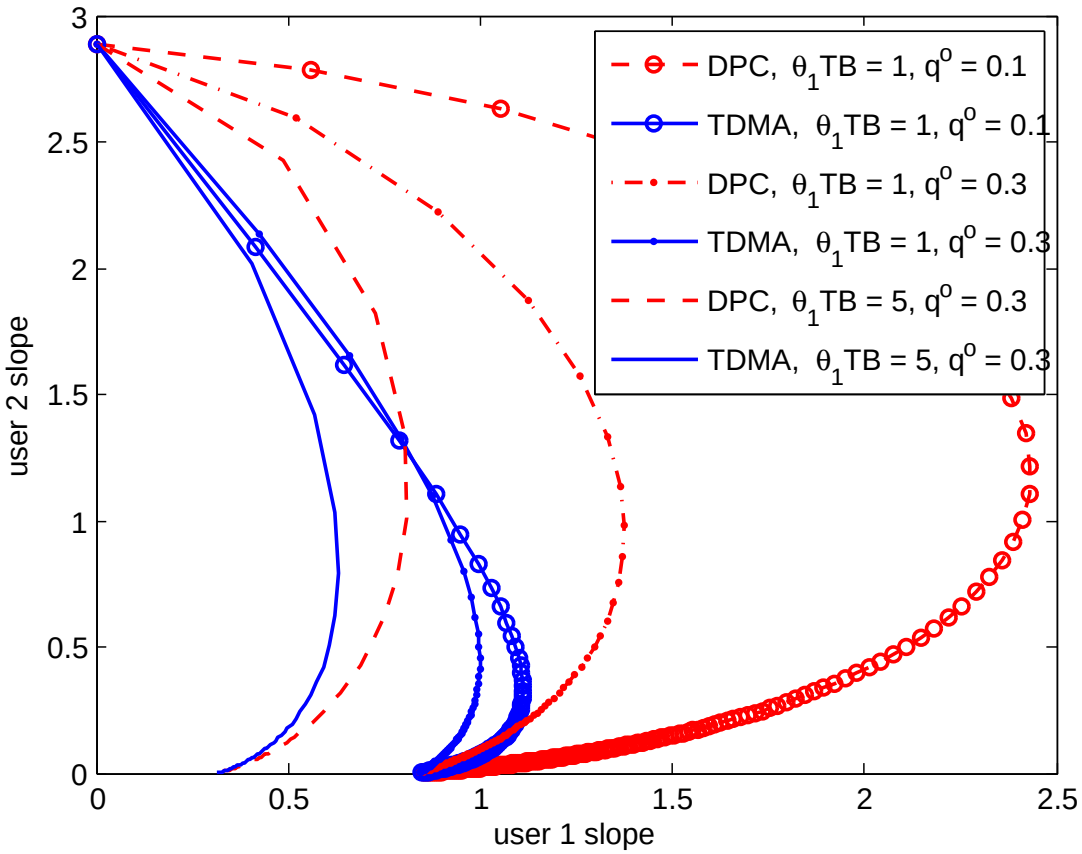

FIGURE 4.6 – Slope region in hybrid Rayleigh fading

of all, for fast fading scenario, where both users are using effective capacity metrics, given power sharing factor α, the sum effective capacity using DPC scheme can be written as (4.48):

$$C_{sum}^{DPC} = -\frac{1}{\theta_1 TB}\log_e \mathbb{E}\left[e^{-\theta_1 TB\log_2(1+\alpha z_1 \mathrm{SNR})}\right] - \frac{1}{\theta_2 TB}\log_e \mathbb{E}\left[e^{-\theta_2 TB\log_2\left[1+\frac{(1-\alpha)z_2\mathrm{SNR}}{1+\alpha z_2 \mathrm{SNR}}\right]}\right]. \quad (4.48)$$

Given time sharing factor α, the sum effective capacity using TDMA scheme can be expressed as (4.49):

$$C_{sum}^{TDMA} = -\frac{1}{\theta_1 TB}\log_e \mathbb{E}\left[e^{-\theta_1 TB\alpha\log_2(1+z_1 \mathrm{SNR})}\right] - \frac{1}{\theta_2 TB}\log_e \mathbb{E}\left[e^{-\theta_2 TB(1-\alpha)\log_2(1+z_2 \mathrm{SNR})}\right]. \quad (4.49)$$

Also, the hybrid fading scenario will be studied, where user 1 is in fast fading using

effective capacity and user 2 is in slow fading using outage capacity. Given power sharing factor α, the sum hybrid capacity in DPC mode can be written as (4.50):

$$C_{sum}^{DPC} = -\frac{1}{\theta_1 TB}\log_e \mathbb{E}\left[e^{-\theta_1 TB\log_2(1+\alpha z_1 \mathrm{SNR})}\right] + \log_2\left(1+\frac{(1-\alpha)z_{th}\mathrm{SNR}}{1+\alpha z_{th}\mathrm{SNR}}\right). \quad (4.50)$$

Given time sharing factor α, the sum hybrid capacity using TDMA can be written as (4.51):

$$C_{sum}^{TDMA} = -\frac{1}{\theta_1 TB}\log_e \mathbb{E}\left[e^{-\theta_1 TB\alpha\log_2(1+z_1 \mathrm{SNR})}\right] + (1-\alpha)\log_2\left(1+z_{th}\mathrm{SNR}\right). \quad (4.51)$$

4.4.1 High SNR Slope and Power Offset

To quantify the impact of the QoS constraints on the performance in high SNR regime, high SNR slope S_∞ and power offset L_∞ are investigated. Denote C as the general normalized capacity. According to [79], S_∞ denotes the high SNR slope with unit as bits/s/Hz/3dB, and it is defined as:

$$S_\infty = \lim_{\mathrm{SNR}\to\infty} \frac{C(\mathrm{SNR})}{\log_2 \mathrm{SNR}} \text{ (bits/s/Hz/3dB)}. \quad (4.52)$$

L_∞ is the power offset with respect to a reference channel having the same high SNR slope (in 3 dB units) [71], specifically it is defined as:

$$L_\infty = \lim_{\mathrm{SNR}\to\infty}\left(\log_2 \mathrm{SNR} - \frac{C(\mathrm{SNR})}{S_\infty}\right). \quad (4.53)$$

Note that $C(\mathrm{SNR})$ represents the sum effective/hybrid capacity in this section.

With the definitions of high SNR slope and power offset, the sum capacity in high SNR regime can be approximated as:

$$C(\mathrm{SNR}) = \mathrm{S}_\infty(\log_2 \mathrm{SNR} - \mathrm{L}_\infty) + \mathrm{o}(1) \text{ (bits/s/Hz)}. \quad (4.54)$$

4.4.2 High SNR Slope and Power Offset for Sum Effective Capacity and Sum Hybrid Capacity

This subsection will obtain the S_∞ and L_∞ for DPC and TDMA scheme in fast fading and hybrid fading scenarios, respectively. As mentioned before, the performance of sum effective capacity for fast fading scenario and sum hybrid capacity in hybrid fading scenario will be studied.

For DPC scheme, its high SNR performance is denoted in Theorem 4.4.

Theorem 4.4. *Using DPC scheme, for given power sharing factor α ($0 < \alpha < 1$), if $0 < \mathbb{E}[z_1^{-\theta_1 TB \log_2 e}] < \infty$, both fast fading and hybrid fading scenario have the same high SNR slope and power offset as follows:*

$$S_\infty^{DPC} = 1, \tag{4.55}$$

$$L_\infty^{DPC} = \frac{1}{\theta_1 TB} \log_e \mathbb{E}[z_1^{-\theta_1 TB log_2 e}]. \tag{4.56}$$

Proof. In fast fading scenario, according to the sum effective capacity denoted in (4.48), and the definition of high SNR slope in (4.52), S_∞^{DPC} can be calculated in (4.57). Next, L_∞^{DPC} can be obtained in (4.58) according to its definition in (4.53).

$$\begin{aligned}
S_\infty^{DPC} &= \lim_{\mathrm{SNR}\to\infty} \frac{C_{sum}^{DPC}}{\log_2 \mathrm{SNR}} \\
&= \lim_{\mathrm{SNR}\to\infty} \frac{-\frac{1}{\theta_1 TB}\log_e \mathbb{E}\left[e^{-\theta_1 TB \log_2(1+\alpha z_1 \mathrm{SNR})}\right] - \frac{1}{\theta_2 TB}\log_e \mathbb{E}\left[e^{-\theta_2 TB \log_2\left[1+\frac{(1-\alpha)z_2 \mathrm{SNR}}{1+\alpha z_2 \mathrm{SNR}}\right]}\right]}{\log_2 \mathrm{SNR}} \\
&= \lim_{\mathrm{SNR}\to\infty} \frac{-\frac{1}{\theta_1 TB} \log_e \mathbb{E}[e^{-\theta_1 TB \log_2(\alpha z_1 \mathrm{SNR})}] - \frac{1}{\theta_2 TB} \log_e \mathbb{E}\left[e^{-\theta_2 TB \log_2 \frac{1}{a}}\right]}{\log_2 \mathrm{SNR}} \\
&= \lim_{\mathrm{SNR}\to\infty} \frac{\log_2 a + \log_2 \mathrm{SNR} - \frac{1}{\theta_1 TB} \log_2 \mathbb{E}[z_1^{-\theta_1 TB \log_2 e}] + \log_2 \frac{1}{a}}{\log_2 \mathrm{SNR}} \\
&= 1 + \lim_{\mathrm{SNR}\to\infty} \frac{-\frac{1}{\theta_1 TB} \log_2 \mathbb{E}[z_1^{-\theta_1 TB \log_2 e}]}{\log_2 \mathrm{SNR}} \\
&= 1
\end{aligned} \tag{4.57}$$

$$
\begin{aligned}
L_{\infty}^{DPC} &= \lim_{\mathrm{SNR}\to\infty}\left(\log_2\mathrm{SNR} - \frac{C_{sum}^{DPC}}{S_{\infty}^{DPC}}\right) \\
&= \lim_{\mathrm{SNR}\to\infty}\left(\log_2\mathrm{SNR} + \frac{\frac{1}{\theta_1 TB}\log_e\mathbb{E}\left[e^{-\theta_1 TB\log_2(1+\alpha z_1\mathrm{SNR})}\right]}{1}\right. \\
&\quad \left. + \frac{\frac{1}{\theta_2 TB}\log_e\mathbb{E}\left[e^{-\theta_2 TB\log_2\left[1+\frac{(1-\alpha)z_2\mathrm{SNR}}{1+\alpha z_2\mathrm{SNR}}\right]}\right]}{1}\right) \\
&= \lim_{\mathrm{SNR}\to\infty}\left(\log_2\mathrm{SNR} - \frac{\log_2 a + \log_2\mathrm{SNR} - \frac{1}{\theta_1 TB}\log_2\mathbb{E}[z_1^{-\theta_1 TB\log_2 e}] + \log_2\frac{1}{a}}{1}\right) \\
&= \frac{1}{\theta_1 TB}\log_2\mathbb{E}[z_1^{-\theta_1 TB\log_2 e}] \qquad (4.58)
\end{aligned}
$$

For hybrid fading, the sum hybrid capacity is denoted in (4.50), its high SNR slope and power offset are the same as that in fast fading scenario.

□

Remark 4.4. *Note that this conclusion for DPC are based on canceling user 2 from user 1. Similarly, when canceling user 1 from user 2,* $S_{\infty}^{DPC} = 1$ *and* $L_{\infty}^{DPC} = \frac{1}{\theta_2 TB}\log_e\mathbb{E}[z_2^{-\theta_2 TB\log_2 e}]$ *are obtained. Therefore, when* $\frac{1}{\theta_1 TB}\log_e\mathbb{E}[z_1^{-\theta_1 TB\log_2 e}] \le \frac{1}{\theta_2 TB}\log_e\mathbb{E}[z_2^{-\theta_2 TB\log_2 e}]$*, the optimal DPC cancellation order is to pre-cancel user 2 from user 1; otherwise, pre-cancel user 1 from user 2.*

Regarding to TDMA scheme, its high SNR performance is given in Theorem 4.5.

Theorem 4.5. *Using TDMA scheme, in fast fading scenario, given time sharing factor* α $(0 < \alpha < 1)$*, if conditions* $0 < \mathbb{E}[z_1^{-\alpha\theta_1 TB\log_2 e}] < \infty$ *and* $0 < \mathbb{E}[z_2^{-(1-\alpha)\theta_2 TB\log_2 e}] < \infty$ *are met, the high SNR slope and power offset of sum effective capacity are:*

$$
\begin{aligned}
S_{\infty}^{TDMA} &= 1, \qquad (4.59)\\
L_{\infty}^{TDMA} &= \frac{1}{\theta_1 TB}\log_e\mathbb{E}[z_1^{-\alpha\theta_1 TB\log_2 e}] + \frac{1}{\theta_2 TB}\log_e\mathbb{E}[z_2^{-(1-\alpha)\theta_2 TB\log_2 e}]. \qquad (4.60)
\end{aligned}
$$

In hybrid fading scenario, given α $(0 < \alpha < 1)$*, if* $0 < \mathbb{E}[z_1^{-\alpha\theta_1 TB\log_2 e}] < \infty$ *is met, the*

high SNR slope and the power offset of sum hybrid capacity become:

$$S_{\infty}^{TDMA} = 1, \tag{4.61}$$

$$L_{\infty}^{TDMA} = \frac{1}{\theta_1 TB} \log_e \mathbb{E}[z_1^{-\alpha\theta_1 TB \log_2 e}] - (1-\alpha)\log_2 z_{th}. \tag{4.62}$$

Proof. In fast fading scenario, the sum effective capacity using TDMA scheme is expressed in (4.49). According to the definition of high SNR slope in (4.52) and power offset in (4.53), its S_{∞}^{TDMA} and L_{∞}^{TDMA} can be calculated by (4.63) and (4.64), respectively.

$$\begin{aligned}
S_{\infty}^{TDMA} &= \lim_{\mathrm{SNR}\to\infty} \frac{C_{sum}^{TDMA}}{\log_2 \mathrm{SNR}} \\
&= \lim_{\mathrm{SNR}\to\infty} \frac{-\frac{1}{\theta_1 TB}\log_e \mathbb{E}\left[e^{-\theta_1 TB\alpha\log_2(1+z_1\mathrm{SNR})}\right] - \frac{1}{\theta_2 TB}\log_e \mathbb{E}\left[e^{-\theta_2 TB(1-\alpha)\log_2(1+z_2\mathrm{SNR})}\right]}{\log_2 \mathrm{SNR}} \\
&= \lim_{\mathrm{SNR}\to\infty} \frac{-\frac{1}{\theta_1 TB}\log_e \mathbb{E}\left[e^{-\theta_1 TB\alpha\log_2(z_1\mathrm{SNR})}\right] - \frac{1}{\theta_2 TB}\log_e \mathbb{E}\left[e^{-\theta_2 TB(1-\alpha)\log_2(z_2\mathrm{SNR})}\right]}{\log_2 \mathrm{SNR}} \\
&= \lim_{\mathrm{SNR}\to\infty} \frac{\alpha\log_2 \mathrm{SNR} - \frac{1}{\theta_1 TB}\log_e \mathbb{E}[z_1^{-\alpha\theta_1 TB\log_2 e}] + (1-\alpha)\log_2 \mathrm{SNR}}{\log_2 \mathrm{SNR}} + \\
&\quad \frac{-\frac{1}{\theta_2 TB}\log_e \mathbb{E}[z_1^{-\theta_2 TB(1-\alpha)\log_2 e}]}{\log_2 \mathrm{SNR}} \\
&= 1
\end{aligned} \tag{4.63}$$

$$\begin{aligned}
L_{\infty}^{TDMA} &= \lim_{\mathrm{SNR}\to\infty} \left(\log_2 \mathrm{SNR} - \frac{C_{sum}^{TDMA}}{S_{\infty}^{TDMA}}\right) \\
&= \lim_{\mathrm{SNR}\to\infty} \left(\log_2 \mathrm{SNR} + \frac{\frac{1}{\theta_1 TB}\log_e \mathbb{E}\left[e^{-\theta_1 TB\alpha\log_2(1+z_1\mathrm{SNR})}\right]}{1} + \right. \\
&\quad \left. \frac{\frac{1}{\theta_2 TB}\log_e \mathbb{E}\left[e^{-\theta_2 TB(1-\alpha)\log_2(1+z_2\mathrm{SNR})}\right]}{1} \right) \\
&= \lim_{\mathrm{SNR}\to\infty} \left(\log_2 \mathrm{SNR} - \log_2 \mathrm{SNR} + \frac{1}{\theta_1 TB}\log_e \mathbb{E}[z_1^{-\alpha\theta_1 TB\log_2 e}] + \right. \\
&\quad \left. \frac{1}{\theta_2 TB}\log_e \mathbb{E}[z_1^{-\theta_2 TB(1-\alpha)\log_2 e}] \right) \\
&= \frac{1}{\theta_1 TB}\log_e \mathbb{E}[(z_1)^{-\alpha\theta_1 TB\log_2 e}] + \frac{1}{\theta_2 TB}\log_e \mathbb{E}[(z_2)^{-(1-\alpha)\theta_2 TB\log_2 e}].
\end{aligned} \tag{4.64}$$

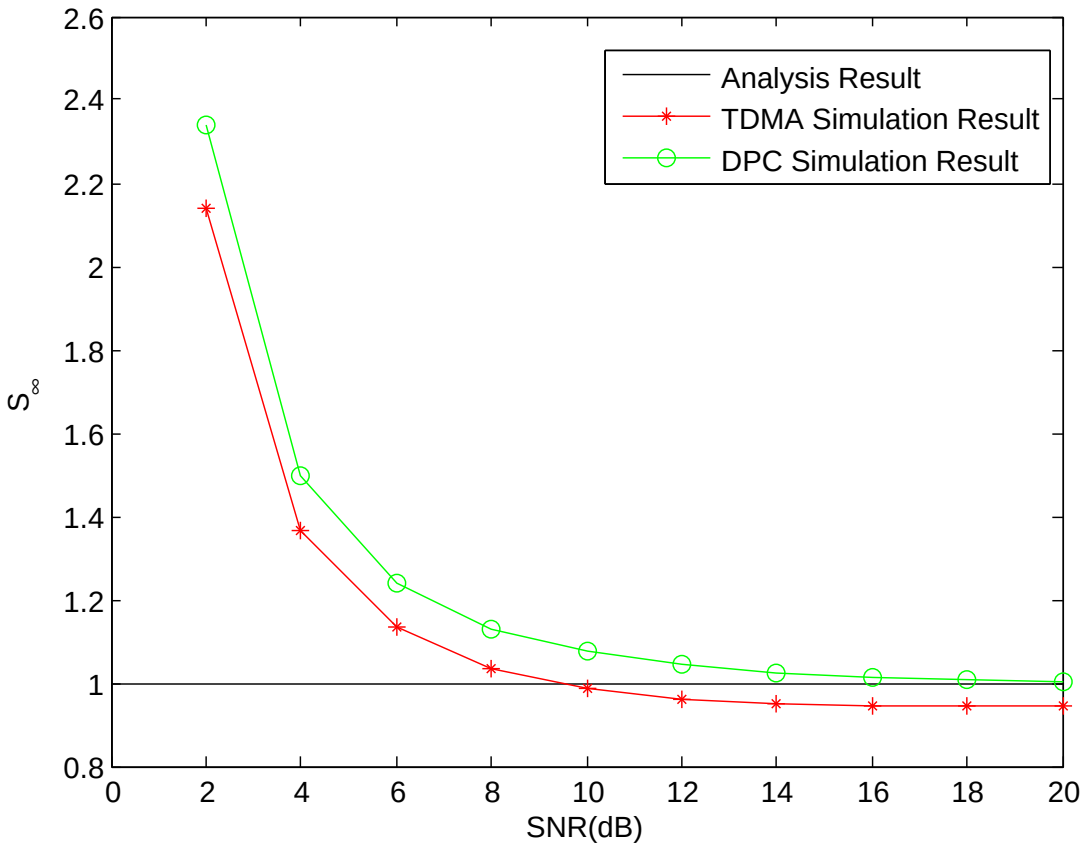

FIGURE 4.7 – High SNR slope approximation.

Similarly, the high SNR slope and power offset can be obtained for hybrid fading.

□

In Rayleigh fading channel, when $\mathbb{E}\{z_1\} = 2$, $\mathbb{E}\{z_2\} = 1$, for $\theta_1 = \theta_2 = 0.1$, given $\alpha = 0.5$, Figure 4.7 – 4.9 show that the approximation results obtained in Theorem 4.4 and 4.5 can well approximate the simulation results obtained from the expressions in (4.52)-(4.54) directly.

Recall that Theorem 4.4 and 4.5 both contain conditions to reach the conclusions on high SNR regime. For Rayleigh fading, such conditions can be further reduced to the requirements on delay QoS exponent θ_i, as denoted in Lemma 4.3.

Lemma 4.3. *In Rayleigh fading channels, for DPC scheme, the condition* $0 < \mathbb{E}[z_1^{-\theta_1 TB\log_2 e}] < \infty$ *becomes* $\theta_1 < \frac{1}{TB\log_2 e}$*; for TDMA scheme, the condition* $0 < \mathbb{E}[z_1^{-\alpha\theta_1 TB\log_2 e}] < \infty$

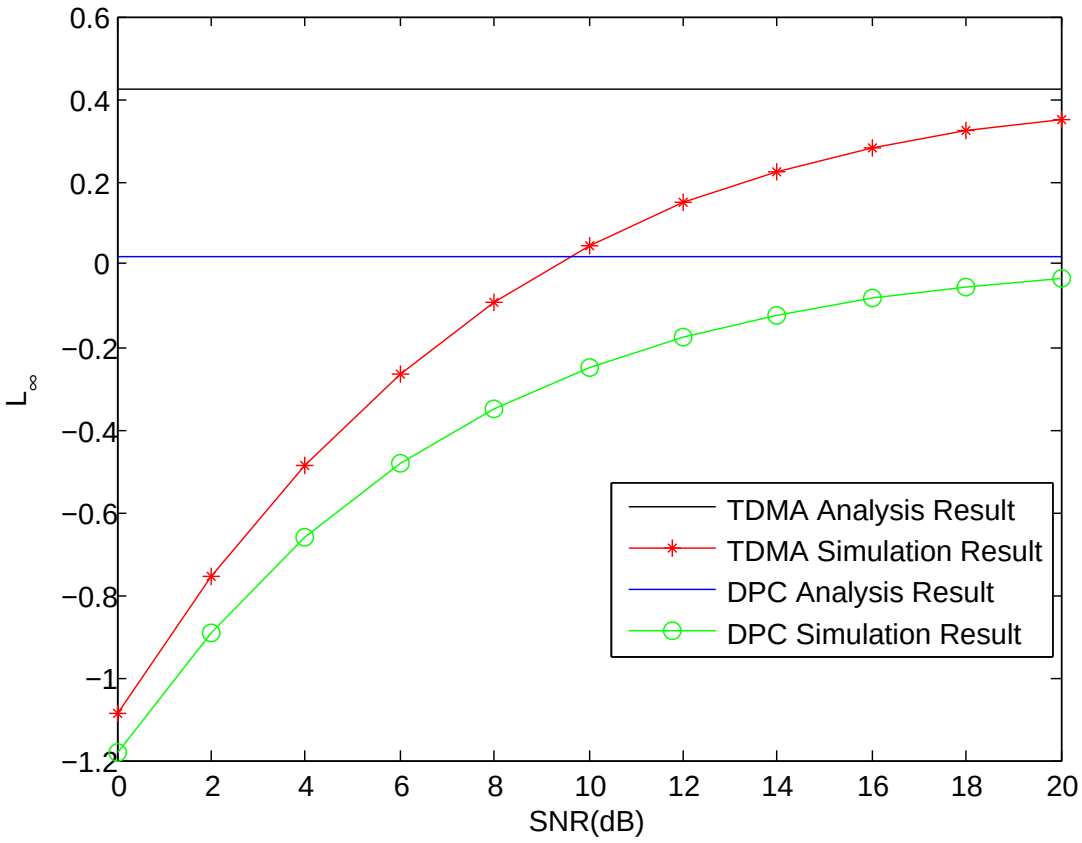

FIGURE 4.8 – Power offset approximation.

restricts $\theta_1 < \frac{1}{TB\alpha \log_2 e}$, *and* $0 < \mathbb{E}[z_2^{-(1-\alpha)\theta_2 TB \log_2 e}] < \infty$ *requires* $\theta_2 < \frac{1}{TB(1-\alpha) \log_2 e}$.

Proof. In Rayleigh fading channels, the channel power gain belongs to exponential distribution. Assume $z_i \sim exp(\lambda_i)$, then $\mathbb{E}\left[{z_i}^{-\eta\theta_i TB\log_2 e}\right]$ can be further expressed as

$$\begin{aligned} & \mathbb{E}\left[{z_i}^{-\eta\theta_i TB\log_2 e}\right] \\ = \quad & \int_0^\infty z_i^{-\eta\theta_i TB \log_2 e} \lambda_i e^{-\lambda_i z_i} dz_i \\ \xlongequal{(\text{let } z = \lambda_i z_i)} \quad & \lambda_i^{\eta\theta_i TB \log_2 e} \int_0^\infty z^{-\eta\theta_i TB \log_2 e} e^{-z} dz. \end{aligned} \tag{4.65}$$

Note that for $\int_0^\infty z^a e^{-z} dz$, $0 < \int_0^\infty z^a e^{-z} dz < \infty$ holds when $a > -1$; and $\int_0^\infty z^a e^{-z} dz = \infty$ when $a \leq -1$. Hence, $0 < \mathbb{E}\left[{z_i}^{-\eta\theta_i TB\log_2 e}\right] < \infty$, only if $\eta\theta_i TB \log_2 e < 1$. Accordingly, the Lemma 4.3 is proved. □

Lemma 4.4. *Regarding to the QoS's impact on the sum effective/hybrid capacity in high*

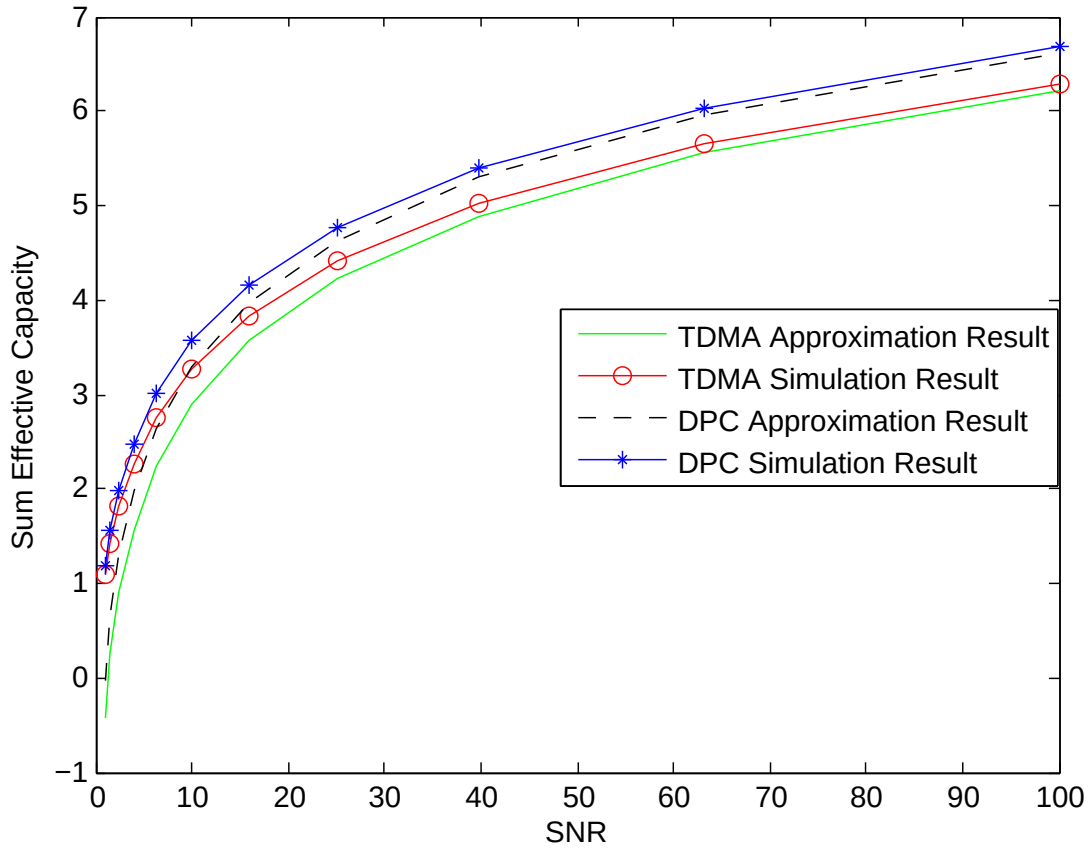

FIGURE 4.9 – Sum effective capacity approximation.

SNR regime:

- L_{∞}^{DPC} *is a non-decreasing function of QoS exponent* θ_1*, when precanceling user 2 from user 1.*

- *In fast fading scenario,* L_{∞}^{TDMA} *in* (4.60) *is a non-decreasing function of the delay QoS exponent* θ_1 *and* θ_2*.*

- *In hybrid fading scenario,* L_{∞}^{TDMA} *in* (4.62) *is a non-decreasing function of the delay QoS exponent* θ_1 *and is a non-increasing function of outage probability* q_o*.*

Proof. Note that $\frac{1}{\theta TB}\log_e \mathbb{E}[z^{-\theta TB\log_2 e}]$ can be expressed as $\log_e\left(\mathbb{E}[z^{-\theta TB\log_2 e}]\right)^{\frac{1}{\theta TB}}$. According to Holder's inequality that: $(\mathbb{E}\{|x|^m\})^{1/m} \leq (\mathbb{E}\{|x|^n\})^{1/n}$ for $0 < m < n$,

$\frac{1}{\theta TB}\log_e \mathbb{E}[z^{-\theta TB\log_2 e}]$ is a non-decreasing function of θ can be proved. Hence, Lemma 4.4 is proved. □

Lemma 4.5. *In high SNR regime, the approximated sum effective/hybrid capacity obtained by DPC is invariant to the resource sharing factor; however, the approximated sum effective/hybrid capacity obtained by TDMA is a function of the resource sharing factor.*

Given $\mathbb{E}\{z_1\} = 2$, $\mathbb{E}\{z_2\} = 1$ and $\mathrm{SNR} = 30$ dB, numerical simulations have been done on sum effective capacity when $\theta_1 = \theta_2 = 0.1$ and when $(\theta_1 = 0.5, \theta_2 = 0.3)$. Figure 4.10 is the sum effective capacity obtained using the DPC scheme. The sum effective capacity decreases as the delay QoS requirements become more stringent, also it does not change much with the power sharing factor. Figure 4.11 shows the sum effective capacity obtained under TDMA scheme. Similarly, the sum effective capacity decreases with the delay QoS requirements, however, it varies with the power sharing factor drastically. It is well known that without QoS constraint, the TDMA scheme can achieve maximum sum capacity by allocating all resource to the user with highest channel gain. However, considering the delay requirements, wireless resource may need to be shared between two users in order to achieve the maximum sum effective capacity.

4.5 Conclusion

This work investigated the DPC and TDMA scheme in low and high SNR regime of a two-user broadcasting system with QoS constraints. Specifically, it considers two cases: (1) when both users are using effective capacity (2) when one user is using effective capacity and the other user is using outage capacity. It is assumed that the receivers have perfect CSI knowledge and the transmitter only knows statistical CSI information.

In the low power regime, minimum transmission energy per bit and wideband

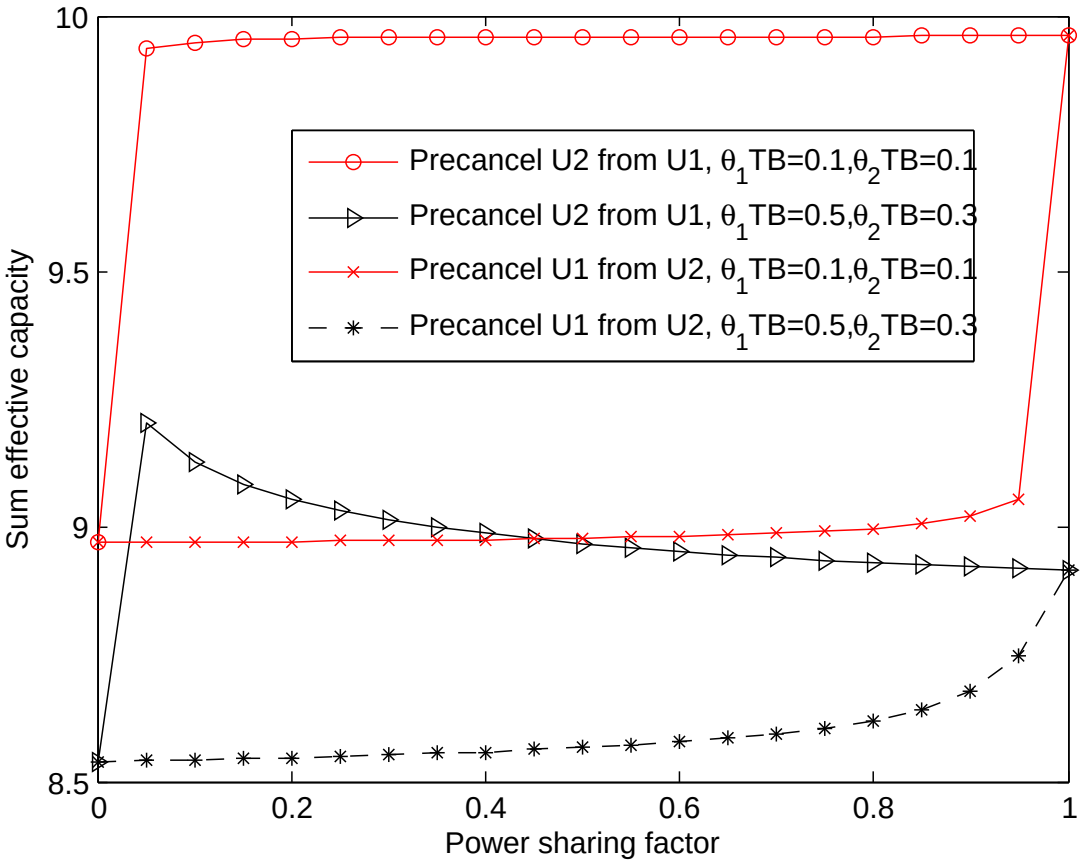

FIGURE 4.10 – DPC sum effective capacity vs α.

slope region are obtained in closed forms for effective capacity region and hybrid capacity region, respectively.

- For both users are using effective capacity, the main observations and contributions are as follows:

    1. Minimum transmission energy per bit for both TDMA and DPC strategies are the same and is not affected by the delay QoS exponents θ_i, however, the wideband slope region decreases when any user's delay constraint becomes stringent.

    2. The turning point of user 1's and user 2's wideband slope are provided in closed forms.

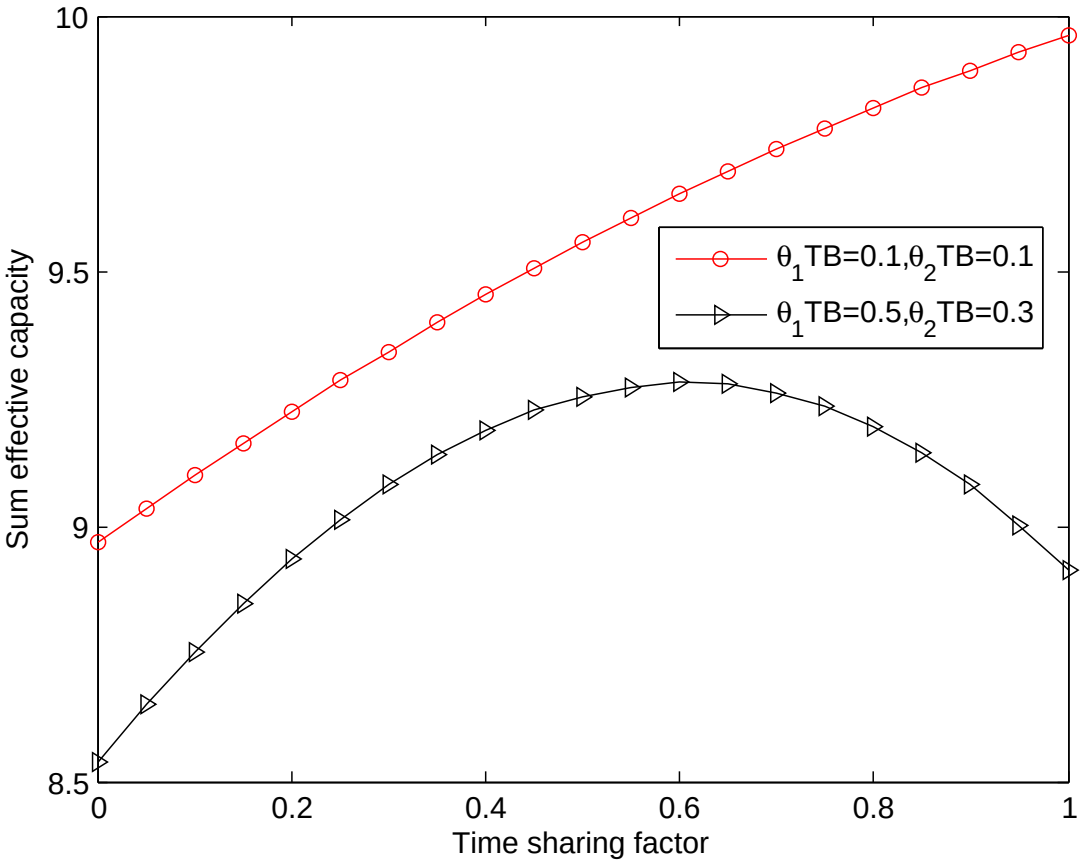

FIGURE 4.11 – TDMA sum effective capacity vs α.

3. Ratio of DPC wideband slope over TDMA wideband slope (a.k.a bandwidth expansion factor σ) are provided.

4. Results on Rayleigh fading channels are given, and more concise conclusions are derived. Also, σ is shown to increase with $\frac{\mathbb{E}\{z_1\}}{\mathbb{E}\{z_2\}}$ and decrease with delay QoS requirements.

5. The optimal DPC cancellation order in low SNR regime is to precancel user 2's interference to user 1 when $\frac{\mathbb{E}\{z_1^2\}}{\mathbb{E}\{z_1\}} \geq \frac{\mathbb{E}\{z_2^2\}}{\mathbb{E}\{z_2\}}$.

6. The resource sharing factor to achieve the rate region for DPC an TDMA are approximated using its first order approximation, and numerical results are also provided.

- For hybrid capacity region (when user 1 is using effective capacity and user 2 is using outage capacity), the main findings and contributions are:

    1. Minimum transmission energy per bit for both TDMA and DPC strategies are the same and is affected by the outage probability but not by the delay QoS exponent θ_1.
    2. The bandwidth expansion factor is obtained.
    3. The optimal DPC cancellation order is to cancel user 2 from user 1 when $\mathbb{E}\{z_1^2\} \geq \mathbb{E}\{z_1\} z_{th}$.
    4. When the optimal cancellation order is to precancel user 2 from user 1, user 1's wideband slope is a mono-increasing function of k, where k is the rate ratio between user 1 and user 2; and the turning point of user 2's wideband slope is provided in closed form.
    5. Analysis on Rayleigh fading channels are provided.

In high SNR regime, the high SNR slope and power offset are obtained for D-PC and TDMA in terms of sum effective capacity and sum hybrid capacity, however, with certain conditions on limitation operations. Such conditions in Rayleigh fading are further reduced into the constraint on the delay QoS component θ_i. The optimal DPC cancellation order is to pre-cancel user 2 from user 1 when $\frac{1}{\theta_1 TB} \log_e \mathbb{E}[z_1^{-\theta_1 TB \log_2 e}] \leq \frac{1}{\theta_2 TB} \log_e \mathbb{E}[z_2^{-\theta_2 TB \log_2 e}]$. Both DPC and TDMA power offsets are proved to be non-decreasing functions of QoS requirement. The sum effective/hybrid capacity using DPC is invariant to the resource sharing factor, while the sum effective/hybrid capacity using TDMA varies with resource sharing factor.

CHAPTER 5
CONCLUSION AND FUTURE WORK

Three frequency sharing schemes for coexisting networks were investigated independently in this dissertation: (1) multiple networks coexist following the interweave cognitive radio paradigm, i.e., the secondary network can only transmit when the primary network is "silent"; (2) multiple networks coexist as an underlay cognitive radio system, i.e., the secondary network transmits simultaneously with the primary network under the premise that its interference to the primary network is below certain threshold; (3) multiple networks converged by using the common transmitter sending signals simultaneously, and the interference is precanceled using DPC pre-coding.

Chapter 2 investigated the resource allocation of the interweave cognitive radio. The novel optimization objective was proposed in this dissertation, i.e., minimizing the primary network's required spectrum as long as its QoS requirements can be met. With this frequency saving objective, the primary system can release the unnecessary frequencies for secondary users. Moreover, efficient near-optimal algorithms and simulations were provided for both downlink and uplink OFDMA-based primary networks. Chapter 3 focused on the resource allocation of the distributed secondary network that underlays the primary network. The secondary network is to maximize its overall capacity under individual user's power constraint and primary user's rate constraint. The distributed MCDD algorithm was provided and proved to converge to the global optimal solution. To reduce the computational complexity and convergence time of MCDD algorithm, the GSLA algorithm has been proposed to obtain a near optimal solution. Chapter 4 analyzed the performance of DPC scheme in a delay sensitive broadcasting system,

where the common transmitter serves different users. For comparison purpose, the T-DMA scheme is also investigated. The delay sensitive requirements were incorporated by using effective capacity for fast fading channel and outage capacity for slow fading channel. Extensive performance analysis was carried out in both low SNR regime and high SNR regime.

Future work on the frequency sharing schemes towards the coexisting networks includes but not limited to:

- Incorporate the admission control into the frequency saving optimization problem in the interweave cognitive radio. Jointly solving the frequency saving and admission control problem at one step may reduce the operational delay and provide further optimization gains.
- When the transmitter has imperfect CSI, the resource allocation algorithms for both underlay and interweave cognitive radio.
- When the transmitter has perfect CSI, the performance of DPC and TDMA for delay sensitive multiuser system.
- In general SNR regime, the performance of DPC vs. TDMA for delay sensitive multiuser system.
- The resource allocation for the DPC scheme in delay sensitive multi-user systems.

Note that most of the work presented in this dissertation have been published in [70, 80–84].

REFERENCES

[1] "Global industry analysts, inc., 3g/3.5g - a global market report," 2011. [Online]. Available: http://www.strategyr.com/3GMarketReport.asp.

[2] "The world in 2011: Ict facts and figures," 2011. [Online]. Available: http://www.itu.int/ITUD/ict/facts/2011/index.html

[3] G. Intelligence, "Infographic: Global 4g-lte connections forecast: 2010 to 2020," Feb. 2014. [Online]. Available: https://gsmaintelligence.com/

[4] "Cisco visual networking index: Global traffic forcast update, 2013 - 2018," Feb. 2014. [Online]. Available: http://www.cisco.com

[5] C. Shannon, "A mathematical theory of communication," *Bell System Technical Journal*, vol. 27, pp. 379–423, 623–656, July, October 1948.

[6] T. S. Rappaport *et al.*, *Wireless communications: principles and practice*. Prentice Hall PTR New Jersey, 1996, vol. 2.

[7] "Lte enb- evolving to lte enb as a node upgrade," 2014. [Online]. Available: http://www.rcrwireless.com/lte/lte-enb.html.

[8] R. Prasad, *OFDM for wireless communications systems*, 3rd ed. Artech House Publishers, 2004.

[9] G. Li and H. Liu, "Downlink radio resource allocation for multi-cell ofdma system," *IEEE Transactions on Wireless Communications*, vol. 5, no. 12, pp. 3451–3459, 2006.

[10] H. Li, Y. Kim, and H. Liu, "Ofdma capacity analysis and subcarrier allocation in mimo channels," *European Wireless 2008*, 2008.

[11] Y. Peng, S. M. Armour, and J. P. McGeehan, "An investigation of dynamic subcarrier allocation in mimo–ofdma systems," *IEEE Transactions on Vehicular Technology*, vol. 56, no. 5, pp. 2990–3005, 2007.

[12] G. Staple and K. Werbach, "The end of spectrum scarcity [spectrum allocation and utilization]," *IEEE Spectrum*, vol. 41, no. 3, pp. 48–52, 2004.

[13] S. Haykin, "Cognitive radio: brain-empowered wireless communications," *IEEE Journal on Selected Areas in Communications*, vol. 23, no. 2, pp. 201–220, 2005.

[14] S. Srinivasa and S. A. Jafar, "Cognitive radios for dynamic spectrum access-the throughput potential of cognitive radio: A theoretical perspective," *IEEE Communications Magazine*, vol. 45, no. 5, pp. 73–79, 2007.

[15] L. B. Le and E. Hossain, "Resource allocation for spectrum underlay in cognitive radio networks," *IEEE Transactions on Wireless Communications*, vol. 7, no. 12, pp. 5306–5315, 2008.

[16] I. F. Akyildiz, W.-Y. Lee, and K. R. Chowdhury, "Crahns: Cognitive radio ad hoc networks," *Ad Hoc Networks*, vol. 7, no. 5, pp. 810–836, 2009.

[17] S. Huang, X. Liu, and Z. Ding, "Decentralized cognitive radio control based on inference from primary link control information," *IEEE Journal on Selected Areas in Communications*, vol. 29, no. 2, pp. 394–406, 2011.

[18] M. H. Costa, "Writing on dirty paper (corresp.)," *IEEE Transactions on Information Theory*, vol. 29, no. 3, pp. 439–441, 1983.

[19] H. Chao, Y. Chen, and Z. Hu, "Dirty paper coding with phase reshaping: New integration scheme for broadcast and unicast," in *2009 IEEE 20th International Symposium on Personal, Indoor and Mobile Radio Communications,*. IEEE, 2009, pp. 2355–2359.

[20] S. Gaur, J. Acharya, and L. Gao, "Enhancing zf-dpc performance with receiver processing," *IEEE Transactions on Wireless Communications*, vol. 10, no. 12, pp. 4052–4056, 2011.

[21] M. Sharif and B. Hassibi, "A comparison of time-sharing, dpc, and beamforming for mimo broadcast channels with many users," *IEEE Transactions on Communications*, vol. 55, no. 1, pp. 11–15, 2007.

[22] B. Liu, H. Li, H. Liu, and S. Roy, "Dpc-based hierarchical broadcasting: design and implementation," *IEEE Transactions on Vehicular Technology*, vol. 57, no. 6, p. 3895, 2008.

[23] H. Li, B. Liu, and H. Liu, "Transmission schemes for multicarrier broadcast and unicast hybrid systems," *IEEE Transactions on Wireless Communications*, vol. 7, no. 11, pp. 4321–4330, 2008.

[24] T. Lohmar and U. Horn, "Hybrid broadcast-unicast distribution of mobile tv over 3g networks," in *Proceedings 2006 31st IEEE Conference on Local Computer Networks*. IEEE, 2006, pp. 850–851.

[25] G. Caire and S. Shamai, "On the achievable throughput of a multiantenna gaussian broadcast channel," *IEEE Transactions on Information Theory*, vol. 49, no. 7, pp. 1691–1706, July 2003.

[26] C. T. Ng and A. J. Goldsmith, "Transmitter cooperation in ad-hoc wireless networks: Does dirty-paper coding beat relaying?" in *IEEE Information Theory Workshop*. IEEE, 2004, pp. 277–282.

[27] A. Lioumpas, P. Bithas, and A. Alexiou, "Partitioning of distributed mimo systems based on overhead considerations," *IEEE Wireless Communications Letters*, vol. 2, no. 6, pp. 579–582, 2013.

[28] A. Goldsmith, S. A. Jafar, I. Maric, and S. Srinivasa, "Breaking spectrum gridlock with cognitive radios: An information theoretic perspective," *Proceedings of the IEEE*, vol. 97, no. 5, pp. 894–914, 2009.

[29] E. Axell, G. Leus, E. G. Larsson, and H. V. Poor, "Spectrum sensing for cognitive radio: State-of-the-art and recent advances," *IEEE Signal Processing Magazine*, vol. 29, no. 3, pp. 101–116, 2012.

[30] S. Sadr, A. Anpalagan, and K. Raahemifar, "Radio resource allocation algorithms for the downlink of multiuser ofdm communication systems," *IEEE Communications Surveys & Tutorials*, vol. 11, no. 3, pp. 92–106, 2009.

[31] M. Bohge, J. Gross, A. Wolisz, and M. Meyer, "Dynamic resource allocation in ofdm systems: an overview of cross-layer optimization principles and techniques," *IEEE Network*, vol. 21, no. 1, pp. 53–59, 2007.

[32] K. Huang, V. K. Lau, and Y. Chen, "Spectrum sharing between cellular and mobile ad hoc networks: transmission-capacity trade-off," *IEEE Journal on Selected Areas in Communications*, vol. 27, no. 7, pp. 1256–1267, 2009.

[33] H. Li, G. Ru, Y. Kim, and H. Liu, "Ofdma capacity analysis in mimo channels," *IEEE Transactions on Information Theory*, vol. 56, no. 9, pp. 4438–4446, 2010.

[34] A. Attar, M. R. Nakhai, and A. H. Aghvami, "Cognitive radio game for secondary spectrum access problem," *IEEE Transactions on Wireless Communications*, vol. 8, no. 4, pp. 2121–2131, 2009.

[35] J.-A. Bazerque and G. B. Giannakis, "Distributed scheduling and resource allocation for cognitive ofdma radios," *Mobile Networks and Applications*, vol. 13, no. 5, pp. 452–462, 2008.

[36] M. E. Sahin, I. Guvenc, and H. Arslan, "Opportunity detection for ofdma-based cognitive radio systems with timing misalignment," *IEEE Transactions on Wireless Communications*, vol. 8, no. 10, pp. 5300–5313, 2009.

[37] S. Gao, L. Qian, and D. R. Vaman, "Distributed energy efficient spectrum access in cognitive radio wireless ad hoc networks," *IEEE Transactions on Wireless Communications*, vol. 8, no. 10, pp. 5202–5213, 2009.

[38] R. Ramjee, D. Towsley, and R. Nagarajan, "On optimal call admission control in cellular networks," *Wireless Networks*, vol. 3, no. 1, pp. 29–41, 1997.

[39] S. S. Jeong, J. A. Han, and W. S. Jeon, "Adaptive connection admission control scheme for high data rate mobile networks," in *IEEE 62nd Vehicular Technology Conference, 2005*, vol. 4. IEEE, 2005, pp. 2607–2611.

[40] H. Liu, X. Li, and F. Mu, "Medium access control for orthogonal frequency-division multiple-access (ofdma) cellular networks," Jul. 4 2006, uS Patent 7,072,315.

[41] S.-E. Elayoubi and B. Fourestié, "Performance evaluation of admission control and adaptive modulation in ofdma wimax systems," *IEEE/ACM Transactions on Networking (TON)*, vol. 16, no. 5, pp. 1200–1211, 2008.

[42] Y.-B. Lin, T.-H. Chiu, and Y. T. Su, "Optimal and near-optimal resource allocation algorithms for ofdma networks," *IEEE Transactions on Wireless Communications*, vol. 8, no. 8, pp. 4066–4077, 2009.

[43] M. Ochel and B. Vöcking, "Approximability of ofdma scheduling," in *Algorithms-ESA 2009*. Springer, 2009, pp. 385–396.

[44] M. Pinedo, *Scheduling: theory, algorithms, and systems*. Springer, 2012.

[45] Y. Ma and D. I. Kim, "Rate-maximization scheduling schemes for uplink ofdma," *IEEE Transactions on Wireless Communications*, vol. 8, no. 6, pp. 3193–3205, 2009.

[46] L. P. Qian, Y. J. A. Zhang, and J. Huang, "Mapel: Achieving global optimality for a non-convex wireless power control problem," *IEEE Transactions on Wireless Communications*, vol. 8, no. 3, pp. 1553–1563, 2009.

[47] W. Yu, G. Ginis, and J. M. Cioffi, "Distributed multiuser power control for digital subscriber lines," *IEEE Journal on Selected Areas in Communications*, vol. 20, no. 5, pp. 1105–1115, 2002.

[48] Z.-Q. Luo and J.-S. Pang, "Analysis of iterative waterfilling algorithm for multiuser power control in digital subscriber lines," *EURASIP Journal on Advances in Signal Processing*, vol. 2006, 2006.

[49] W. Yu and R. Lui, "Dual methods for nonconvex spectrum optimization of multi-carrier systems," *IEEE Transactions on Communications*, vol. 54, no. 7, pp. 1310–1322, 2006.

[50] L. P. Qian and Y. Jun, "Monotonic optimization for non-concave power control in multiuser multicarrier network systems," in *IEEE INFOCOM 2009*. IEEE, 2009, pp. 172–180.

[51] F. Wang, M. Krunz, and S. Cui, "Price-based spectrum management in cognitive radio networks," *IEEE Journal of Selected Topics in Signal Processing*, vol. 2, no. 1, pp. 74–87, 2008.

[52] M. Hong and A. Garcia, "Equilibrium pricing of interference in cognitive radio networks," *IEEE Transactions on Signal Processing*, vol. 59, no. 12, pp. 6058–6072, 2011.

[53] S. Geman and D. Geman, "Stochastic relaxation, gibbs distributions, and the bayesian restoration of images," *IEEE Transactions on Pattern Analysis and Machine Intelligence*, no. 6, pp. 721–741, 1984.

[54] L. P. Qian, Y. J. A. Zhang, and M. Chiang, "Globally optimal distributed power control for nonconcave utility maximization," in *2010 IEEE Global Telecommunications Conference (GLOBECOM 2010)*. IEEE, 2010, pp. 1–6.

[55] G. Caire, D. Tuninetti, and S. Verdu, "Suboptimality of tdma in the low-power regime," *IEEE Transactions on Information Theory*, vol. 50, no. 4, pp. 608–620, 2004.

[56] N. Jindal and A. Goldsmith, "Dirty-paper coding versus tdma for mimo broadcast channels," *IEEE Transactions on Information Theory*, vol. 51, no. 5, pp. 1783–1794, May 2005.

[57] N. Jindal, "High snr analysis of mimo broadcast channels," in *Proceedings 2005 International Symposium on Information Theory*, Sept 2005, pp. 2310–2314.

[58] J. Lee and N. Jindal, "High snr analysis for mimo broadcast channels: Dirty paper coding versus linear precoding," *IEEE Transactions on Information Theory*, vol. 53, no. 12, pp. 4787–4792, Dec 2007.

[59] F. Knabe, M. Wiese, C. Huppert, and J. Klotz, "The wideband slope region of bpsk and qpsk for broadcast channels in the low-power regime," in *IEEE Information Theory Workshop, 2009*, Oct 2009, pp. 440–444.

[60] H. Wu, Y. Zhang, and X. Liu, "Laxity-based opportunistic scheduling with flow-level dynamics and deadlines," in *IEEE Wireless Communications and Networking Conference*, Shanghai, China, Apr. 2013.

[61] H. Wu, X. Lin, X. Liu, and Y. Zhang, "Application-level scheduling with deadline constraints," in *IEEE INFOCOM*, Toronto, Canada, 2014.

[62] H. Wu, X. Lin, X. Liu, K. Tan, and Y. Zhang, "Decomposition of large-scale MDPs for wireless scheduling with load- and channel-awareness," in *Information Theory and Applications Workshop (ITA)*, San Diego, CA, Feb. 2014.

[63] D. Wu and R. Negi, "Effective capacity: a wireless link model for support of quality of service," *IEEE Transactions on Wireless Communications*, vol. 2, no. 4, pp. 630–643, 2003.

[64] S. Verdu, "Spectral efficiency in the wideband regime," *IEEE Transactions on Information Theory*, vol. 48, no. 6, pp. 1319–1343, 2002.

[65] M. Gursoy, D. Qiao, and S. Velipasalar, "Analysis of energy efficiency in fading channels under qos constraints," *IEEE Transactions on Wireless Communications*, vol. 8, no. 8, pp. 4252–4263, August 2009.

[66] M. Gursoy, "Mimo wireless communications under statistical queueing constraints," *IEEE Transactions on Information Theory*, vol. 57, no. 9, pp. 5897–5917, Sept 2011.

[67] D. Qiao, M. C. Gursoy, and S. Velipasalar, "Energy efficiency in multiaccess fading channels under qos constraints," *EURASIP Journal on Wireless Communications and Networking*, no. 136, pp. 1–16, 2012.

[68] M. Ozmen, M. Gursoy, and P. Varshney, "Energy efficiency in fading interference channels under qos constraints," in *Proceedings 2012 International Symposium on Information Theory and its Applications (ISITA)*, 2012, pp. 692–696.

[69] A. Host-Madsen, M. Uppal, and Z. Xiong, "On outage capacity in the low power regime," *IEEE Transactions on Information Theory*, vol. 58, no. 2, pp. 888–896, Feb 2012.

[70] G. Ru, H. Li, L. Liu, Z. Hu, and Y. Gan, "Energy efficiency of hybrid cellular with heterogeneous qos provisions," *IEEE Communications Letters*, vol. 18, no. 6, pp. 1003–1006, June 2014.

[71] A. Lozano, A. Tulino, and S. Verdu, "High-snr power offset in multiantenna communication," *IEEE Transactions on Wireless Communications*, vol. 51, no. 12, pp. 4134–4151, Dec 2005.

[72] N. Prasad and M. Varanasi, "Mimo outage capacity in the high snr regime," in *Proceedings 2005 International Symposium on Information Theory*, Sept 2005, pp. 656–660.

[73] L. Liu, "Providing quality-of-service guarantees in wireless networks," *On delay-sensitive communication over wireless systems*, Ph.D. Dissertation, Electrical Engineering, Texas A&M University, College Station, TX, May 2008.

[74] C.-S. Chang, *Performance guarantees in communication networks*. New York: Springer-Verlag, 2000.

[75] L. Liu and J. Chamberland, "On the effective capacities of multiple-antenna gaussian channels," in *Proceedings 2008 IEEE International Symposium on Information Theory*, 2008, pp. 2583–2587.

[76] D. Wu, "Providing quality-of-service guarantees in wireless networks," Ph.D. Dissertation, Department of Electrical and Computer Engineering, Carnegie Mellon University, Pittsburgh, PA, August 2003.

[77] H. Li, B. Liu, and H. Liu, "Transmission schemes for multicarrier broadcast and unicast hybrid systems," *IEEE Transactions on Wireless Communications*, vol. 7, no. 11, pp. 4321–4330, 2008.

[78] M. Shen and A. Host-Madsen, "The wideband slope of interference channels: The large bandwidth case," *IEEE Transactions on Information Theory*, vol. 59, no. 5, pp. 2694–2712, May 2013.

[79] S. Shamai and S. Verdu, "The impact of frequency-flat fading on the spectral efficiency of cdma," *IEEE Transactions on Information Theory*, vol. 47, no. 4, pp. 1302–1327, May 2001.

[80] H. Li, G. Ru, S. Liu, H. Liu, and J.-N. Hwang, *"Introduction to Wireless Communications and Digital Broadcasting", in Digital Front-End in Wireless Communications and Broadcasting, 1st edition*. Cambridge University Press, 2011.

[81] G. Ru, H. Li, G. Li, and S. Liu, "Ofdma resource allocation in wireless communications," *Recent Patents on Electrical Engineering*, vol. 3, pp. 1–8, 2010.

[82] G. Ru, H. Li, S. Liu, W. Lin, L. Liu, and X. Wang, "Spectrum optimization for ofdma based wireless networks," in *Proceedings of the IEEE Vehicular Technology Conference*, San Francisco, USA, Sept. 2011.

[83] G. Ru, H. Li, Y. Lu, Y. Cheng, and W. Lin, "Frequency saving ofdma resource allocation with qos provision," in *IEEE Wicon*, Xi'an, China, Oct. 2011.

[84] G. Ru, H. Li, T. Tran, W. Lin, L. Liu, and H. Wu, "Distributed optimal power control for multicarrier cognitive systems," in *IEEE Global Communications Conference (GLOBECOM)*, Anaheim, USA, Dec. 2012.

CURRICULUM VITA

NAME: Guanying Ru

ADDRESS: Department of Electrical and Computer Engineering
University of Louisville
Louisville, KY 40292

EDUCATION: Ph.D., Electrical Engineering
University of Louisville, 2011-2014

Ph.D. Candidate, Electrical Engineering
North Dakota State University, 2009-2011

M.S., Electrical Engineering
Zhengzhou University, 2006-2009

B.S., Electrical Engineering
Zhengzhou University, 2002-2006

PROFESSIONAL EXPERIENCE: Intern in AT&T Lab,
Jun. 2013-Dec. 2013.

Visiting Student, Computer Science Department,
University of California, Davis,
Jun. 2011-Dec. 2011

AWARDS: Doctoral Dissertation Completion Award, 2013.

Electrical Engineering Outstanding Graduate Student, 2012.

The Theobald Scholarship Award, 2012.

Graduate Researchers Award Nominee, 2011.

Phi Kappa Phi Honor Society Inductee, 2011.

PUBLICATIONS:

JOURNAL:

[1] **Guanying Ru**, Hongxiang Li "TDMA vs. DPC in Delay Sensitive Communication over Broadcast Fading Channels," IEEE Transactions on Information Theory (Under submission).

[2] **Guanying Ru**, Hongxiang Li, Lingjia Liu, Zixia Hu, Yong Gan, "Energy Efficiency of Hybrid Cellular with Heterogeneous QoS Provisions," IEEE Communications Letters, vol.18, no.6, pp.1003–1006, June 2014.

[3] Tuan. T. Tran, Hongxiang Li, **Guanying Ru**, Robert J. Kerczewski, Lingjia Liu, and Samee U. Khan, "Secure Wireless Multicast for Delay-Sensitive Data via Network Coding," IEEE Transactions on Wireless Communications, vol(12), 7, pp.3372–3387, Jul. 2013.

[4] Hongxiang Li, **Guanying Ru**, Younsun Kim, and Hui Liu, "OFDMA Capacity Analysis in MIMO Channels," IEEE Transactions on Information Theory, vol. (56), 9, pp. 4438–4446, Sept. 2010.

[5] **Guanying Ru**, Hongxiang Li, Guoqing Li and Siqian Liu, "OFDMA Resource Allocation in Wireless Communications," Recent Patents on Electrical Engineering, vol(3), pp.1–8, Jun. 2010.

[6] **Guanying Ru**, Shouyi Yang, Yanhui, Lu, and Lin Qi, "Adaptable ZP MB-OFDM System," Communications Technology, vol.(43), 2, Jan. 2010.

BOOK CHAPTER:

[1] Hongxiang Li, **Guanying Ru**, Siqian Liu, Hui Liu and Jenq-Neng Hwang, "Introduction to Wireless Communications and Digital Broadcasting" in Digital Front-End in Wireless Communications and Broadcasting, 1st edition, Cambridge University Press, Sept. 2011.

CONFERENCE:

[1] **Guanying Ru**, Hongxiang Li, Tuan. T. Tran, Weiyao Lin, Lingjia Liu, Huasen Wu, "Distributed Optimal Power Control for Multicarrier Cognitive Systems," IEEE Globecom, Anaheim, USA, Dec, 2012.

[2] **Guanying Ru**, Hongxiang Li, Yanhui Lu, Yong Cheng, Weiyao Lin, "Frequency Saving OFDMA Resource Allocation with QoS Provision," IEEE Wicon, Xi'an, China, Oct. 2011.

[3] **Guanying Ru**, Hongxiang Li, Siqian Liu, Weiyao Lin, Lingjia Liu, Xudong Wang "Spectrum Optimization for OFDMA Based Wireless Networks," IEEE VTC, San Francisco, USA, Sept. 2011.

[4] Siqian Liu, Hongxiang Li, **Guanying Ru**, Weiyao Lin, Lingjia Liu, Yang Yi. "Capacity of Multicarrier Multilayer Broadcast and Unicast Hybrid Cellular System with Independent Channel Coding over Subcarriers," IEEE VTC, San Francisco, USA, Sept. 2011.

[5] **Guanying Ru**, Shouyi Yang, Xiaomin Mu, EnQing Chen, "A Zero-watermark System Based on Combined Spatial and Wavelet Domains," IEEE Chinacom 2008, Hangzhou, China, Aug. 2008.